
DIGITAL ACCESS TO SCHOLARSHIP AT HARVARD
DASH.HARVARD.EDU

HARVARD LIBRARY


A metabolite of branched chain amino acids drives vascular fatty acid transport and causes glucose intolerance

Citation

Jang, Cholsoon. 2016. A metabolite of branched chain amino acids drives vascular fatty acid transport and causes glucose intolerance. Doctoral dissertation, Harvard University, Graduate School of Arts & Sciences.

Link

http://nrs.harvard.edu/urn-3:HUL.InstRepos:26718711

Terms of use

This article was downloaded from Harvard University's DASH repository, and is made available under the terms and conditions applicable to Other Posted Material (LAA), as set forth at

https://harvardwiki.atlassian.net/wiki/external/NGY5NDE4ZjgzNTc5NDQzMGIzZWZhMGFlOWI2M2EwYTg

Accessibility

https://accessibility.huit.harvard.edu/digital-accessibility-policy

Share Your Story

The Harvard community has made this article openly available.
Please share how this access benefits you. Submit a story

A metabolite of branched chain amino acids drives vascular fatty acid transport and causes glucose intolerance

A dissertation presented

By

Cholsoon Jang

to

The Division of Medical Sciences

in partial fulfillment of the requirements

for the degree of

Doctor of Philosophy

in the subject of

Biological and Biomedical Sciences

Harvard University

Cambridge, Massachusetts

September 2015

© 2015 Cholsoon Jang

All rights reserved.

Dissertation Advisor: Dr. Zoltan Arany Cholsoon Jang

A metabolite of branched chain amino acids drives vascular fatty acid transport and causes glucose intolerance

Abstract

Epidemiological and experimental data implicate branched chain amino acids (BCAAs) in the development of insulin resistance, but the mechanisms underlying this link remain unclear. Insulin resistance in skeletal muscle stems from excess accumulation of lipid species, a process that requires blood-borne lipids to first traverse the blood vessel wall. Little is known, however, of how this trans-endothelial transport occurs or is regulated. Here, we identify 3-hydroxy-isobutyrate (3-HIB), a catabolic intermediate of the BCAA valine, as a novel paracrine regulator of trans-endothelial transport of fatty acids. PGC-1α, a transcriptional co-activator that regulates broad programs of fatty acid consumption, induces the secretion from muscle of 3-HIB, which then triggers fatty acid uptake and transport in endothelial cells. Conversely, inhibiting the synthesis of 3-HIB in muscle cells blocks the promotion of endothelial fatty acid uptake. Providing animals with 3-HIB in drinking water, or inducing 3-HIB levels in skeletal muscle by over-expressing PGC-1α, stimulates muscle to take up fatty acids *in vivo*, leading to muscle lipid accumulation, and systemic glucose intolerance. 3-HIB levels are elevated in muscle from patients with diabetes. These data thus unveil a novel mechanism that regulates trans-endothelial flux of fatty acids, revealing 3-HIB as a new bioactive signaling metabolite that links the

regulation of fatty acid flux to BCAA catabolism and provides a mechanistic explanation for how increased BCAA catabolic flux can cause diabetes.

Table of Contents

Abstract iii
Acknowledgements vi
Dedications x
Figures and Tables xi

Chapter 1: Introduction 1
- Lipotoxicity and muscle insulin resistance 2
- Vascular fatty acid transport 4
- Role of PGC-1 co-activators in fatty acid metabolism 8
- Branched chain amino acid metabolism and diabetes 12
- References 14

Chapter 2: Regulation of vascular fatty acid transport by PGC-1s 20
- Attribution 20
- Introduction 21
- Results 25
- Discussion 55
- Materials and methods 62
- References 67

Chapter 3: Role of 3-HIB in glucose homeostasis 70
- Attribution 70
- Introduction 71
- Results 76
- Discussion 92
- Materials and methods 98
- References 108

Chapter 4: Discussion 114
- 3-HIB receptors and downstream signaling 115
- Regulation of BCAA metabolism by PGC-1s 118
- Beyond 3-HIB and beyond muscle 121
- Systemic versus local levels of BCAAs and metabolites 122
- Potential caveats of muscle 3-HIB concentration 123
- Conclusion 125
- References 126

Acknowledgements

My PhD journey has been filled with joy, happiness, struggles and many people who shared all these 'symptoms' with me. Without them, it must have been so boring and lonely.

First of all, I thank Zolt, my PhD mentor, for everything for the past 6 years. He's the number 2 person with whom I have shared the above symptoms the most. Then who's number 1? My wife. I've learned all the essential aspects of the 'true scientist' from him – how to ask critical and interesting questions, how to interpret data, how to solve problems, how to give a good talk, how to criticize data, how to make a funny joke about science and life, how to write a good paper and so on. One day, I was talking to my lab mate and he said 'whenever I discuss with you, I feel like I'm talking with Zolt." That was the best compliment I have ever heard. Zolt, thank you so much for being my mentor!

Dear my honorable past and present Arany lab gangs, I really appreciate and miss you guys' humors, sarcasm, bitter but very helpful scientific comments, and incredible ability to steal food and drinks from seminars. I have learned a lot from you and have enjoyed my life in lab because of you. Let me call each of your names. Glenn, my father-in-lab, thank you for being a good and supportive father since I joined the lab. You know I respect you, right? I miss your weird laughing sounds so much. Sri and Aihua, thank you for threatening and yelling to Glenn whenever he was mean to me. You guys were like my mother-in-lab. MC, thank you for attacking me with your ingenious weapon (dry ice in tight EP tubes). It kept me waking up in lab to make me more productive. Ian, you are the funniest guy I've ever met in this country. I can't easily imagine you are now a serious doctor. Jim, thank you for shouting "Shogo!!!!" in lab late at nights and weekends to blame Shogo for our never-working experiments. It made me convinced I'm not the only crazy person in the entire CLS building. Adeel, thank you for making fun of Glenn so that we appreciate that God is fair – Apparently, Glenn is not a perfect man!

Laura, thank you for spending 5 years with me as my sole fellow graduate student in our lab. I was too shy to tell you in person but I really appreciate all your help, emotional support, and patience whenever I acted like a child. I can't imagine my PhD life without you. George, Yoni, Robyn, Amrita, Nicole, Caitlin, Sophia, Tiffany and Luisa, I also thank you for sharing a wonderful time in lab. Shogo, thank you for being my Chef and drinking fellow. Let's drink until dawn if I can pass my defense exam. Atsushi, you should join our drinking festival! I will do my best to get your wife's permission. Jian, a big brother of our lab. I really appreciate all your efforts to restore lab stuffs vandalized by Arany lab kids including myself. Boa, thank you for being the second Korean member of our lab. After you joined, people now realize Koreans are actually nice. Ayon, Michael, Steven, Zhipeng and Linzi are also my precious lab mates who are already rising stars of our lab.

I am also grateful for members of my dissertation advisory committee (DAC) - Dr. Patricia D'Amore, Dr. Jorge Plutzky and Dr. Steven Gygi. You have been my strongest allies during my PhD war. Your support and encouragement kept me moving forward. I have good memories for each of you. Pat was so kind that she came all the way from MGH to encourage me at an NRB café when I was puzzled by the fact that our lab is moving. I still remember Jorge's really warm email that made me impressed and encouraged (I've never received such a long email from any professor in my life). Also, thank you for giving me precious advices on my future career. Finally, I will never forget an advice Steve once gave me – "It's important to start and proceed with a project. However, it's more important to decide when you finish and wrap up the project." Someday if I have a chance to become a DAC member of a graduate student, I will recollect my DAC committee and ask to myself this question: 'what would my DAC do to help this student?', because that would be the most right thing for the student.

Thank you also for my defense committee members, Dr. Joseph Loscalzo, Dr. David Cohen, Dr. Patricia D'Amore, and Dr. Matthew Vander Heiden. I really appreciate your time, feedbacks and scientific insights to improve my thesis. I would also like to thank to my previous mentors in Korea – Dr. Jongkyung Chung, Dr. Gou Young Koh, and Dr. Minho Shong. Without their mentoring and support, I would have had much harder time during my PhD.

None of this work would have been possible without assistance from collaborators. I just realized that there are too many people to call each person's name here, unless I devote one chapter just to say thank you to each of them. Thank you all. I wish the best of luck to your research and future career.

I also have to thank the people who helped me focus on studying and not worry about money. Dear my Lotte Foundation family - Keunjae Lee, Ohsang Kwon and Donghyun Jung, I really appreciate your financial support and encouragement, and greeting me with delicious Korean food whenever I visited your office. Also, I would like to thank American Heart Association for supporting my PhD work.

I would like to thank the people who have been my refuge, my shelter and my sanctuary. They are now more than half of my Facebook friends. They are the people who made a warm seaweed soup on my birthday and took care of me when I was sick. They are the people who prayed for me with tears. They are the people who I had breakfast for 3 years almost every morning. They are the people who taught me life is enjoyable and grateful. I really appreciate my friends in youth group, a conductor (Keeyoung Kim) and members of chorus, elders (including Mooje Sung, Soo-chan Bae and so on), and a pastor, Tae-Whan Kim, of the First Korean Church in Cambridge.

Finally, thank you to my family. Dear my wife (Gina Lee), thank you for making me the luckiest and happiest man in the world. Dear my mom (Eulsook Kim), dad (Myeongjin Chang) and sister (Sehee Jang), thank you for having me as your family. I can't think of any appropriate words in English (or even in Korean) to express my love and thankfulness. I can't stare at our family pictures on my desk without tears. I really miss you. I also want to thank my grandma, aunts, and all of my cousins. I am so lucky to have you as my sweat family. Dear my mother-in law (Keum-hyung Lee), father-in-law (In-kyun Lee), sister-in-law (Sora Lee and Junga Lee) and brother-in-law (Cholhee Cho), thank you for your emotional support and encouragement. Lastly, thank you God, my father in the heaven and in my heart, for everything.

Dedication

To my father (Myeongjin Chang) and mother (Eulsook Kim)

None of this would have been possible without your

love, encouragement and sacrifices.

Thank you.

Figures and Tables

Chapter 1

Figure 1.1: Imbalanced fatty acid metabolism 3

Figure 1.2: Mechanism of insulin resistance by excess intracellular fat species 4

Figure 1.3: Endothelial fatty acid transport 6

Figure 1.4: VEGF-B regulates endothelial fatty acid transport 7

Figure 1.5: PGC-1α as an orchestrator of fatty acid metabolism 8

Figure 1.6: Hypothesis 10

Chapter 2

Figure 2.1: BCAA catabolism 22

Figure 2.2: Development of a Bodipy-FA uptake assay 26

Figure 2.3: PGC-1α in muscle cells induces secretion of paracrine factors that stimulate endothelial FA transport 27

Figure 2.4: Retrovirus-mediated PGC-1α CM induces endothelial FA uptake 28

Figure 2.5: Characteristics of endothelial FA uptake by C2C12 conditioned media 29

Figure 2.6: Endothelial cells take up long-chain fatty acids upon PGC-1α CM treatment 30

Figure 2.7: PGC-1α CM activity is cell type specific and ATP-dependent 31

Figure 2.8: Primary brain ECs make a tight monolayer and transport FAs upon CM treatment 32

Figure 2.9: Knockout of both PGC-1s is required to reduce the FA uptake-inducing activity in myotube CM 33

Figure 2.10: Blockage of VEGF-B does not suppress FA uptake induced by α-CM 34

Figure 2.11: Deletion of VEGF-B receptors in ECs does not block FA uptake induced by α-CM 35

Figure 2.12: The paracrine factor is a small molecule 36

Figure 2.13: Several metabolites are higher in α-CM compared to Ct-CM 37

Figure 2.14: List of compounds tested to identify signaling pathways in myotubes that affect the PGC-1α CM activity 38

Figure 2.15: Insulin and three inhibitors affect the α-CM activity but not FA uptake by ECs directly 39

Figure 2.16: Schematic of unbiased purification of the paracrine factor 40

Figure 2.17: Fractionation of CMs and activity test 41

Figure 2.18: Identification of a peak that is unique to match with the activity 42

Figure 2.19: MS/MS spectra of four isobaric hydroxybutyrate candidates 43

Figure 2.20: Identification of 3-hydroxyisobutyrate (3-HIB) as the paracrine factor in α-CM that stimulates endothelial FA uptake 44

Figure 2.21: 3-HIB increases endothelial FA transport 45

Figure 2.22: C2C12 myotubes metabolize FAs transported by 3-HIB-treated ECs 46

Figure 2.23: 3-HIB is generated from valine catabolism 48

Figure 2.24: PGC-1α and PGC-1β induce expression of BCAA catabolic enzymes in myotubes 50

Figure 2.25: Deletion of both PGC-1α and PGC-1β suppresses gene expression of valine catabolic enzymes 51

Figure 2.26: Perturbation of 3-HIB production in myotubes affects FA uptake induced by α-CM 52

Figure 2.27: Knockdown of HIBADH in mouse skeletal muscle increases triglycerides levels 53

Figure 2.28: Knockdown of HIBADH in HUVECs does not affect FA uptake 54

Figure 2.29: BCAA catabolism requires glycolysis 56

Chapter 3

Figure 3.1: Protein-mediated fatty acid transport in ECs 72

Figure 3.2: FATPs but not CD36 mediate endothelial FA uptake by α-CM or 3-HIB 77

Figure 3.3: Fatty acid transport proteins mediate endothelial FA uptake by α-CM or 3-HIB 78

Figure 3.4: α-CM or 3-HIB does not affect expression of fatty acid transport-related genes 79

Figure 3.5: α-CM does not affect protein levels of FATP3 and FATP4 80

Figure 3.6: PGC-1α and PGC-1β in muscle regulate valine catabolic enzyme expression 81

Figure 3.7: PGC-1α and PGC-1β cooperate to regulate valine catabolic enzyme expression 82

Figure 3.8: PGC-1α expression in muscle induces fatty acid uptake *in vivo* 83

Figure 3.9: PGC-1α and PGC-1β in muscle regulate glucose tolerance 84

Figure 3.10: Acute feeding of mice with 3-HIB stimulates FA uptake by heart and thigh 85

Figure 3.11: Acute feeding of mice with 3-HIB does not affect vessel permeability or damage muscle 86

Figure 3.12: Effect of two-week 3-HIB feeding on FA metabolism 87

Figure 3.13: 3-HIB induces PKCθ membrane translocation in muscle 88

Figure 3.14: 3-HIB reduces Akt signaling and induces glucose intolerance. 89

Figure 3.15: Mice fed with 3-HIB for 2 weeks show systemic insulin resistance 90

Figure 3.16: Fasting increases muscle and plasma levels of 3-HIB 91

Figure 3.17: 3-HIB is increased in muscle of *db*/*db* mice and human diabetic patients 93

Figure 3.18: Comparison of BCAT and BCKDH gene expression between the liver and muscle subtypes 95

Chapter 4

Figure 4.1: Inhibition of ERRα or PPARδ does not block the induction of valine catabolism genes by PGC-1α 119

Figure 4.2: Knockdown of Klf15 blocks some of valine catabolism genes induced by PGC-1α 120

Figure 4.3: Quantification of 3-HIB in muscle interstitial fluid 124

Chapter 1: Introduction

Lipotoxicity and muscle insulin resistance

Modern society is one of vast over-consumption of calories and fats, and fats have been increasingly implicated as critical to the pathology of cardiovascular and metabolic diseases. Epidemiological and animal studies have demonstrated a clear causal relationship between obesity and diabetes (Guilherme A et al. 2008). How obesity causes diabetes at a molecular level, however, is not fully understood. One of potential mechanisms is a model of lipotoxicity-induced insulin resistance. In normal physiological conditions, dietary fats are esterified to form triglycerides in the liver and stored in the liver and adipose tissues throughout the body. During fasting or increased physical activity such as exercise, these fats are consumed by metabolically active organs such as the heart and skeletal muscle to generate energy through mitochondrial beta-oxidation. However, excess supply of dietary fats can overwhelm the storage capacity of adipose tissues. The overloading of fats in adipose tissues is known to trigger inflammation marked by increased macrophage infiltration. Adipose tissues under inflammation elevate lipolysis, which further limits their fat storage capacity. The released excess fats then circulate and eventually accumulate in other tissues such as the heart and skeletal muscle (Figure 1.1). Skeletal muscle utilizes its abundant mitochondria to consume a large amount of fats. However, surplus fat entry into muscle results in accumulation of incompletely oxidized fatty acids, which interfere with various cell signaling pathways in myocytes (Itani SI et al. 2002). One of the most critical pathways affected is the insulin signaling pathway (Figure 1.2). Incompletely oxidized fatty acid species (e.g. ceramides, diglycerides and acyl-carnitines) are known to activate cellular stress signaling pathways such as c-Jun N-terminal kinase (JNK) and protein kinase C (PKC) (Szendroedi J et al. 2014). These activated stress kinases directly phosphorylate a critical inhibitory phosphorylation site (Ser 1101) of insulin receptor substrate-1 (IRS-1), a key downstream target of insulin signaling pathway (Griffin ME et al. 1999; Yu C et al. 2002).

Normally, IRS-1 dependent downstream signaling cascades activate Akt protein kinase, which then induces translocation of glucose transporters to the plasma membrane to increase cellular glucose uptake upon insulin stimulation. In diabetic conditions, however, this molecular event is severely blunted by IRS-1 inhibition through JNK / PKC activation. Indeed, muscle biopsies from patients with type II diabetes and muscle from rodent models of diabetes (e.g. leptin receptor mutated *db*/*db* mice and Zucker diabetic rats) show highly increased levels of incompletely oxidized fatty acid species and consequently decreased phosphorylation of Akt (Dresner A et al. 1999; Cline GW et al. 1999). Many genetic and pharmaceutical approaches have been tried in the rodent models to restore the insulin signaling pathway by directly inhibiting stress kinases or activating insulin pathway components, with only a partial success

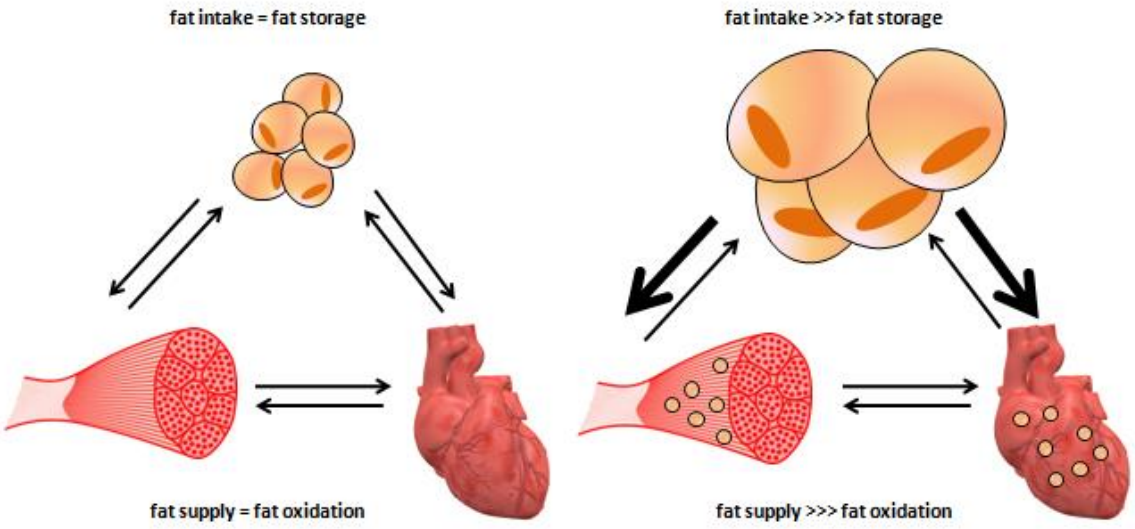


Figure 1.1: Imbalanced fatty acid metabolism. In a normal state, fats are stored in adipose tissues as triglycerides. Upon fasting or increased physical activity like exercise, stored fats are secreted and transported to metabolically active organs such as the heart and skeletal muscle where fats are oxidized to generate energy. When dietary fat intake is too much, excess fats cannot be stored in adipose tissues and accumulate in the heart and skeletal muscle, causing lipotoxicity and insulin resistance in these organs.

because of complexity of the signaling pathway (Mayerson AB et al. 2002; Kim JK et al. 2004; Choi CS et al. 2007; Morino K et al. 2008; Camporez JP et al. 2013). Therefore, new strategies that target more fundamental upstream events are necessary. Finding ways to modulate entry of fatty acids into myocytes would thus provide novel therapeutic targets for the treatment of diabetes and its complications.

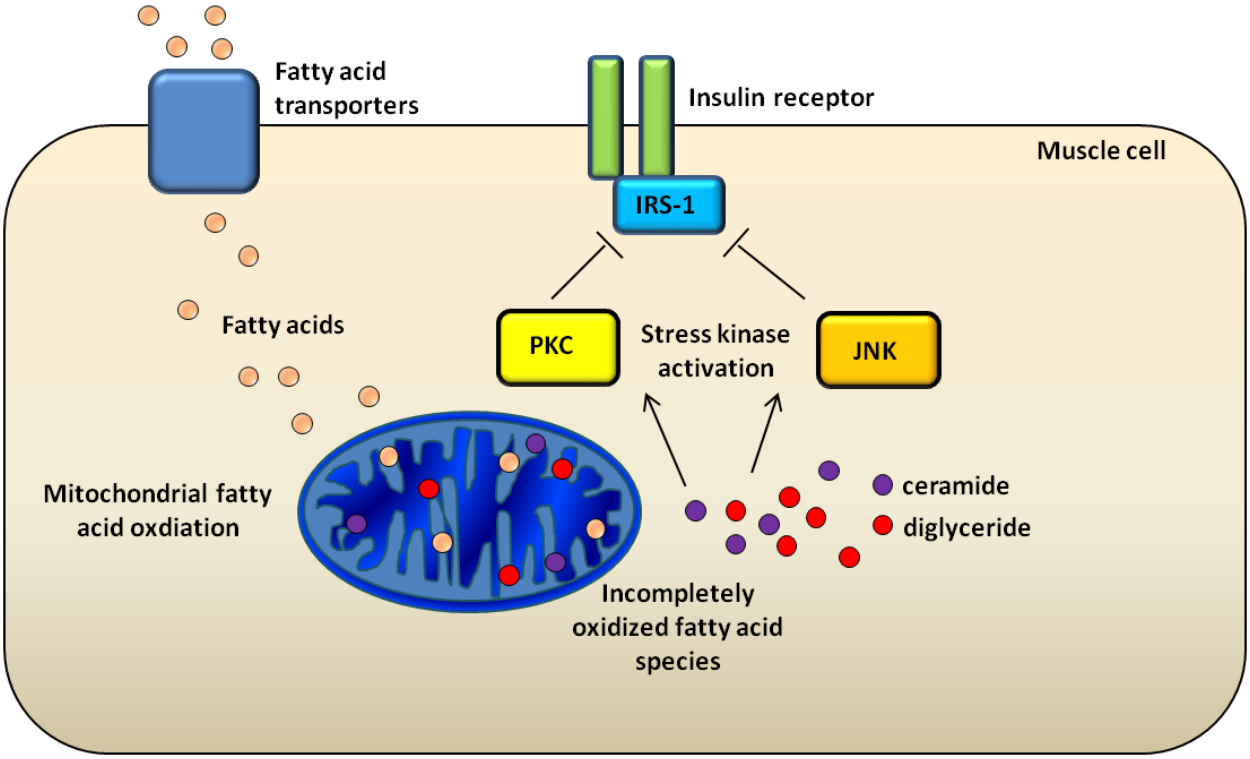


Figure 1.2: Mechanism of insulin resistance by excess intracellular fat species. Excess amount of fatty acids cannot be completely oxidized by mitochondria in muscle cells, which results in accumulation of toxic lipid species such as ceramides and diglycerides. These lipid species are known to activate stress kinases such as Protein kinase C (PKC) and Jun N-terminal kinase (JNK), leading to increased inhibitory phosphorylation of Insulin receptor substarate-1 (IRS-1). Inhibition of IRS-1 thus renders cells resistant to insulin stimulation (insulin resistance).

Vascular fatty acid transport

Fatty acids are mostly circulating in blood either as esterified triglycerides in lipoprotein particles (e.g. VLDL, LDL, chylomicrons) or as non-esterified fatty acids bound to albumin proteins. Esterified fats destined for muscle cells must be unesterified at the luminal endothelial

surface by lipoprotein lipase, a protein generated and secreted by muscle cells and transported to endothelial cells (Davies BS et al. 2010; Davies BS et al. 2012). The expression, activity, and transport of lipoprotein lipase are tightly regulated, involving multiple signaling pathways and regulatory proteins (Wang Y et al. 2015). It is relatively unknown how fatty acids are released from albumin on the endothelial surface. Free fatty acids must then traverse the vessel wall to reach the underlying tissue. How do fatty acids get across the endothelium? Remarkably little is known about this question. Two mechanisms have primarily been proposed. In the first, fatty acids incorporate into the endothelial plasma membrane and then rapidly diffuse within the membrane, ultimately being delivered to interstitial albumin or other carrier proteins (Hamilton JA and Kamp F. 1999). However, experimentally measured kinetics of endothelial fatty acid transport is much faster than calculated kinetics of fatty acid diffusion, indicating that there are facilitated transport mechanisms (Kampf JP et al. 2006; Bonen A et al. 2007). In fact, studies have provided clear evidence that proteins mediate endothelial fatty acid transport. For instance, it was shown that mild treatment of cells with protease such as trypsin to cleave only membrane proteins abrogated fatty acid uptake by the cell (Bonen A et al. 1998; Luiken JJ et al. 1999). These data favor the second proposal: fatty acids are transported across the endothelial cells, either via vesicular transport or specific transport proteins. The identifications of fatty acid transporters (FATPs) and fatty acid translocase (FAT or CD36) have strengthened the argument for this type of trans-endothelial transport (Figure 1.3) (Abumrad NA et al. 1993; Schaffer JE and Lodish HF. 1994; Hirsch D et al. 1998; Gimeno RE et al. 2003). FATPs are transmembrane proteins with acyl-CoA synthetase activity that converts fatty acids to acyl-CoA. This enzymatic activity of FATPs seems to be important to facilitate uptake of extracellular fatty acids across the membrane by a vectorial acylation mechanism (Digel M et al. 2011). This is similar to the

mechanism of glucose uptake, in which there is a rapid conversion of intracellular glucose to glucose-6-phosphate to keep the glucose gradient high outside and low inside cells. Moreover, hydrophilic moieties of CoA and phosphate in acyl-CoA and glucose-6-phosphate, respectively, efficiently block free diffusion across the plasma membrane. Fatty acid binding proteins (FABPs) that bind to fatty acids directly in cytoplasm or the plasma membrane are also known to modulate fatty acid uptake with as of yet unidentified mechanisms (Stremmel W et al. 1985; Schwieterman W et al. 1988). Studies using genetic deletion of individual members of FATPs or CD36 in various tissues have demonstrated their importance to fatty acid transport

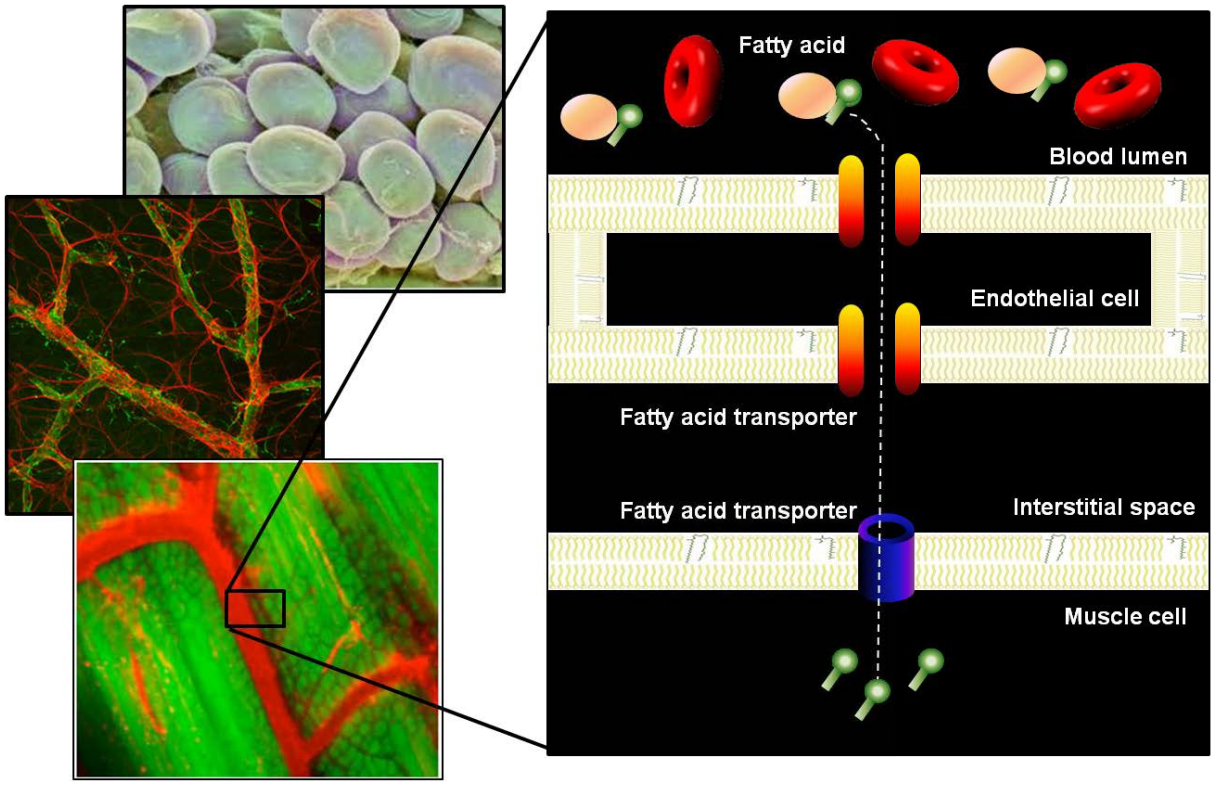


Figure 1.3: Endothelial fatty acid transport. Fatty acids released from adipose tissues are bound to albumin in the blood and transferred to muscle through blood vessels. There are three plasma membrane boundaries between the blood lumen and cytoplasm of muscle cell – two endothelial cell membranes and one muscle cell membrane. Various fatty acid transporter proteins such as FATPs and CD36 localize on these membranes, thereby facilitating fatty acid transport from blood to muscle cells. How this process is regulated is poorly understood.

(Coburn CT et al. 2000; Gimeno RE et al. 2003). However, the data for FATPs or FABPs specifically in endothelial cells are scant (Iso T et al. 2013). Thus, much remains to be learned about the transport of fats across the endothelium. In particular, almost nothing is known of how trans-capillary fatty acid transfer is regulated by systemic and local cues. Two pivotal recent studies by the same group have shown that vascular endothelial growth factor-B (VEGF-B), a cousin of VEGF-A, regulates endothelial fatty acid transport (Hagberg CE et al. 2010; Hagberg CE et al. 2012). VEGF-B binds to its membrane receptors, VEGFR1 and co-receptor NRP1, and activates downstream pathways to elevate gene expression of FATP3 and FATP4 in endothelial cells (Figure 1.4). Genetic deletion of VEGF-B in mice dramatically reduced fatty acid transport into the heart and skeletal muscle. Interestingly, the authors also found that increased fatty acid

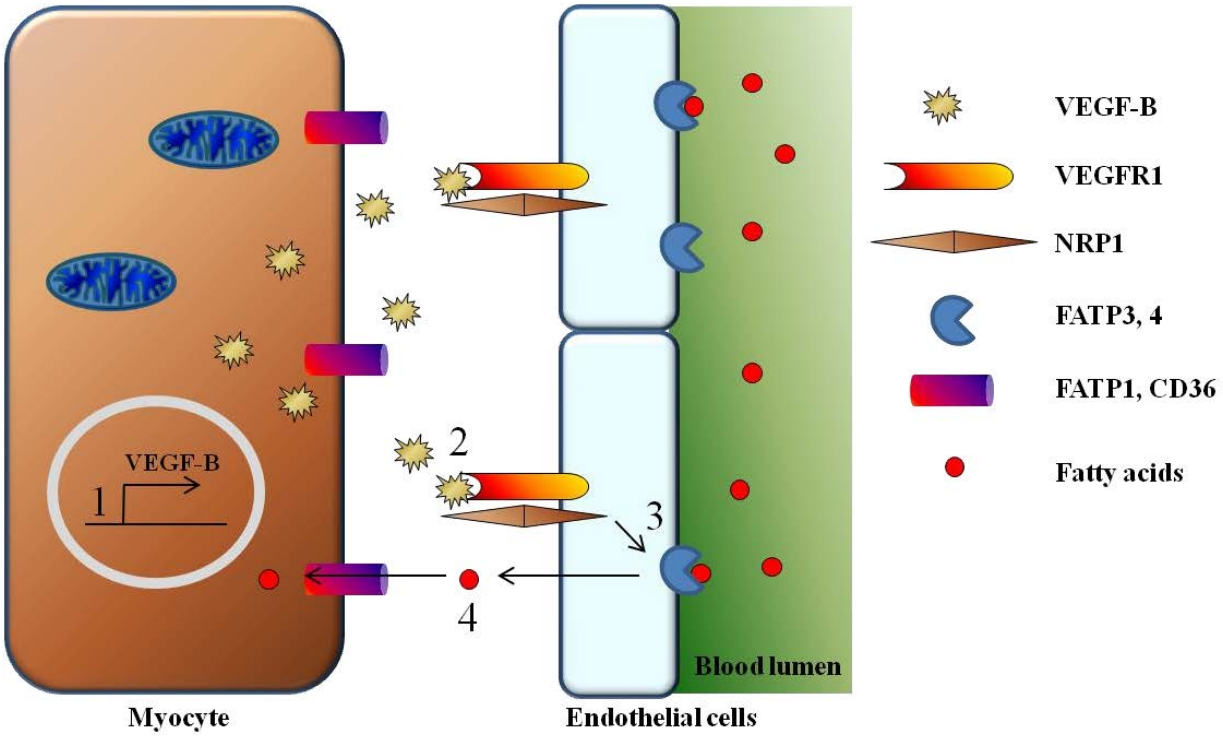


Figure 1.4: VEGF-B regulates endothelial fatty acid transport. Myocyte-derived VEGF-B (1) binds to its receptors VEGFR1 and NRP1 in the endothelial cell plasma membrane (2), thereby transducing signaling pathways to increase gene expression of FATP3 and FATP4 (3). These fatty acid transporters then increase transport of fatty acids from blood to myocyte (4). This figure is modified from Hagberg CE et al. *Physiology* 28:125-134, 2013.

shunt to white adipose tissues and improved whole body insulin sensitivity. Consistently, VEGF-B knockout mice were highly resistant to diabetes even on high-fat diet or in a *db*/*db* genetic background by reducing fat accumulation in skeletal muscle. Furthermore, injection of VEGF-B blocking antibody into the mouse models of type II diabetes dramatically restored glucose sensitivity and lipid homeostasis, strongly proposing a therapeutic potential of VEGF-B blockage for the treatment of diabetes. Little is known, however, whether there are other mechanisms underlying the regulation of fatty acid transport in endothelial cells.

Role of PGC-1 co-activators in fatty acid metabolism

PPARγ co-activator alpha (PGC-1α) and beta (PGC-1β) are transcriptional co-activators

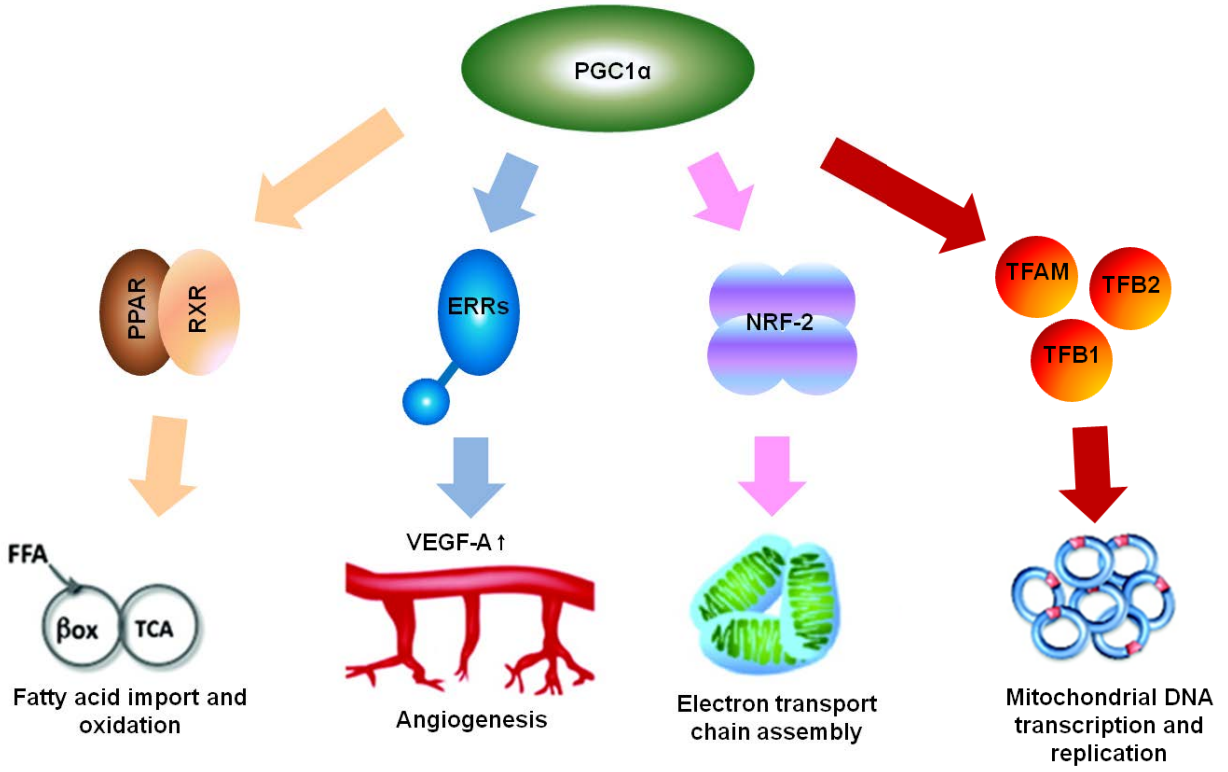


Figure 1.5: PGC-1α as an orchestrator of fatty acid metabolism. PGC-1α binds to and activates multiple nuclear receptor transcription factors to regulate a variety of biological processes related to fatty acid metabolism. It increases expression of fatty acid oxidation enzymes, induces angiogenesis through VEGF-A, stimulates mitochondrial electron transport chain assembly and mitochondrial biogenesis.

that powerfully regulate cellular metabolism in numerous tissues, including the heart and skeletal muscle. Transcriptional co-activators are proteins that dock on transcription factors and alter chromatin structure and the transcription machinery to stimulate gene expression (Hermanson O et al. 2002; Spiegelman BM and Heinrich R. 2004). Recently, co-activators have emerged as potent regulatory targets of physiological stimuli and hormones (Handschin C and Spiegelman BM. 2006). PGC-1α was first identified as a cold-inducible PPARγ binding protein in brown fat (Puigserver P et al. 1998). PGC-1α expression is highly induced in the liver by fasting, which in turn induces genes responsible for gluconeogenesis. In skeletal muscle, exercise is the most well-known stimulator of PGC-1α expression. Induction of PGC-1α by exercise increases fatty acid uptake, oxidation and mitochondrial biogenesis. These diverse, tissue-specific effects of PGC-1α are shown to occur through direct binding and activation of several nuclear receptor transcription factors, including PPARs and estrogen related receptors (ERRs) (Figure 1.5). PGC-1α is most highly expressed in the heart and skeletal muscle and is preferentially expressed in oxidative fibers that use fatty acids as a major energy source (Lin J et al. 2002). Transgenic expression of PGC-1α in skeletal muscle leads to activation of genes typical of slow fibers, and induces a broad genetic program of mitochondrial biology and fatty acid oxidation, mimicking some aspects of chronic exercise (Wende AR et al. 2007; Calvo JA et al. 2008). PGC-1β, a cousin of PGC-1α, has a similar role in mitochondrial biology, but its regulatory mechanisms and downstream effects are slightly different from PGC-1α (Rowe GC and Arany Z. 2014). For example, PGC-1β expression is relatively unchanged by the physiological cues that strongly induce PGC-1α (e.g. fasting and exercise). Nonetheless, transgenic mice expressing PGC-1β specifically in skeletal muscle show similar phenotypes to PGC-1α muscle-specific transgenic

mice, suggesting their overlapping roles in skeletal muscle biology (Rowe GC et al. 2011). PGC-1α or PGC-1β whole body knockout mice are viable and grossly normal (Leone TC et al. 2005; Sonoda J et al. 2007). However, their double knockout mice are embryonic lethal (Lai L et al. 2008), indicating important cooperative and compensatory roles of the proteins.

Recently, our lab showed that PGC-1α also powerfully regulates angiogenesis in the heart and skeletal muscle (Arany Z et al. 2008; Chinsomboon J et al. 2009; Patten IS et al. 2012). Gain-of-function studies showed that PGC-1α strongly induces expression of VEGF-A, and other angiogenic factors like PDGF-B and Angiopoietin-2, in cultured cardiomyocytes and in the

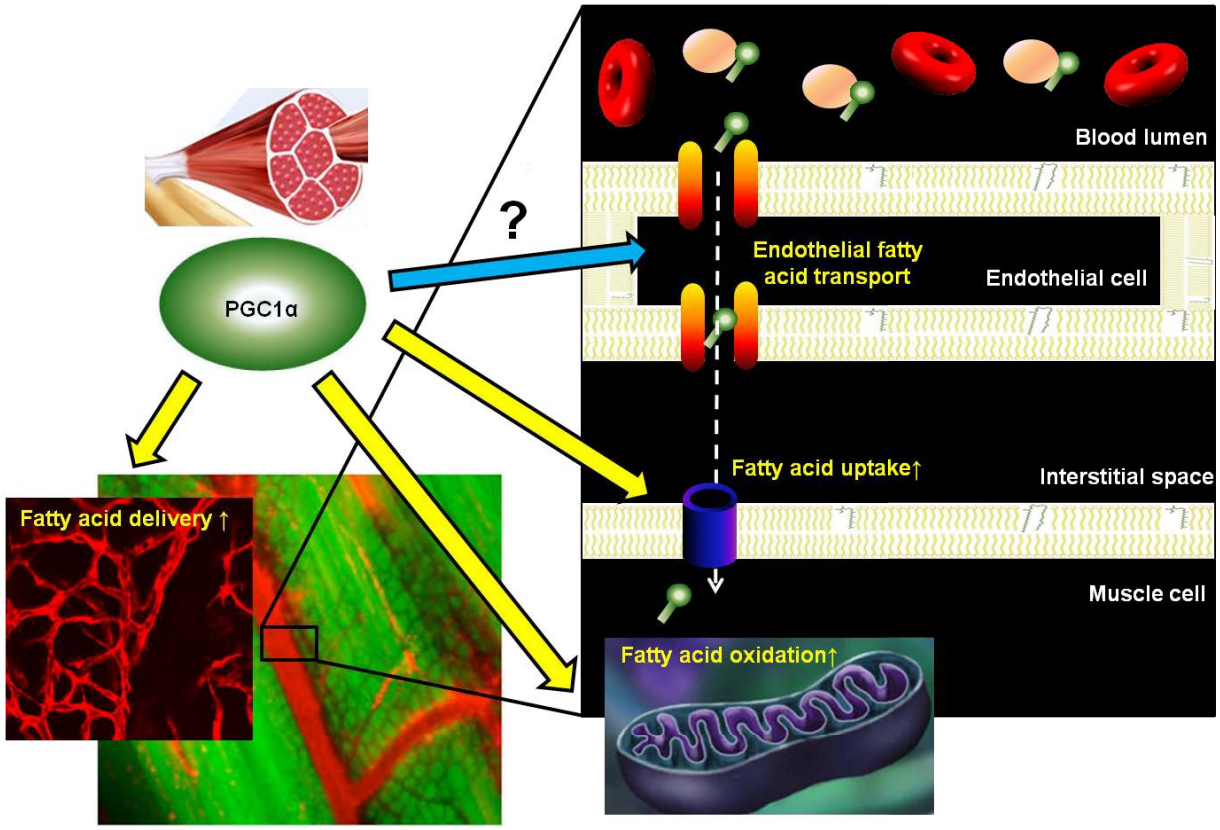


Figure 1.6: Hypothesis. PGC-1α regulates many steps of fatty acid metabolism in muscle cells – from fatty acid delivery through angiogenesis, fatty acid oxidation through mitochondrial biogenesis, to fatty acid uptake through CD36 induction. Thus, it is possible that PGC-1α can also regulate endothelial fatty acid transport.

heart and skeletal muscle *in vivo*. Transgenic expression of PGC-1α in cardiac and skeletal muscle dramatically increased capillary density. Loss-of-function studies, using mice lacking PGC-1α specifically in cardiomyocytes or myocytes, demonstrated that PGC-1α is required for physiological angiogenesis (e.g. mediated by exercise). Thus, PGC-1α coordinates the formation of new blood vessels (which facilitate fat and oxygen delivery to tissues) with fatty acid oxidation in mitochondria (fat and oxygen consumption). However, it is unknown whether PGC-1α can also regulate endothelial fatty acid transport (Figure 1.6).

The finding that PGC-1α in muscle cells directly regulates VEGF-A is particularly interesting because VEGF-A is a secreted factor that can influence other cells. In fact, recent studies have further expanded the role of muscle PGC-1α in the regulation of secreted factors that exhibit paracrine/endocrine action, collectively known as "myokines" (Correia JC et al. 2015). Mice transgenically expressing PGC-1α specifically in skeletal muscle (MCKα mice) show increased browning of white adipose tissues with higher thermogenesis, potentially through a muscle-derived endocrine hormone and/or bioactive metabolite (Bostrom P et al. 2012; Roberts LD et al. 2014). Furthermore, aged MCKα mice show significantly improved whole-body health and increased life span, suggesting that increased expression of PGC-1α in skeletal muscle is sufficient to delay various aging processes in the whole body (Wenz T et al. 2009). On the other hand, MCKα mice are more insulin resistant than wild type mice upon high-fat feeding (Choi CS et al. 2008). This is a cautionary note of increased PGC-1α expression in muscle without physical activity. As a mechanism of this paradoxical effect of PGC-1α, increased accumulation of fatty acid species and inhibition of insulin signaling by PKC was suggested. Interestingly, these MCKα mice show improved glucose tolerance when exercised (Summermatter S et al. 2013), demonstrating that PGC-1α overexpression in skeletal muscle must be accompanied with

physical activity to obtain its full beneficial effects. To summarize, PGC-1α in muscle not only regulates intracellular processes but also intercellular communication through secreted factors.

Branched chain amino acid metabolism and diabetes

Valine, isoleucine and leucine, collectively known as branched chain amino acids (BCAAs), have many characteristics distinct from other amino acids (Lynch CJ and Adams SH. 2014). First, they are the most abundant essential amino acids in the body. For example, about 30% of muscle proteins are composed of BCAAs. They are also the most hydrophobic amino acids rendering them essential structural components of globular proteins, membrane proteins, and coiled-coil structures of many transcription factors. Second, the catabolism of BCAAs initiates in skeletal muscle contrary to other amino acids whose catabolism mostly occurs in the liver. This explains why the pattern of blood BCAA levels is quite different from that of other amino acids during the fed-fast cycle. Finally, BCAAs are directly involved in regulating biological processes such as protein synthesis and neurotransmitter synthesis. BCAAs are potent activators of the mammalian target of rapamycin (mTOR) (Dodd KM and Tee AR. 2012). mTOR is a master regulator kinase of cell size and proliferation. Its two distinct complexes (mTORC1 and mTORC2) regulate a variety of cellular functions through S6K- and Akt-dependent protein translation and cell cycle, respectively (Wang X and Proud CG. 2006). Since mTOR is directly activated by BCAAs, and the mTOR pathway is frequently deregulated in metabolic diseases, numerous studies have focused on how BCAA metabolism is altered in various patho-physiological settings (Wang TJ et al. 2011; Wurtz P et al. 2012; McCormack SE et al. 2013). Data from the Framingham Heart Study, for example, unexpectedly revealed that elevated BCAA levels in blood are the strongest predictor of developing diabetes a decade later (Wang TJ et al. 2011). Consistently, animal models of diabetes including *db*/*db* mice and Zucker diabetic

rats also show high BCAA blood levels (She P et al. 2007; Lackey DE et al. 2013; Olson KC et al. 2014). Importantly, feeding rats with a high BCAA diet exacerbated insulin resistance by the high-fat diet (Newgard CB et al. 2009), implicating a strong causal relationship between high BCAA and insulin resistance (Felig P et al. 1969; Newgard CB. 2012). Further studies are required to elucidate how increased BCAA levels contribute to the development of insulin resistance.

References

Abumrad NA, el-Maghrabi MR, Amri EZ, Lopez E, Grimaldi PA. (1993). Cloning of a rat adipocyte membrane protein implicated in binding or transport of long-chain fatty acids that is induced during preadipocyte differentiation. Homology with human CD36. J Biol Chem. 268:17665-8.

Arany Z, Foo SY, Ma Y, Ruas JL, Bommi-Reddy A, Girnun G, Cooper M, Laznik D, Chinsomboon J, Rangwala SM, Baek KH, Rosenzweig A, Spiegelman BM. (2008). HIF-independent regulation of VEGF and angiogenesis by the transcriptional coactivator PGC-1α. Nature. 451:1008-12.

Bonen A, Luiken JJ, Liu S, Dyck DJ, Kiens B, Kristiansen S, Turcotte LP, Van Der Vusse GJ, Glatz JF. (1998). Palmitate transport and fatty acid transporters in red and white muscles. Am J Physiol. 275:471-8.

Bonen A, Chabowski A, Luiken JJ, Glatz JF. (2007). Is membrane transport of FFA mediated by lipid, protein, or both? Mechanisms and regulation of protein-mediated cellular fatty acid uptake: molecular, biochemical, and physiological evidence. Physiology. 22:15-29.

Bostrom P, Wu J, Jedrychowski MP, Korde A, Ye L, Lo JC, Rasbach KA, Bostrom EA, Choi JH, Long JZ, Kajimura S, Zingaretti MC, Vind BF, Tu H, Cinti S, Hojlund K, Gygi SP, Spiegelman BM. (2012). A PGC1-α-dependent myokine that drives brown-fat-like development of white fat and thermogenesis. Nature. 481:463-8.

Calvo JA, Daniels TG, Wang X, Paul A, Lin J, Spiegelman BM, Stevenson SC, Rangwala SM. (2008). Muscle-specific expression of PPAR{gamma} coactivator-1{alpha} improves exercise performance and increases peak oxygen uptake. J Appl Physiol. 104:1304-12.

Camporez JP, Jornayvaz FR, Petersen MC, Pesta D, Guigni BA, Serr J, Zhang D, Kahn M, Samuel VT, Jurczak MJ, Shulman GI. (2013). Cellular mechanisms by which FGF21 improves insulin sensitivity in male mice. Endocrinology. 154:3099-109.

Chinsomboon J, Ruas J, Gupta RK, Thom R, Shoag J, Rowe GC, Sawada N, Raghuram S, Arany Z. (2009). The transcriptional coactivator PGC-1{alpha} mediates exercise-induced angiogenesis in skeletal muscle. Proc Natl Acad Sci U S A. 106:21401-6.

Choi CS, Fillmore JJ, Kim JK, Liu ZX, Kim S, Collier EF, Kulkarni A, Distefano A, Hwang YJ, Kahn M, Chen Y, Yu C, Moore IK, Reznick RM, Higashimori T, Shulman GI. (2007). Overexpression of uncoupling protein 3 in skeletal muscle protects against fat-induced insulin resistance. J Clin Invest. 117:1995-2003.

Choi CS, Befroy DE, Codella R, Kim S, Reznick RM, Hwang YJ, Liu ZX, Lee HY, Distefano A, Samuel VT, Zhang D, Cline GW, Handschin C, Lin J, Dodd KM, Tee AR. (2012). Leucine and mTORC1: a complex relationship. Am J Physiol Endocrinol Metab. 302:E1329-42.

Cline GW, Petersen KF, Krssak M, Shen J, Hundal RS, Trajanoski Z, Inzucchi S, Dresner A, Rothman DL, Shulman GI. (1999). Impaired glucose transport as a cause of decreased insulin-stimulated muscle glycogen synthesis in type 2 diabetes. N Engl J Med. 341:240-6.

Coburn CT, Knapp FF Jr, Febbraio M, Beets AL, Silverstein RL, Abumrad NA. (2000). Defective uptake and utilization of long chain fatty acids in muscle and adipose tissues of CD36 knockout mice. J Biol Chem. 275:32523-9.

Correia JC, Ferreira DM, Ruas JL. (2015). Intercellular: local and systemic actions of skeletal muscle PGC-1s. Trends Endocrinol Metab. 26:305-14.

Davies BS, Beigneux AP, Barnes RH 2nd, Tu Y, Gin P, Weinstein MM, Nobumori C, Nyren R, Goldberg I, Olivecrona G, Bensadoun A, Young SG, Fong LG. (2010). GPIHBP1 is responsible for the entry of lipoprotein lipase into capillaries. Cell Metab. 12:42-52.

Davies BS, Goulbourne CN, Barnes RH 2nd, Turlo KA, Gin P, Vaughan S, Vaux DJ, Bensadoun A, Beigneux AP, Fong LG, Young SG. (2012). Assessing mechanisms of GPIHBP1 and lipoprotein lipase movement across endothelial cells. J Lipid Res.53:2690-7.

Digel M, Staffer S, Ehehalt F, Stremmel W, Ehehalt R, Fullekrug J. (2011). FATP4 contributes as an enzyme to the basal and insulin-mediated fatty acid uptake of C2C12 muscle cells. Am J Physiol Endocrinol Metab. 301:785-96.

Dresner A, Laurent D, Marcucci M, Griffin ME, Dufour S, Cline GW, Slezak LA, Andersen DK, Hundal RS, Rothman DL, Petersen KF, Shulman GI. (1999). Effects of free fatty acids on glucose transport and IRS-1-associated phosphatidylinositol 3-kinase activity. J Clin Invest. 103:253-9.

Felig P, Marliss E, Cahill GF Jr. (1969). Plasma amino acid levels and insulin secretion in obesity. N. Engl. J. Med. 281:811-6.

Gimeno RE, Hirsch DJ, Punreddy S, Sun Y, Ortegon AM, Wu H, Daniels T, Stricker-Krongrad A, Lodish HF, Stahl A. (2003). Targeted deletion of fatty acid transport protein-4 results in early embryonic lethality. J Biol Chem. 278:49512-6.

Gimeno RE, Ortegon AM, Patel S, Punreddy S, Ge P, Sun Y, Lodish HF, Stahl A. (2003). Characterization of a heart-specific fatty acid transport protein. J Biol Chem. 278:16039-44.

Griffin ME, Marcucci MJ, Cline GW, Bell K, Barucci N, Lee D, Goodyear LJ, Kraegen EW, White MF, Shulman GI. (1999). Free fatty acid-induced insulin resistance is associated with activation of protein kinase C theta and alterations in the insulin signaling cascade. Diabetes. 48:1270-4.

Guilherme A, Virbasius JV, Puri V, Czech MP. (2008). Adipocyte dysfunctions linking obesity to insulin resistance and type 2 diabetes. Nat Rev Mol Cell Biol. 9:367-77.

Hagberg CE, Falkevall A, Wang X, Larsson E, Huusko J, Nilsson I, van Meeteren LA, Samen E, Lu L, Vanwildemeersch M, Klar J, Genove G, Pietras K, Stone-Elander S, Claesson-Welsh L, Yla-Herttuala S, Lindahl P, Eriksson U. (2010). Vascular endothelial growth factor B controls endothelial fatty acid uptake. Nature. 464:917-21.

Hagberg CE, Mehlem A, Falkevall A, Muhl L, Fam BC, Ortsater H, Scotney P, Nyqvist D, Samen E, Lu L, Stone-Elander S, Proietto J, Andrikopoulos S, Sjoholm A, Nash A, Eriksson U. (2012). Targeting VEGF-B as a novel treatment for insulin resistance and type 2 diabetes. Nature. 490:426-30.

Hamilton JA, Kamp F. (1999). How are free fatty acids transported in membranes? Is it by proteins or by free diffusion through the lipids? Diabetes. 48:2255-69.

Handschin C, Spiegelman BM. (2006). Peroxisome proliferator-activated receptor gamma coactivator 1 coactivators, energy homeostasis, and metabolism. Endocr Rev. 27:728-35.

Hermanson O, Glass CK, Rosenfeld MG. (2002). Nuclear receptor coregulators: multiple modes of modification. Trends Endocrinol Metab. 13:55-60.

Hirsch D, Stahl A, Lodish HF. (1998). A family of fatty acid transporters conserved from mycobacterium to man. Proc Natl Acad Sci U S A. 95:8625-9.

Iso T, Maeda K, Hanaoka H, Suga T, Goto K, Syamsunarno MR, Hishiki T, Nagahata Y, Matsui H, Arai M, Yamaguchi A, Abumrad NA, Sano M, Suematsu M, Endo K, Hotamisligil GS, Kurabayashi M. (2013). Capillary endothelial fatty acid binding proteins 4 and 5 play a critical role in fatty acid uptake in heart and skeletal muscle. Arterioscler Thromb Vasc Biol. 33:2549-57.

Itani SI, Ruderman NB, Schmieder F, Boden G. (2002). Lipid-induced insulin resistance in human muscle is associated with changes in diacylglycerol, protein kinase C, and IkappaB-alpha. Diabetes. 51:2005-11.

Kampf JP, Cupp D, Kleinfeld AM. (2006). Different mechanisms of free fatty acid flip-flop and dissociation revealed by temperature and molecular species dependence of transport across lipid vesicles. J Biol Chem. 281:21566-74.

Kim JK, Fillmore JJ, Sunshine MJ, Albrecht B, Higashimori T, Kim DW, Liu ZX, Soos TJ, Cline GW, O'Brien WR, Littman DR, Shulman GI. (2004). PKC-theta knockout mice are protected from fat-induced insulin resistance. J Clin Invest. 114:823-7.

Lackey DE, Lynch CJ, Olson KC, Mostaedi R, Ali M, Smith WH, Karpe F, Humphreys S, Bedinger DH, Dunn TN, Thomas AP, Oort PJ, Kieffer DA, Amin R, Bettaieb A, Haj FG, Permana P, Anthony TG, Adams SH. (2013). Regulation of adipose branched-chain amino acid catabolism enzyme expression and cross-adipose amino acid flux in human obesity. Am J Physiol Endocrinol Metab. 304:E1175-87.

Lai L, Leone TC, Zechner C, Schaeffer PJ, Kelly SM, Flanagan DP, Medeiros DM, Kovacs A, Kelly DP. (2008). Transcriptional coactivators PGC-1α and PGC-lbeta control overlapping programs required for perinatal maturation of the heart. Genes Dev. 22:1948-61.

Leone TC, Lehman JJ, Finck BN, Schaeffer PJ, Wende AR, Boudina S, Courtois M, Wozniak DF, Sambandam N, Bernal-Mizrachi C, Chen Z, Holloszy JO, Medeiros DM, Schmidt RE, Saffitz JE, Abel ED, Semenkovich CF, Kelly DP. (2005). PGC-1α deficiency causes multi-system energy metabolic derangements: muscle dysfunction, abnormal weight control and hepatic steatosis. PLoS Biol. 3:e101.

Lin J, Wu H, Tarr PT, Zhang CY, Wu Z, Boss O, Michael LF, Puigserver P, Isotani E, Olson EN, Lowell BB, Bassel-Duby R, Spiegelman BM. (2002). Transcriptional co-activator PGC-1 alpha drives the formation of slow-twitch muscle fibres. Nature. 418:797-801.

Luiken JJ, Turcotte LP, Bonen A. (1999). Protein-mediated palmitate uptake and expression of fatty acid transport proteins in heart giant vesicles. J Lipid Res. 40:1007-16.

Lynch CJ, Adams SH. (2014). Branched-chain amino acids in metabolic signalling and insulin resistance. Nat Rev Endocrinol. 10:723-36.

Mayerson AB, Hundal RS, Dufour S, Lebon V, Befroy D, Cline GW, Enocksson S, Inzucchi SE, Shulman GI, Petersen KF. (2002). The effects of rosiglitazone on insulin sensitivity, lipolysis, and hepatic and skeletal muscle triglyceride content in patients with type 2 diabetes. Diabetes. 51:797-802.

McCormack SE, Shaham O, McCarthy MA, Deik AA, Wang TJ, Gerszten RE, Clish CB, Mootha VK, Grinspoon SK, Fleischman A. (2013). Circulating branched-chain amino acid concentrations are associated with obesity and future insulin resistance in children and adolescents. Pediatr Obes. 8:52-61.

Morino K, Neschen S, Bilz S, Sono S, Tsirigotis D, Reznick RM, Moore I, Nagai Y, Samuel V, Sebastian D, White M, Philbrick W, Shulman GI. (2008). Muscle-specific IRS-1 Ser->Ala transgenic mice are protected from fat-induced insulin resistance in skeletal muscle. Diabetes. 57:2644-51.

Newgard CB, An J, Bain JR, Muehlbauer MJ, Stevens RD, Lien LF, Haqq AM, Shah SH, Arlotto M, Slentz CA, Rochon J, Gallup D, Ilkayeva O, Wenner BR, Yancy WS Jr, Eisenson H, Musante G, Surwit RS, Millington DS, Butler MD, Svetkey LP. (2009). A branched-chain amino acid-related metabolic signature that differentiates obese and lean humans and contributes to insulin resistance. Cell Metab. 9:311-26.

Newgard, C.B. (2012). Interplay between lipids and branched-chain amino acids in development of insulin resistance. Cell Metab 15, 606-14.

Olson KC, Chen G, Xu Y, Hajnal A, Lynch CJ. (2014). Alloisoleucine differentiates the branched-chain aminoacidemia of Zucker and dietary obese rats. Obesity. 22:1212-5.

Patten IS, Rana S, Shahul S, Rowe GC, Jang C, Liu L, Hacker MR, Rhee JS, Mitchell J, Mahmood F, Hess P, Farrell C, Koulisis N, Khankin EV, Burke SD, Tudorache I, Bauersachs J, del Monte F, Hilfiker-Kleiner D, Karumanchi SA, Arany Z. (2012). Cardiac angiogenic imbalance leads to peripartum cardiomyopathy. Nature. 485:333-8.

Petersen KF, Spiegelman BM, Shulman GI. (2008). Paradoxical effects of increased expression of PGC-1α on muscle mitochondrial function and insulin-stimulated muscle glucose metabolism. Proc Natl Acad Sci U S A. 105:19926-31.

Puigserver P, Wu Z, Park CW, Graves R, Wright M, Spiegelman BM. (1998). A cold-inducible coactivator of nuclear receptors linked to adaptive thermogenesis. Cell. 92:829-39.

Roberts LD, Bostrom P, O'Sullivan JF, Schinzel RT, Lewis GD, Dejam A, Lee YK, Palma MJ, Calhoun S, Georgiadi A, Chen MH, Ramachandran VS, Larson MG, Bouchard C, Rankinen T, Souza AL, Clish CB, Wang TJ, Estall JL, Soukas AA, Cowan CA, Spiegelman BM, Gerszte RE. (2014). β-Aminoisobutyric acid induces browning of white fat and hepatic β-oxidation and is inversely correlated with cardiometabolic risk factors. Cell Metab. 19:96-108.

Rowe GC, Jang C, Patten IS, Arany Z. (2011). PGC-1β regulates angiogenesis in skeletal muscle. Am J Physiol Endocrinol Metab. 301:155-63.

Rowe GC, Arany Z. (2014). Genetic models of PGC-1 and glucose metabolism and homeostasis. Rev Endocr Metab Disord. 15:21-9.

Schaffer JE, Lodish HF. (1994). Expression cloning and characterization of a novel adipocyte long chain fatty acid transport protein. Cell. 79:427-36.

Schwieterman W, Sorrentino D, Potter BJ, Rand J, Kiang CL, Stump D, Berk PD. (1988). Uptake of oleate by isolated rat adipocytes is mediated by a 40-kDa plasma membrane fatty acid binding protein closely related to that in liver and gut. Proc Natl Acad Sci U S A. 85:359-63.

She P, Van Horn C, Reid T, Hutson SM, Cooney RN, Lynch CJ. (2007). Obesity-related elevations in plasma leucine are associated with alterations in enzymes involved in branched-chain amino acid metabolism. Am J Physiol Endocrinol Metab. 293:E1552-63.

Shulman GI. (2014). Ectopic fat in insulin resistance, dyslipidemia, and cardiometabolic disease. N Engl J Med. 371:1131-41.

Sonoda J, Mehl IR, Chong LW, Nofsinger RR, Evans RM. (2007). PGC-1β controls mitochondrial metabolism to modulate circadian activity, adaptive thermogenesis, and hepatic steatosis. Proc Natl Acad Sci U S A. 104:5223-8.

Spiegelman BM, Heinrich R. (2004). Biological control through regulated transcriptional coactivators. Cell. 119:157-67.

Stremmel W, Strohmeyer G, Borchard F, Kochwa S, Berk PD. (1885). Isolation and partial characterization of a fatty acid binding protein in rat liver plasma membranes. Proc Natl Acad Sci U S A. 82:4-8.

Summermatter S, Shui G, Maag D, Santos G, Wenk MR, Handschin C. (2013). PGC-1α improves glucose homeostasis in skeletal muscle in an activity-dependent manner. Diabetes. 62:85-95.

Szendroedi J, Yoshimura T, Phielix E, Koliaki C, Marcucci M, Zhang D, Jelenik T, Muller J, Herder C, Nowotny P, Shulman GI, Roden M. (2014). Role of diacylglycerol activation of PKCtheta in lipid-induced muscle insulin resistance in humans. Proc Natl Acad Sci U S A. 111:9597-602.

Wang TJ, Larson MG, Vasan RS, Cheng S, Rhee EP, McCabe E, Lewis GD, Fox CS, Jacques PF, Fernandez C, O'Donnell CJ, Carr SA, Mootha VK, Florez JC, Souza A, Melander O, Clish CB, Gerszten RE. (2011). Metabolite profiles and the risk of developing diabetes. Nat Med. 17:448-53.

Wang X and Proud CG. (2006). The mTOR pathway in the control of protein synthesis. Physiology. 21:362-9.

Wang Y, Rodrigues B. (2015). Intrinsic and extrinsic regulation of cardiac lipoprotein lipase following diabetes. Biochim Biophys Acta. 1851:163-71.

Wende AR, Schaeffer PJ, Parker GJ, Zechner C, Han DH, Chen MM, Hancock CR, Lehman JJ, Huss JM, McClain DA, Holloszy JO, Kelly DP. (2007). A role for the transcriptional coactivator PGC-1α in muscle refueling. J Biol Chem. 282:36642-51.

Wenz T, Rossi SG, Rotundo RL, Spiegelman BM, Moraes CT. (2009). Increased muscle PGC-1α expression protects from sarcopenia and metabolic disease during aging. Proc Natl Acad Sci U S A. 106:20405-10.

Wurtz P, Makinen VP, Soininen P, Kangas AJ, Tukiainen T, Kettunen J, Savolainen MJ, Tammelin T, Viikari JS, Ronnemaa T, Kahonen M, Lehtimaki T, Ripatti S, Raitakari OT, Jarvelin MR, Ala-Korpela M. (2012). Metabolic signatures of insulin resistance in 7,098 young adults. Diabetes. 61:1372-80.

Yu C, Chen Y, Cline GW, Zhang D, Zong H, Wang Y, Bergeron R, Kim JK, Cushman SW, Cooney GJ, Atcheson B, White MF, Kraegen EW, Shulman GI. (2002). Mechanism by which fatty acids inhibit insulin activation of insulin receptor substrate-1 (IRS-1)-associated phosphatidylinositol 3-kinase activity in muscle. J Biol Chem. 277:50230-6.

Chapter 2:

Regulation of vascular fatty acid transport by PGC-1s

Attributions: Cholsoon Jang performed all experiments for this section unless otherwise stated. Dr. Sungwhan Oh performed all the mass spectrometry analysis. Dr. Wenyun Lu and Dr. Joshua Rabinowitz (Penn Metabolomics Core) performed metabolomics flux analysis. Dr. Chandra Ghosh and Dr. Samir Parikh performed trans-endothelial electrical resistance experiments.

Abstract

Insulin resistance in skeletal muscle stems from excess accumulation of lipid species, a process that requires blood-borne lipids to first traverse the blood vessel wall. Little is known, however, of how this trans-endothelial transport occurs or is regulated. PGC-1α in skeletal muscle coordinates the consumption of fatty acids in mitochondria with their delivery via blood vessels. We reasoned here that PGC-1α, in order to maximize delivery of fatty acids to muscle, would likely also instruct these new vessels to have a higher capacity for trans-endothelial fatty acid transport. Indeed, conditioned media from PGC-1α-overexpressing muscle cells highly induces endothelial fatty acid uptake. Biochemical fractionation and mass-spectrometry analysis show that the responsible factor is not VEGF-B but 3-hydroxyisobutyrate (3-HIB), a catabolic intermediate of the BCAA valine. PGC-1α induces almost all genes of valine catabolic enzymes and the secretion of 3-HIB from muscle cells. Inhibiting the synthesis of 3-HIB in muscle cells blocks the promotion of endothelial fatty acid uptake. These data thus unveil a novel mechanism that regulates trans-endothelial flux of fatty acids, revealing 3-HIB as a new bioactive signaling metabolite that links the regulation of fatty acid flux to BCAA catabolism.

Introduction

BCAA catabolism

BCAA catabolism is tightly regulated and unique in many aspects (Figure 2.1). All three BCAAs share the first two enzymes in their catabolism pathway. The first enzyme is BCAA aminotransferase (BCAT), which transfers an amino group from BCAAs to alpha-keto glutarate, a TCA intermediate. There are two BCAT isoenzymes – cytoplasmic BCAT (BCAT1) and

mitochondrial BCAT (mBCAT or BCAT2) encoded in different genes. BCATs are reversible enzymes. Skeletal muscle highly expresses both BCAT1 and BCAT2, while the liver does not (Torres N et al. 1998). Therefore, the initial catabolism of BCAAs probably occurs in

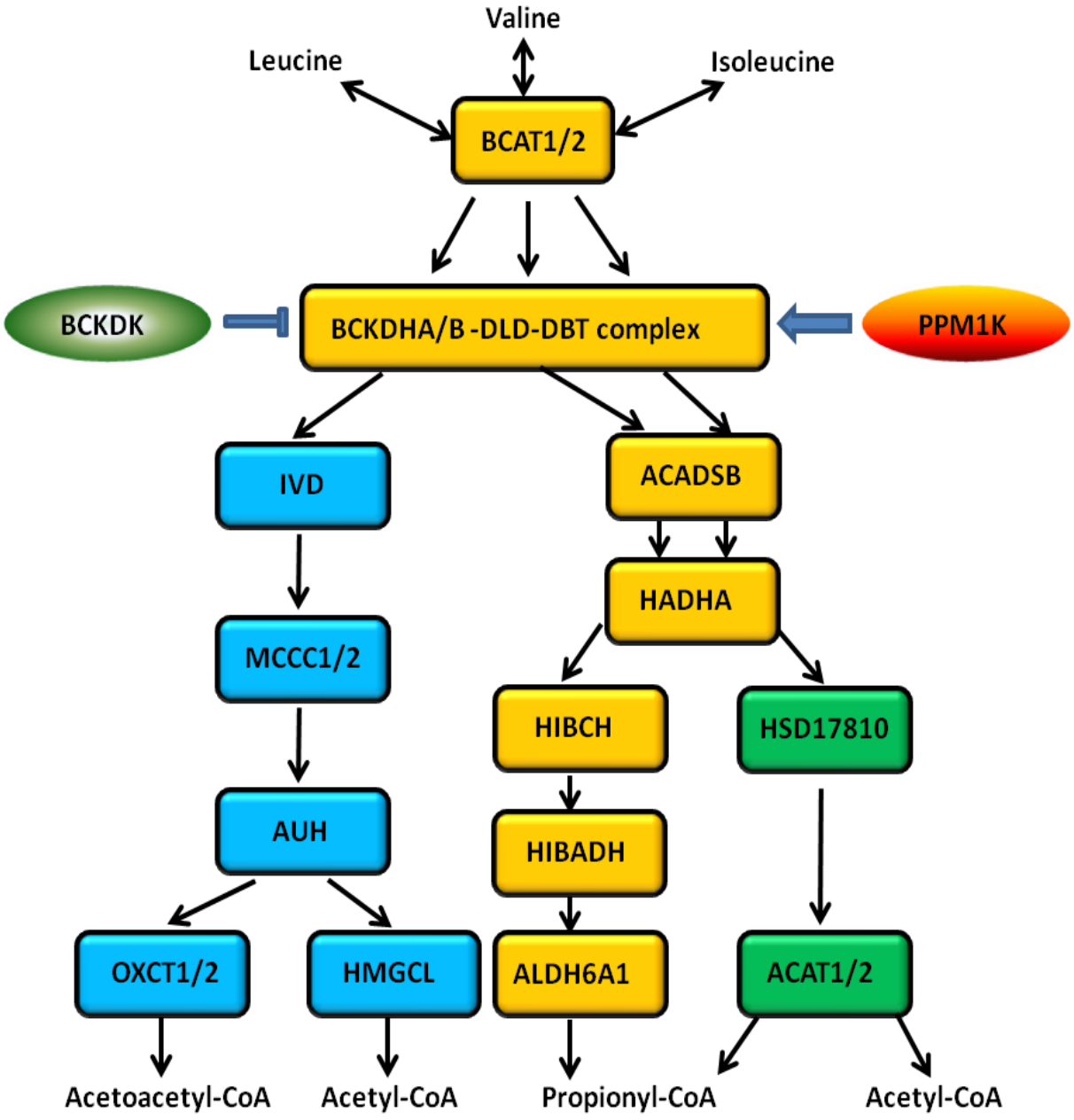


Figure 2.1: BCAA catabolism. Three BCAAs share the first two enzymes, BCAT1/2 and BCDKH complex. BCKDH complex is regulated by phosphorylation / dephosphorylation by BCKDK and PPM1K, respectively. Downstream enzymes are fairly unique for each BCAA. The final products of BCAAs are acetyl-CoA, propionyl-CoA or acetoacetyl-CoA.

muscle cells. The products of BCAT activity are alpha-keto acids, which can be further catabolized in muscle cells or secreted and transported to other tissues such as the liver. This shuttle of alpha-keto acids from muscle to the liver has been suggested based on the fact that the liver does not express BCATs and alpha-keto acids are detected in blood. However, this view has been challenged recently by several studies that employed highly sensitive mass-spectrometry to measure BCAA-related metabolites (Newgard CB et al. 2009). In fact, muscle cells seem to catabolize a major portion of alpha-keto acids. The detailed experimental evidences are discussed more in Chapter 4. The second enzyme that catabolizes alpha-keto acids is branched chain keto acid dehydrogenase (BCKDH). Again, there are two isoenzymes – BCKDH-A and BCKDH-B. BCKDH-A localizes in mitochondria, while BCKDH-B localizes in cytoplasm. Muscle cells highly express both enzymes, as do hepatocytes. BCKDHs are the rate limiting step and irreversible, which is thus considered the flux-generating step. BCKDHs are composed of three component enzymes that catalyze consecutive steps (Brosnan JT and Brosnan ME. 2006). Through BCKDHs, alpha-keto acids obtain a bulky and hydrophilic CoA residue, which helps cells efficiently trap the products of the enzymes inside mitochondria for further catabolism. BCKDHs are highly regulated enzymes. First, they are inhibited or activated by phosphorylation or dephosphorylation, respectively. Both kinase (BCKDH kinase or BCKDK) and phosphatase (Protein Phosphatase, Mg2+/Mn2+ dependent 1K or PPM1K) responsible for BCKDH regulation were identified. The expression and activity of BCKDK is tightly regulated by extracellular cues such as insulin and exercise (Nellis MM et al. 2002; Shimomura Y et al. 2004). The regulation mechanisms of PPM1K are relatively unknown. Second, the very substrates of BCKDHs, alpha-keto acids, are potent allosteric inhibitors of BCKDK, thereby activating BCKDHs as a positive feedback loop. Among three alpha-keto acids, alpha-keto isocaproate

(derived from leucine) is the strongest activator. With this elegant mechanism, the body enhances BCAA disposal when BCAAs are excess and conversely saves BCAAs when these essential amino acids are less available. Third, BCKDK is also allosterically inhibited by NADH and the CoA esters that arise from BCAA catabolism. Finally, studies suggest inter-organ regulatory mechanisms of BCAA catabolism. For instance, insulin signaling in the brain is shown to regulate expression of hepatic BCKDH through unknown circulating factors (Shin AC et al. 2014). After BCKDHs, three BCAAs have unique downstream enzymes (Figure 2.1). The tissue expression profiles and regulation of these enzymes are poorly studied.

Hypothesis

PGC-1α in muscle cells orchestrates almost all steps of fatty acid metabolism: making new blood vessels through VEGF-A, increasing fatty acid uptake by muscle cells through CD36, and generating new mitochondria and fatty acid oxidation machinery. It thus follows that muscle PGC-1α could also regulate endothelial fatty acid transport. If so, then the question arises of how muscle cells expressing PGC-1α can communicate with adjacent endothelium to do so. Hence the proposed hypothesis driving the experiments is as follows: expression of PGC-1α in muscle cells causes the secretion of factors that instruct adjoining endothelial cells to increase uptake of fatty acids from the circulation and transport them to underlying myocytes. If so, then both the factors, and the receptors and pathways involved in endothelial cells, may be novel targets for pharmaceutical modulation of fatty acid trafficking in the heart and skeletal muscle.

Why envision pharmaceutical modulation of trans-endothelial fatty acid transport? Excess accumulation of unesterified fatty acids in muscle is now thought to be a critical initiating event in the development of insulin resistance and diabetes (Shulman GI. 2014). Blocking

endothelial transport of fatty acids into muscle could therefore treat diabetes at its root. This notion has recently received strong support from studies with VEGF-B, a factor secreted from muscle that modulates trans-endothelial fatty acid transport (Hagberg CE et al. 2010). Strikingly, blocking endothelial lipid transport by blocking VEGF-B led to reduced fat accumulation in myocytes and restored insulin sensitivity in rodent models of type II diabetes (Hagberg CE et al. 2012). Interestingly, we have identified a factor that regulates endothelial fatty acid transport and it is different from VEGF-B (see below). Identifying the receptor and downstream signaling pathways in endothelial cells would thus unveil novel potential targets for the treatment of diabetes.

Results

To test if PGC-1α in skeletal muscle regulates endothelial fatty acid transport, we devised an assay in which conditioned medium (CM) from C2C12 skeletal myotubes was added to human umbilical vein endothelial cells (HUVECs), after which the ability of the HUVECs to take up fatty acids was measured by the import of the fluorescent fatty acid analog Bodipy-C12 (Figure 2.2). These dyes have been used extensively to measure uptake of long-chain fatty acids in many cell types, and were instrumental in the cloning of FATPs (Gimeno RE et al. 2003; DiRusso CC et al. 2005). It should also be noted that Bodipy fluorophore covalently bound at the hydrophobic end of 12 carbon fatty acid (Bodipy-C12) generates a molecule that has an overall length approximately equivalent to 18-carbon fatty acids, and which thus behaves like long chain fatty acids in multiple assays (Rambold AS et al. Dev. Cell 2015). Strikingly, CM from C2C12

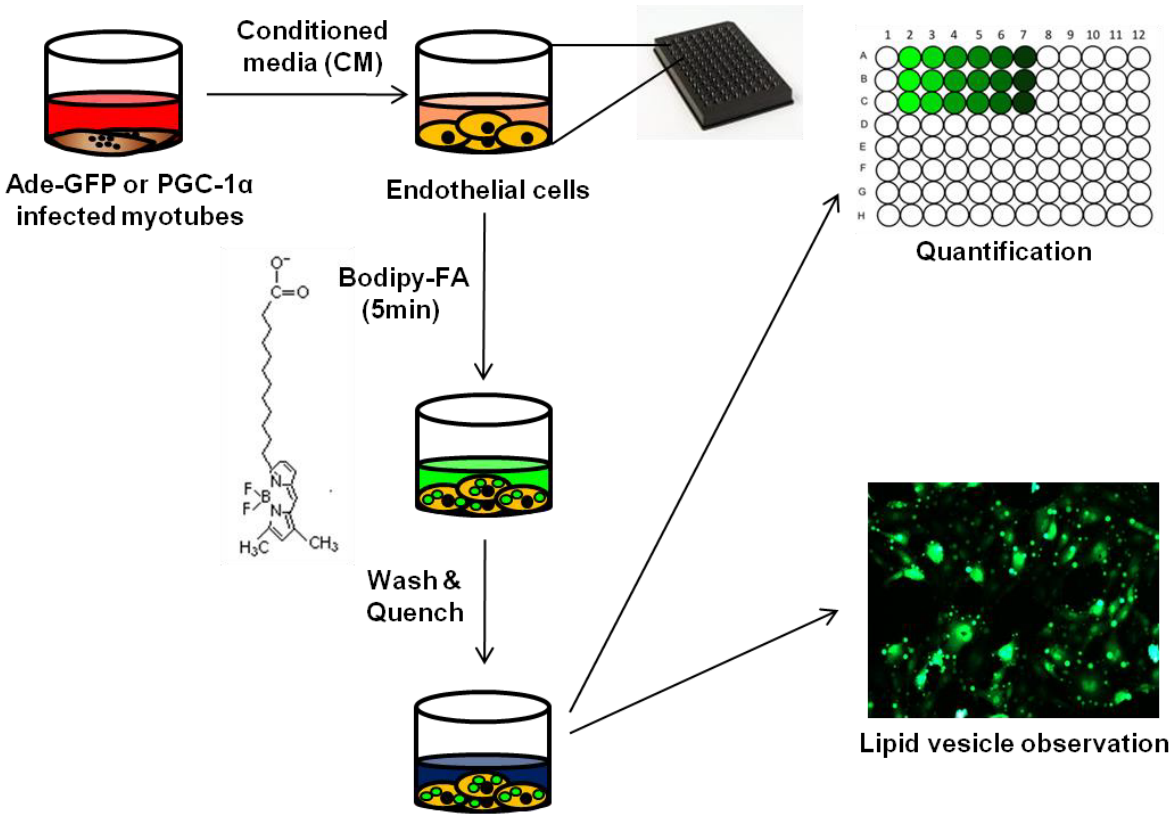


Figure 2.2: Development of a Bodipy-FA uptake assay. Differentiated myotubes were infected with adenovirus expressing GFP or PGC-1α for 48 hr, and the conditioned media (CM) were harvested. Endothelial cells in a 96 well plate were treated with CMs for 1 hr and incubated with Bodipy-conjugated fatty acids (Bodipy-FA) for 5 min. After the cells were washed and quenched with trypan blue, intracellular Bodipy-FA was measured by a plate reader or visualized with a fluorescence microscope.

myotubes over-expressing PGC-1α via adenovirus infection (α-CM) led to much stronger uptake of fatty acids in HUVECs (Figure 2.3a), suggesting the existence of a PGC-1α-regulated paracrine factor that induces endothelial fatty acid uptake. We chose fatty acid concentrations (2-16 μM) for further experiments based on numerous other studies using this approach (Li H et al. 2008; Hagberg CE et al. 2010; Dubikovskaya E et al. 2014). In addition, we have performed fatty acid uptake assay with a wide range of fatty acids from 1 to 250 μM and it showed a saturation effect from >50 μM fatty acids (Figure 2.3b). To rule out effects of adenoviral

contamination, C2C12 cells stably expressing PGC-1α were generated with retrovirus. As a

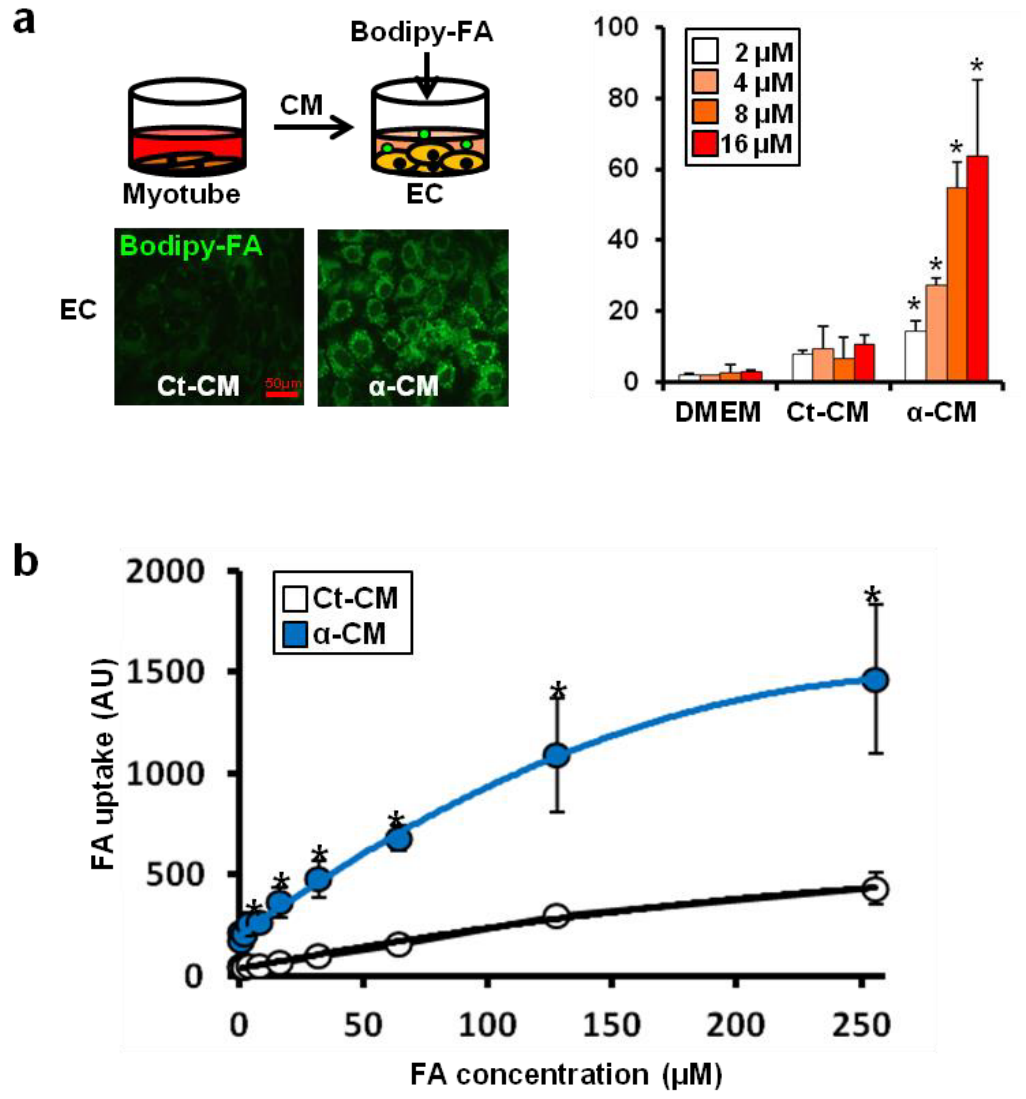


Figure 2.3: PGC-1α in muscle cells induces secretion of paracrine factors that stimulate endothelial FA transport. a, Experimental strategy (top), representative images (bottom) and quantification (right) of Bodipy-FA (2-16 μM) uptake by endothelial cells (ECs) after exposure to conditioned media from myotubes expressing GFP (Ct-CM) or PGC-1α (α-CM). **b**, FA uptake by ECs was saturated by high FA concentrations after 5 min of FA addition. *p<.05 vs. control. Data are mean ± s.d. of at least three biological replicates.

result, retroviral over-expression of PGC-1α yielded similar results (Figure 2.4a and b). Co-staining of Bodipy-fatty acids in endothelial cells with mitotracker (a mitochondrial marker) or

with anti-Calnexin antibody (an ER marker) indicates that fatty acids partially co-localize with

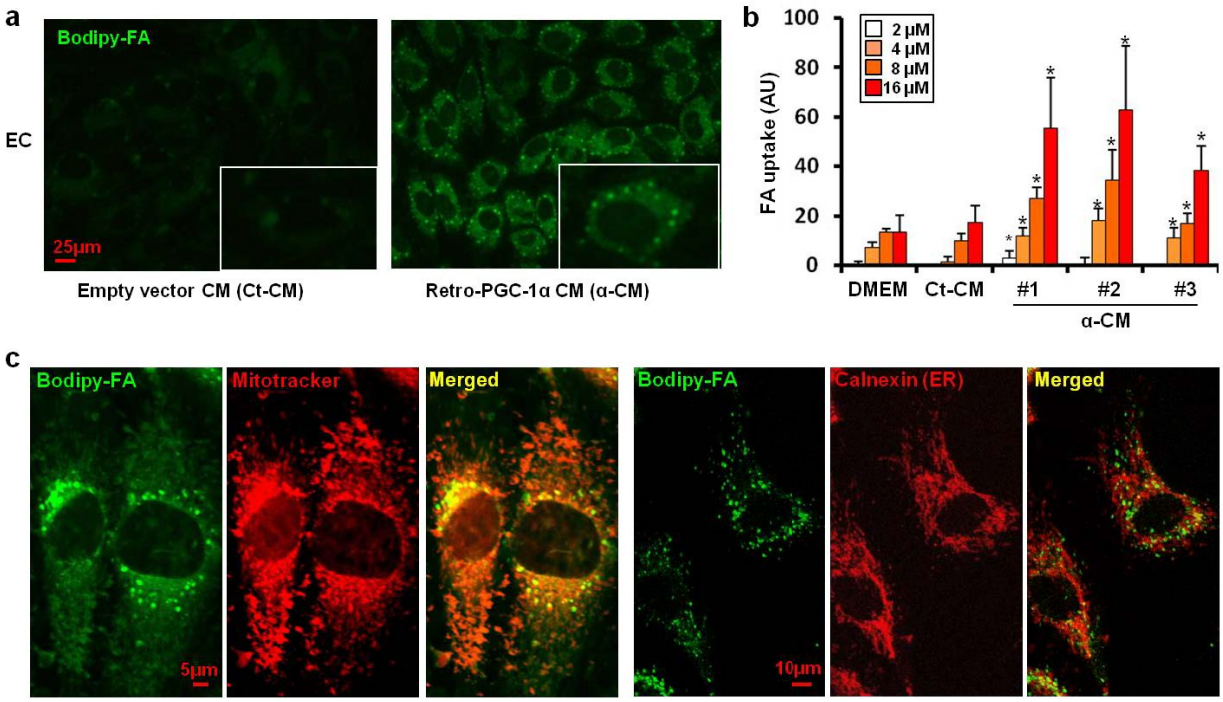


Figure 2.4: Retrovirus-mediated PGC-1α CM induces endothelial FA uptake. a, Representative images of endothelial cells (ECs) that take up Bodipy-fatty acids after treatment with CMs from C2C12 myotubes infected with retrovirus expressing vector control (Ct-CM) or PGC-1α (α-CM). **b**, Quantification of Bodipy-FA (2-16 μM) uptake by ECs. Numbers (#1, 2, 3) indicate independent stable cell lines. **c**, ECs that take up Bodipy-FA (green) after treatment of α-CM were stained with mitotracker (red, left) or immunostained with anti-Calnexin antibody (red, right) as an ER marker. *p<.05 vs. control. Data are mean ± s.d. of at least three biological replicates.

mitochondria but not with ER (Figure 2.4c). The uptake of fatty acids by endothelial cells was rapid (Figure 2.5a), could be competed by equimolar concentrations of unlabeled oleic acid (Figure 2.5b), and remained detectable after dilution of α-CM (Figure 2.5c). Prolonged exposure of endothelial cells to α-CM in the presence of unlabeled fats increased intracellular lipids, as measured by staining with oil red O or unconjugated Bodipy (Figure 2.6a). We also used Bodipy-C16 as another long chain fatty acid tracer, and observed increased endothelial Bodipy-

C16 uptake upon α-CM treatment (Figure 2.6b). On the other hand, endothelial cells do not take up Bodipy-C5 (Figure 2.6b), consistent with a specific long-chain fatty acid transport process. Various endothelial cells, including HUVECs, human umbilical cord blood-derived endothelial colony-forming cells (hECFCs) as well as an established mouse endothelial cell line (MS-1), have been tested and yielded similar results (Figure 2.7a). On the other hand, other cell types, including fibroblasts, macrophages, adipocytes, hepatocytes, and smooth muscle cells did not respond to α-CM, suggesting that this process is fairly endothelial cell-specific (Figure 2.7a).

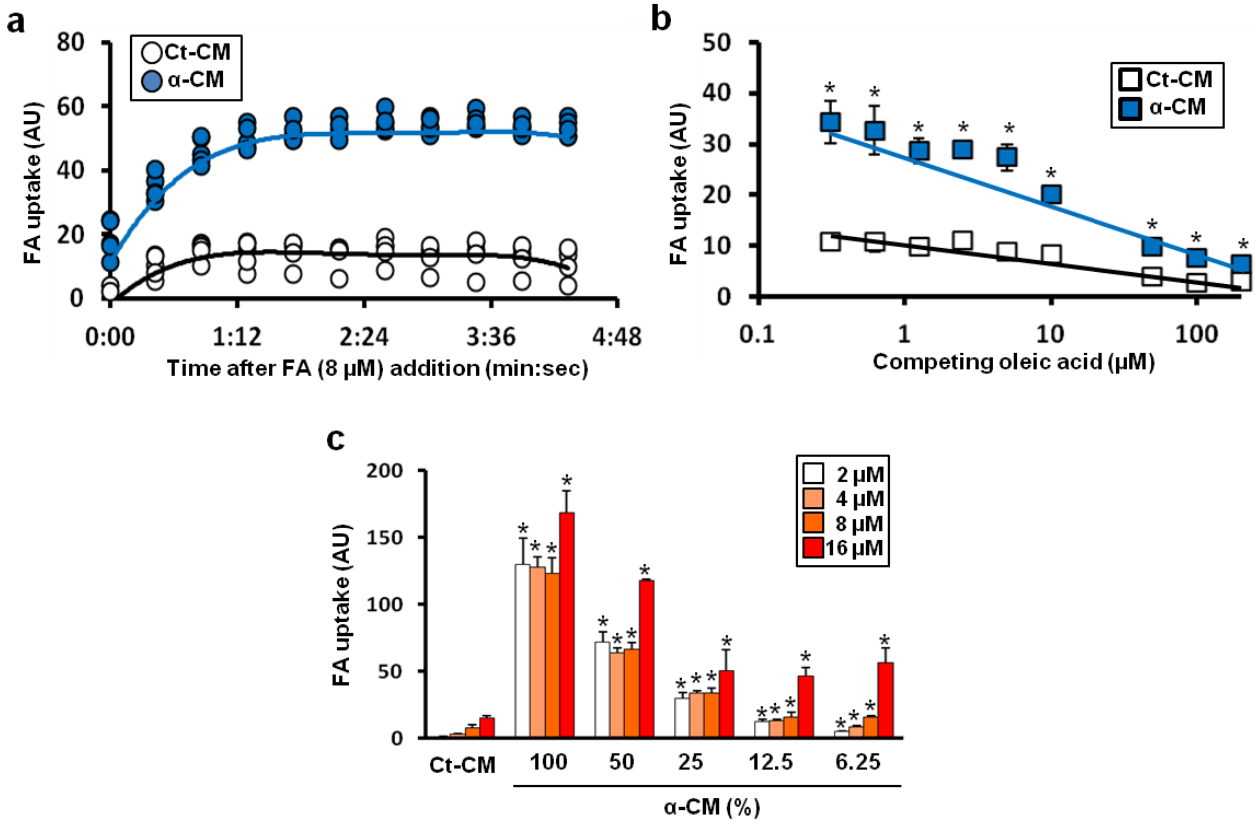


Figure 2.5: Characteristics of endothelial FA uptake by C2C12 conditioned media. a-b, FA uptake is rapid (**a**) and competed by unlabeled oleic acid after 5min of FA addition (**b**). **c**, α-CM sequentially diluted with Ct-CM partially retains its activity. *p<.05 vs. control. Data are mean ± s.d. of at least three biological replicates.

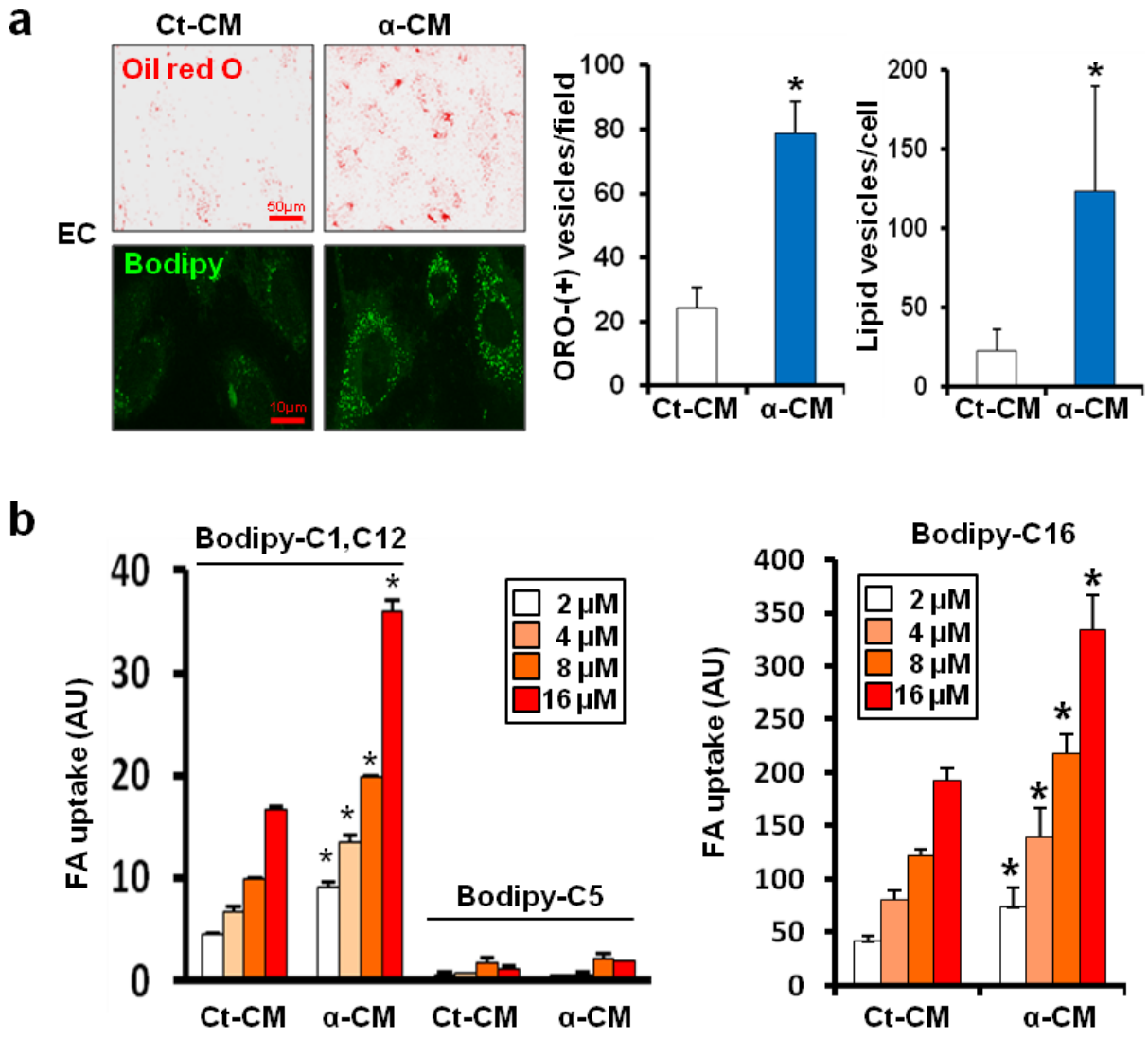


Figure 2.6: Endothelial cells take up long-chain fatty acids upon PGC-1α CM treatment. a, Prolonged exposure (24 hrs) to α-CM increases intracellular neutral lipids in ECs. Representative images (left) and quantification (right). **b**, ECs were treated with Bodipy-conjugated long-chain FA (Bodipy-C1, C12 or Bodipy-C16) or short-chain FA (Bodipy-C5) after exposure to CMs, and FA uptake was measured. *p<.05 vs. control. Data are mean ± s.d. of at least three biological replicates.

The induction of fatty acid uptake by endothelial cells occurred within 15-60 minutes of exposure to α-CM (Figure 2.7b) and was ATP-dependent (Figure 2.7c). To directly measure trans-endothelial transport of fatty acids, we used primary rat brain endothelial cells. These cells were chosen because they have a higher capacity to form tight junctions, as confirmed by a high

trans-endothelial electrical resistance (>1500Ω/cm2) (Figure 2.8a) and expression of tight junction proteins (Figure 2.8b) (Matter K and Balda MS. 2003). After incubation with CM,

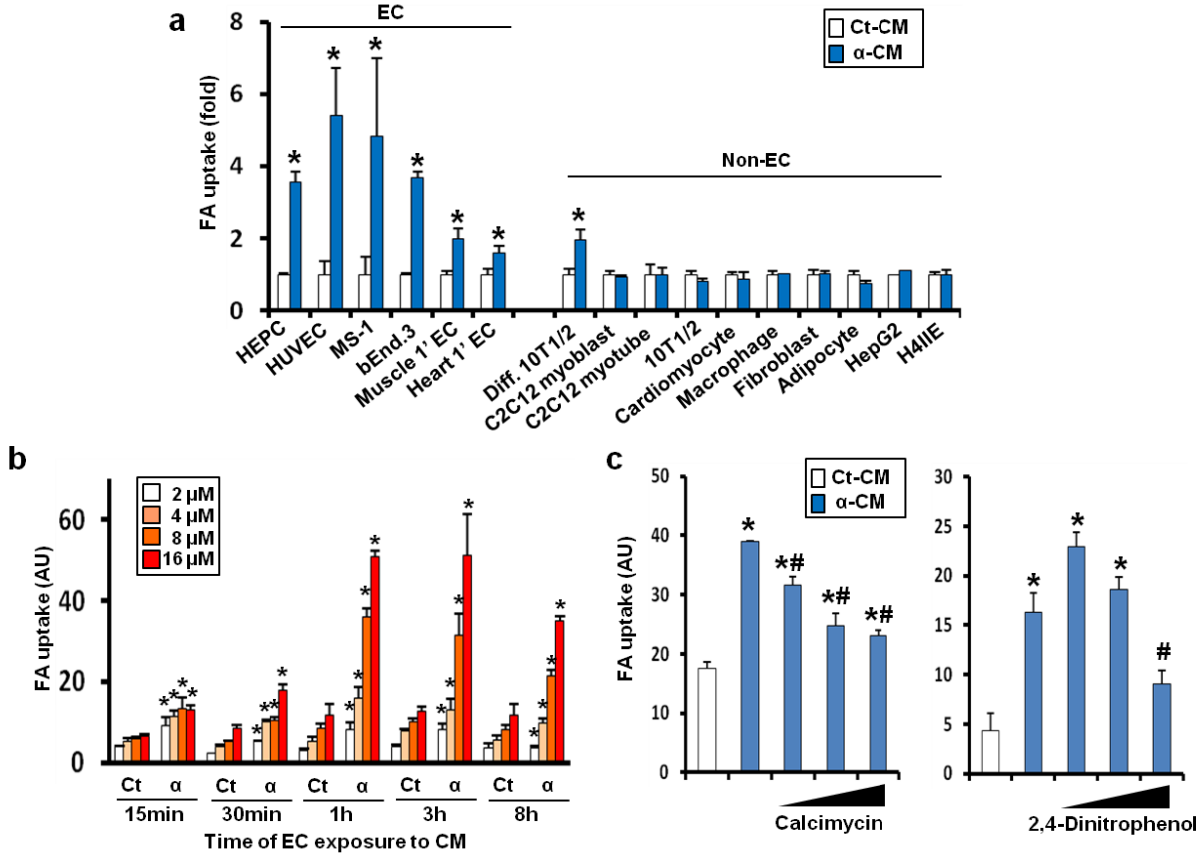


Figure 2.7: PGC-1α CM activity is cell type specific and ATP-dependent. a, FA (2 μM) uptake by each cell type was measured after exposure to CMs for 1 hr. **b**, Enhanced FA uptake occurs within 1 hr of exposure to α-CM. **c**, FA (2 μM) uptake by HUVECs was measured after pre-treatment with Calcimycin (left, 12.5-50 μM) or 2, 4-Dinitrophenol (right, 125-500 μM) for 30 min followed by treatment with CMs with or without drug for an additional hour. *p<.05 vs. control. #p<.05 vs. α-CM alone. Data are mean ± s.d. of at least three biological replicates.

endothelial cells on transwells were transferred to a plate containing myotubes, and then Bodipy-fatty acids was added to the upper compartment and its transport through an endothelial cell monolayer to the bottom compartment was measured (Figure 2.8c left). Endothelial cells pretreated with α-CM highly increased transport of fatty acids (Figure 2.8c middle). This was prevented by pretreatment of endothelial cells with sulfo-N-succinimidyl oleic acid (SSO), a

fatty acid analog that blocks cellular fatty acid uptake (Figure 2.8c middle) (Kuda O et al. 2013). Myotubes under the endothelial cells treated with α-CM also showed much higher intracellular Bodipy-fatty acids (Figure 2.8c right).

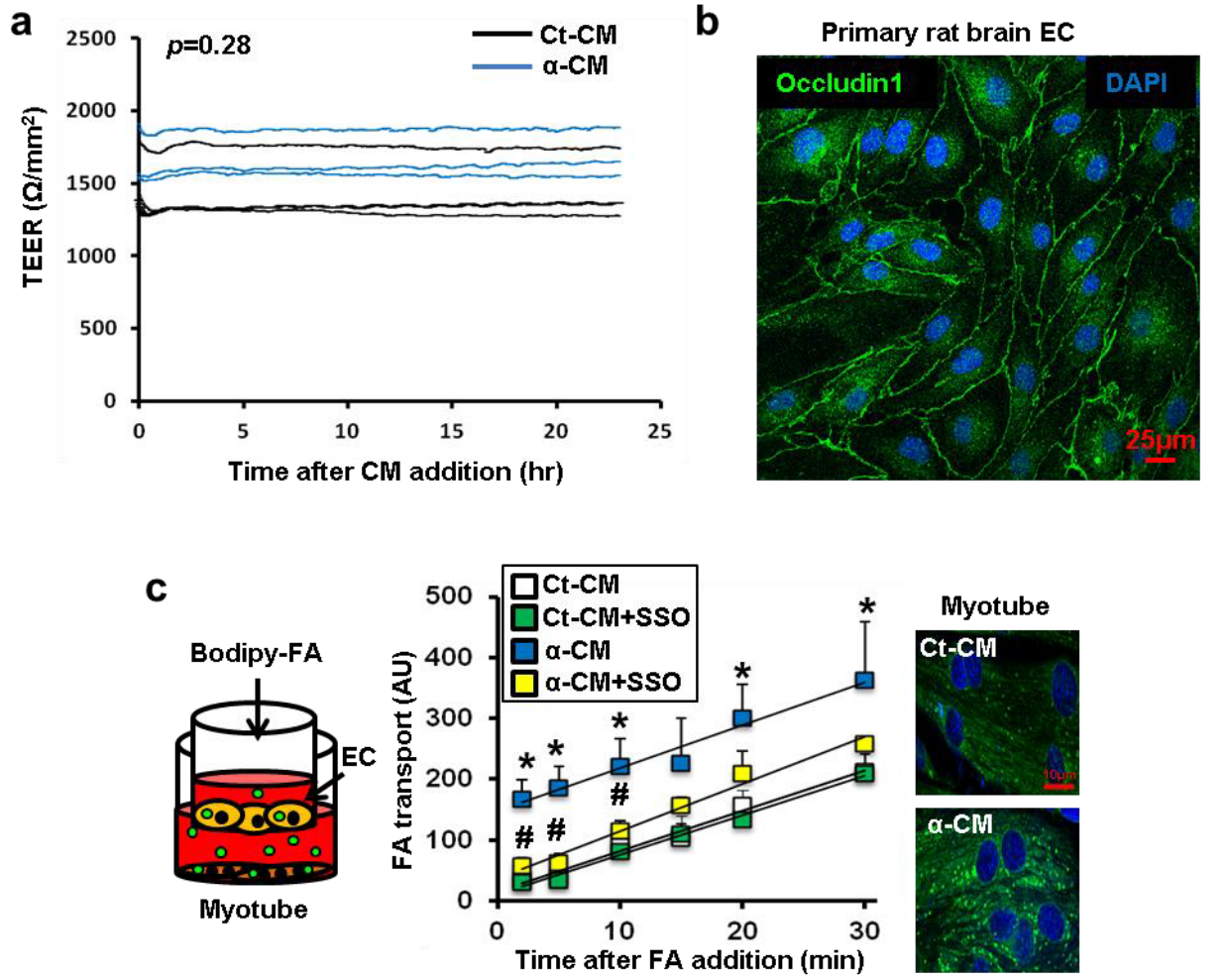


Figure 2.8: Primary brain ECs make a tight monolayer and transport FAs upon CM treatment. a, Measurement of trans-endothelial electrical resistance (TEER) of an EC monolayer after exposure to CMs for 24 hr. **b**, Confluent primary rat brain ECs were immunostained with anti-Occludin1 antibody (green, tight junctions) and DAPI (blue, nuclei). **c**, α-CM stimulates FA transport across a tight EC monolayer. *p<.05 vs. control. #p<.05 vs. α-CM. ANOVA was used for **c**. Data are mean ± s.d. of at least three biological replicates.

These data indicate that PGC-1α CM increases not only uptake but also transport of fatty acids by endothelial cells. Conversely, an endothelial monolayer treated with CM from myotubes lacking both PGC-1α and PGC-1β showed reduced fatty acid transport (Figure 2.9a). However,

an endothelial monolayer treated with CM from myotubes lacking only PGC-1α did not show any significant difference (Figure 2.9b). This observation is likely explained by our findings that 1) the expression level of PGC-1α in C2C12 myotubes is already quite low compared to muscle (Figure 2.9c), and 2) there is significant redundancy between PGC-1α and PGC-1β (see below). Together, these data demonstrate the existence of paracrine factor(s), induced in myotubes by PGC-1α, which stimulate(s) endothelial fatty acid uptake and transport.

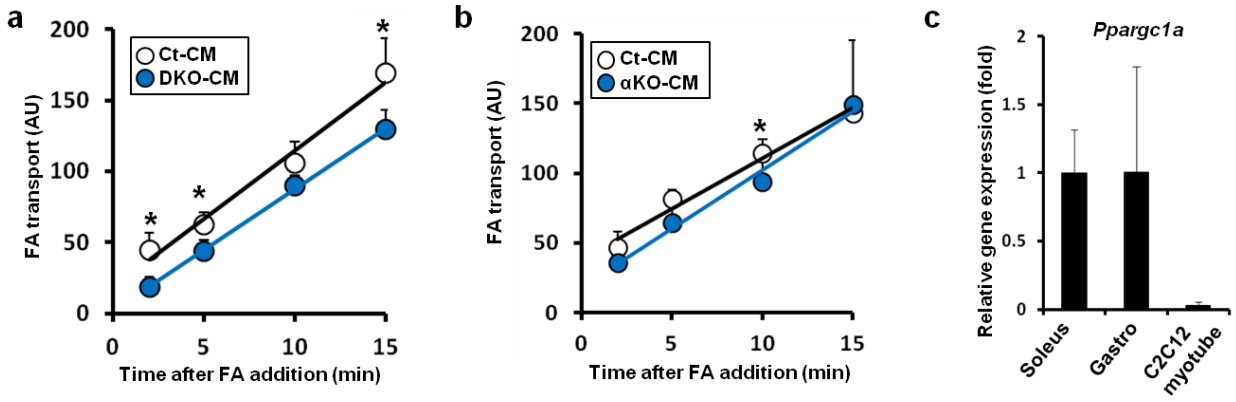


Figure 2.9: Knockout of both PGC-1s is required to reduce the FA uptake-inducing activity in myotube CM. a-b, CM from myotubes lacking both PGC-1α and PGC-1β (**a**, DKO-CM) decreased FA (8 μM) transport by ECs, while CM from myotubes lacking PGC-1α alone (**b**, αKO-CM) did not. **c**, qPCR analysis of PGC-1α expression in the soleus or gastrocnemius skeletal muscle and C2C12 myotubes. Note that C2C12 myotubes express much less PGC-1α than skeletal muscle does. *p<.05 vs. DKO-CM (**a**) or αKO-CM (**b**). Data are mean ± s.d. of at least three biological replicates.

A recent report has suggested that VEGF-B may regulate endothelial fatty acid uptake (Hagberg CE et al. 2010). Interestingly, we found that PGC-1α induces the expression of VEGF-B, both in cell culture and in transgenic animals (Figure 2.10a), suggesting that the paracrine factor can be VEGF-B. In fact, conditioned media from VEGF-B-overexpressing 293T cells increased fatty acid uptake (Figure 2.10b). To test if the factor in α-CM is VEGF-B, we first validated reagents that are known to block VEGF-B signaling. Endothelial cells treated with

recombinant VEGF-B or VEGF-A showed rapid induction of ERK-1/2 phosphorylation (Figure 2.10c). However, fatty acid uptake and ERK-1/2 phosphorylation were blocked by pre-incubation of VEGF-A or -B proteins with neutralizing soluble receptor (sFlt1) or pre-treatment of ECs with VEGF receptor inhibitor (SU11248) (Figure 2.10b and c). Surprisingly, the same treatment had no impact on the ability of α-CM to increase fatty acid uptake by endothelial cells

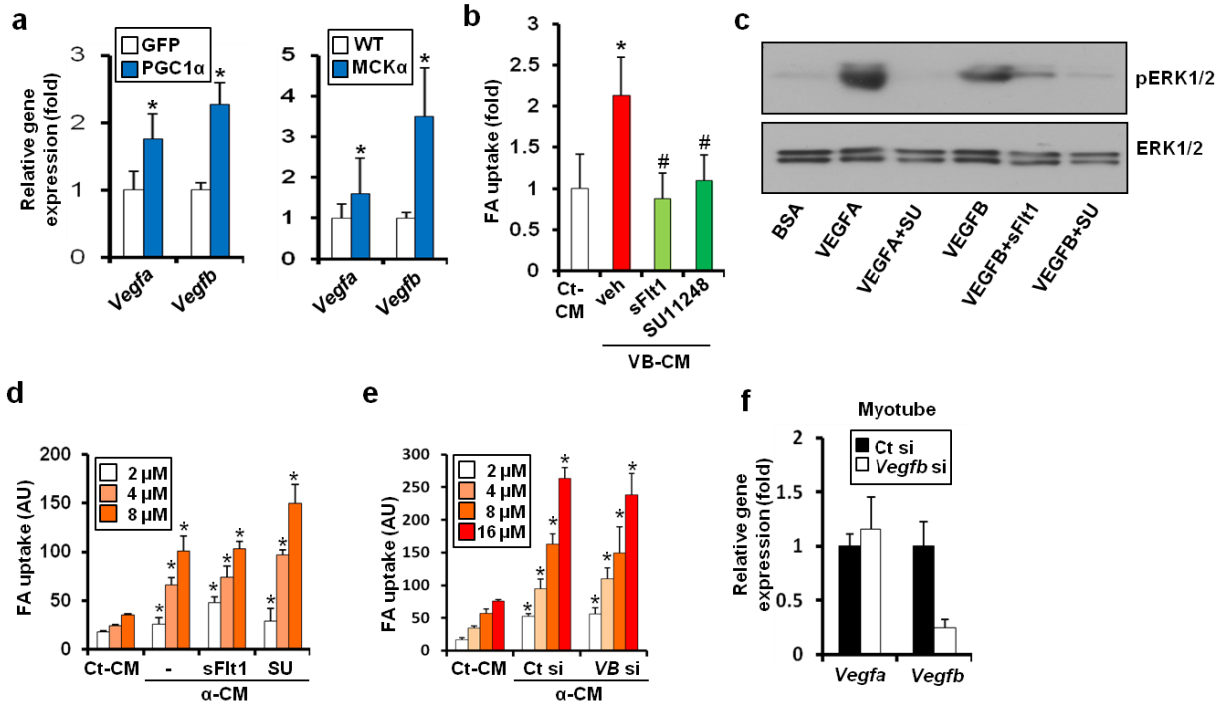


Figure 2.10: Blockage of VEGF-B does not suppress FA uptake induced by α-CM. a, qPCR analysis of C2C12 myotubes (left) expressing GFP or PGC-1α via adenovirus, or skeletal muscle (right) from wild type or MCKα mice. **b**, FA (2 μM) uptake by ECs was measured after exposure to control (Ct-CM) or VEGF-B CM (VB-CM) for 24 hr with vehicle (veh) or inhibitors. **c**, Western blot analysis of ECs treated with recombinant VEGF-A or VEGF-B (100 ng/mL) for 10 min with or without inhibitors (sFlt1 or SU11248). **d-e**, Blockade of VEGF-B signaling with sFlt1 or SU11248 (**d**), or knockdown of Vegfb in myotubes (**e**) failed to block the paracrine activity. **f**, qPCR analysis of C2C12 myotubes after transfection with control or Vegfb siRNA for 48 hr. *p<.05 vs. control. #p<.05 vs. α-CM. ANOVA was used for **b**. Data are mean ± s.d. of at least three biological replicates.

(Figure 2.10d). Also, α-CM from muscle cells transfected with VEGF-B siRNA still highly induced fatty acid uptake (Figure 2.10e and f). Finally, genetic knockdown or deletion of either

or both VEGFR1 (FLT1) and VEGFR2 (FLK1), known VEGF-B receptors, also failed to inhibit α-CM activity (Figure 2.11a-d). It thus appears that the paracrine factor in α-CM is not VEGFB.

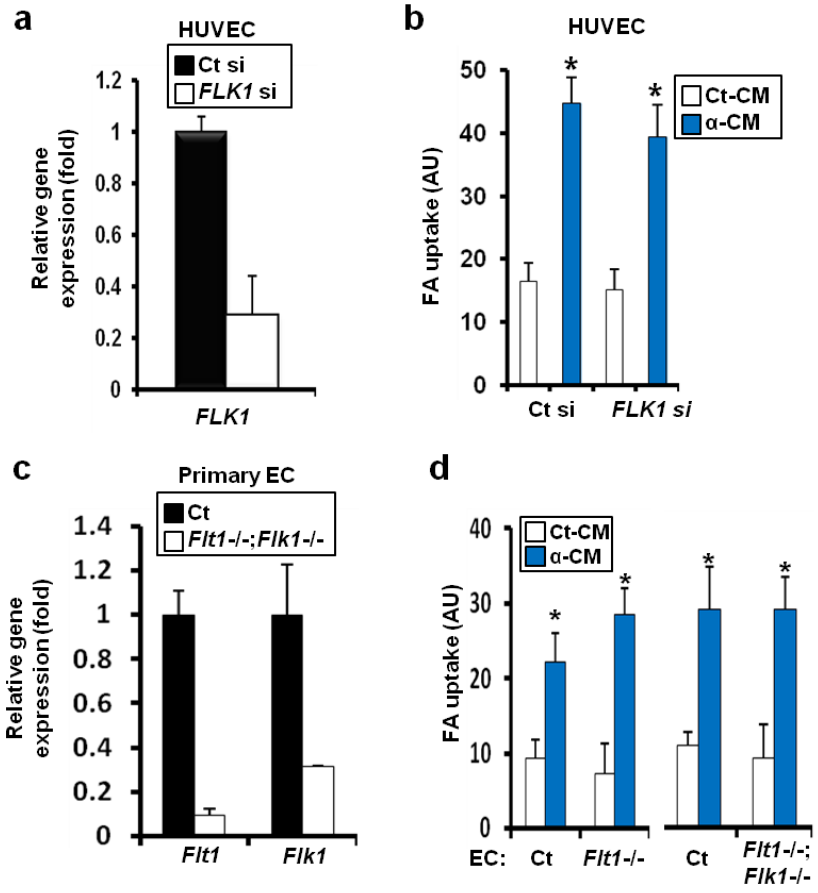


Figure 2.11: Deletion of VEGF-B receptors in ECs does not block FA uptake induced by α-CM. a-b, qPCR analysis (**a**) and FA (2 μM) uptake assay (**b**) of HUVECs after transfection with control or FLK1 siRNA for 48 hr. **c-d**, qPCR analysis (**c**) and FA uptake assay (**d**) of primary ECs isolated from Flt1 flox/flox or Flt1 flox/flox; Flk1 flox/flox mice after infection with adenovirus expressing Cre recombinase for 48 hr. *p<.05 vs. control. Data are mean ± s.d. of at least three biological replicates.

If not VEGF-B, then what is the paracrine factor? To investigate the nature of the factor, α-CM was heated to 80°C for 1 hr to heat-inactivate proteins prior to placement on ECs. Intriguingly, this did not kill the activity of the factor (Figure 2.12a). Moreover, the factor was not inactivated by trypsin treatment and it passed through a 3kDa membrane filter (Figure 2.12b and c). Thus,

the factor is a small molecule, potentially a heat-stable short peptide, metabolite or lipid. To

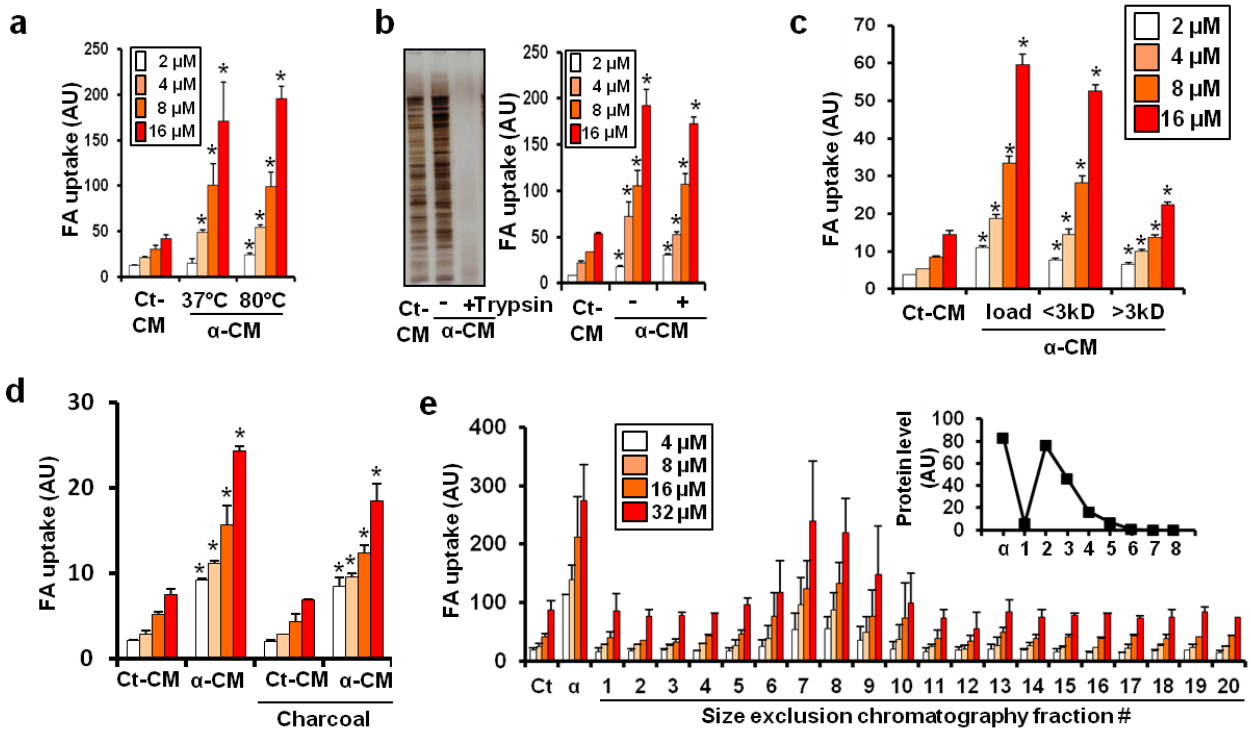


Figure 2.12: The paracrine factor is a small molecule. a-c, The paracrine factor is resistant to heat (**a**) and trypsin (**b**), and is smaller than 3kDa (**c**). **d**, FA (2-16 μM) uptake by ECs was measured after exposure to CMs pre-incubated with charcoal. **e**, The α-CM activity was fractionated by size-exclusion chromatography. *p<.05 vs. control. Data are mean ± s.d. of at least three biological replicates.

directly test if the factor is a lipid, we used charcoal, which absorbs lipids and strongly hydrophobic molecules. However, charcoal treatment also failed to inactivate the factor (Figure 2.12d). Consistent with the results using different molecular sizes of membrane filters (Figure 2.12c), biochemical fractionation of α-CM with size exclusion chromatography showed the fatty acid uptake-inducing activity in fractions containing small molecules, and few proteins (Figure 2.12e). We next performed metabolomics analysis of Ct-CM versus α-CM to identify the factor. There are more than 20 metabolites that are highly enriched (>5 fold) in α-CM (Figure

2.13). However, treatment of ECs with each of these candidate metabolites was not sufficient to

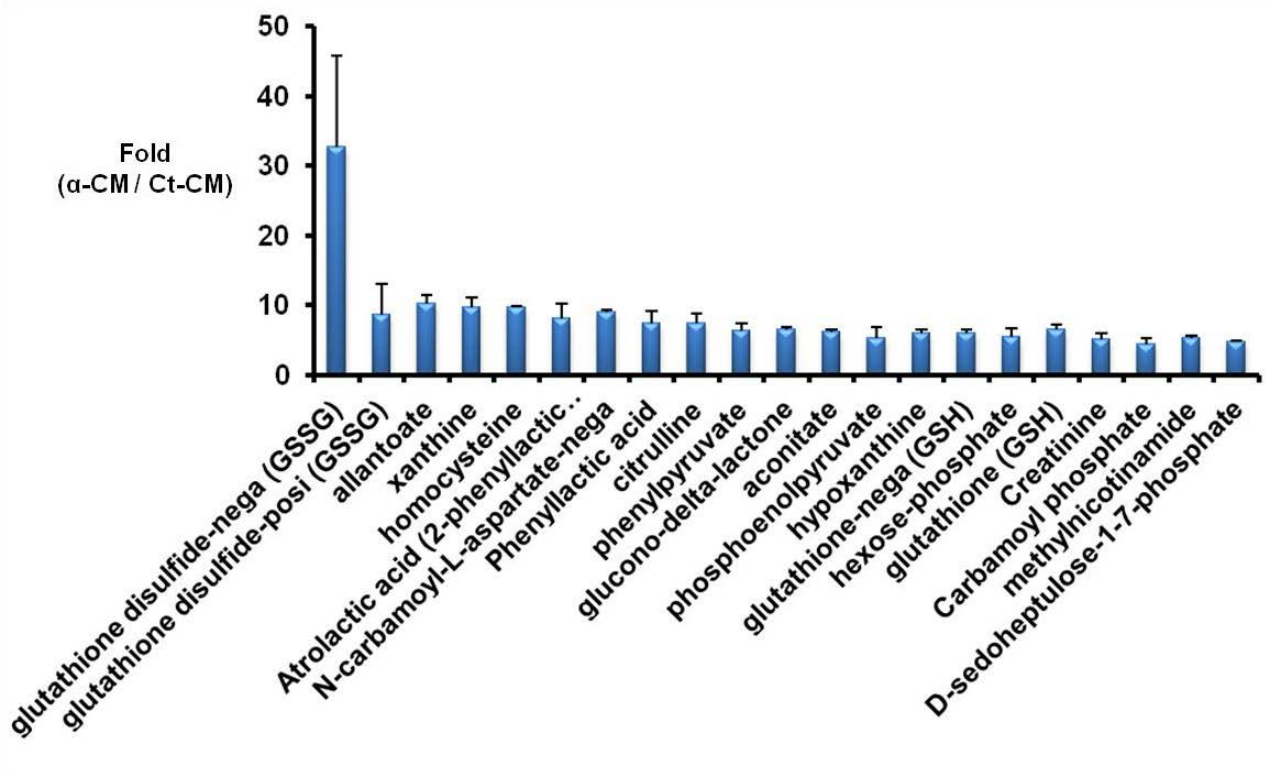


Figure 2.13: Several metabolites are higher in α-CM compared to Ct-CM. Targeted metabolomics analysis with CMs revealed that 21 metabolites are at least 5 fold higher in α-CM compared to control CM (Ct-CM).

induce fatty acid uptake (data not shown). To investigate the pathways that may regulate the synthesis and secretion of the paracrine factor, and to identify tools with which to purify the factor, we treated PGC-1α-expressing C2C12 myotubes with an array of compounds, and assayed the CM for fatty acid uptake-inducing activity in HUVECs. Interestingly, a number of inhibitors targeting components of the PI3K pathway (including PI3K, Akt, and mTORC2) suppressed the paracrine activity, while insulin itself slightly induced the activity (Figures 2.14

and 2.15a). 2-deoxy-glucose (2DG), an inhibitor of glycolysis, and CHC (alpha-cyano-4-

Compound	Target	α-CM activity
U0126	MEK1/2 ↓	-
SB203580	P38 ↓	-
U73122	PLCγ ↓	-
Akt VIII	Akt ↓	↓↓
LY294002	PI3K ↓	↓↓
Rapamycin	mTORC1 ↓	-
Torin	mTORC1,2 ↓	↓↓
Insulin	InR ↑	↑
PD98059	ERK1,2 ↓	-
Compound C	AMPK ↓	↓
AICAR	AMPK ↑	-
SP600125	JNK↓	-

Compound	Target	α-CM activity
Phenylephrine	α1 AR ↑	-
Ritodrine	β2 AR ↑	-
Isoproterenol	β1 AR ↑	-
CL316243	β3 AR ↑	-
XCT790	ERRα ↓	↓
GW0742	PPARδ ↑	-
Rosiglitazone	PPARγ ↑	↑
Dexamethasone	Glucocorticoid ↑	-
2DG	Glycolysis ↓	↓↓
CHC	MCT ↓	↓↓
FCCP	OXPHOS ↓	-
Rotenone	OXPHOS ↓	-

Figure 2.14: List of compounds tested to identify signaling pathways in myotubes that affect the PGC-1α CM activity. C2C12 myotubes expressing PGC-1α via retrovirus were treated with the indicated compound during CM generation for 48 hr, and the activity of CM on enhancing FA (2 μM) uptake by ECs was measured. ECs were also incubated with media containing the indicated compound for 1 hr to test if the compound directly affects FA uptake by ECs. The effects of compound are indicated with arrows. Note that inhibitors of PI3K-mTORC2 pathway strongly suppress the α-CM activity. InR, insulin receptor; AR, adrenergic receptor; MCT, monocarboxylate transporter; OXPHOS, oxidative phosphorylation.

hydroxycinnamate), a monocarboxylate transporter inhibitor, also blocked the paracrine activity (Figure 2.15b). We have tested if insulin and the inhibitors affect FA uptake by ECs directly. None of treatment inhibited FA uptake by ECs (Figure 2.15c), suggesting that these treatment acts on the level of muscle cells for 3-HIB production / secretion. Based on the inhibitor screen results, we assumed that glycolysis can be an important driver for the generation of the paracrine factor. To test this idea, we added an excess amount of pyruvate in the media to overcome inhibition of glycolysis by the inhibitors. Intriguingly, addition of pyruvate indeed partially restored the fatty acid uptake activity of α-CM inhibited by Akt inhibitor (Akt VIII) and 2DG, but not by CHC (Figure 2.15d). The potential molecular mechanisms of the pyruvate addition effect will be discussed below.

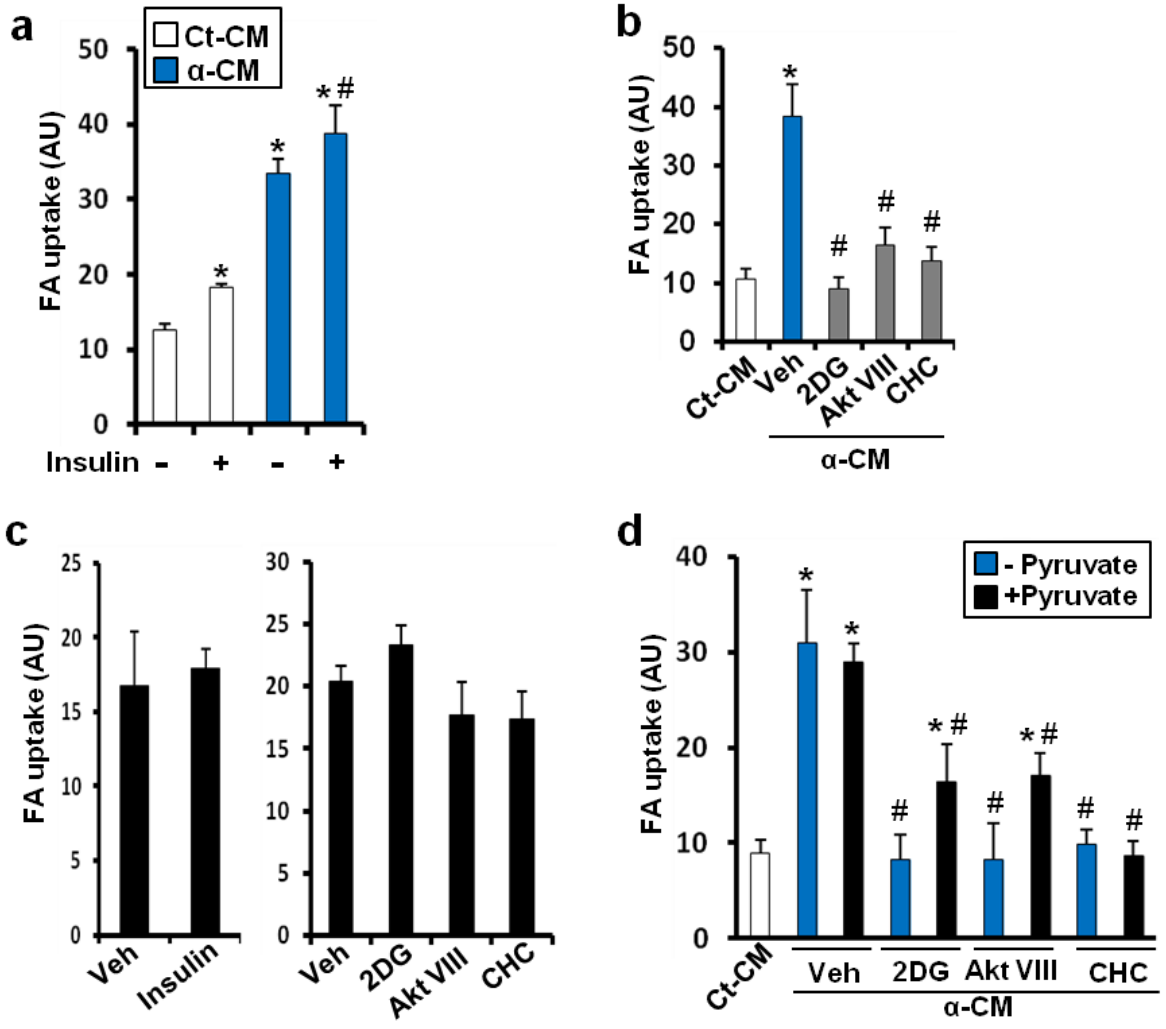


Figure 2.15: Insulin and three inhibitors affect the α-CM activity but not FA uptake by ECs directly. a-b, FA (2 μM) uptake by ECs was measured after exposure to α-CMs generated from C2C12 myotubes treated with insulin (**a**, 10 nM) or the indicated inhibitor (**b**). **c**, FA (2 μM) uptake by ECs was measured after treatment with insulin (left) or the indicated inhibitor (right) for 1 hr. **d**, FA (2 μM) uptake by ECs was measured after exposure to α-CMs generated from C2C12 myotubes treated with the indicated inhibitors with or without pyruvate (50 mM). *p<.05 vs. control. #p<.05 vs. α-CM. Data are mean ± s.d. of at least three biological replicates.

The identification of these inhibitors allowed us to use CM from PGC-1α-expressing myotubes that were pre-treated with the inhibitors as discerning negative controls for further chromatography and mass-spectrometry. The CMs were treated with charcoal to remove hydrophobic compounds, and first fractionated by open column silica-gel chromatography

(Figure 2.16). The activity was found in later fractions after elution with n-BuOH:MeOH=1:1

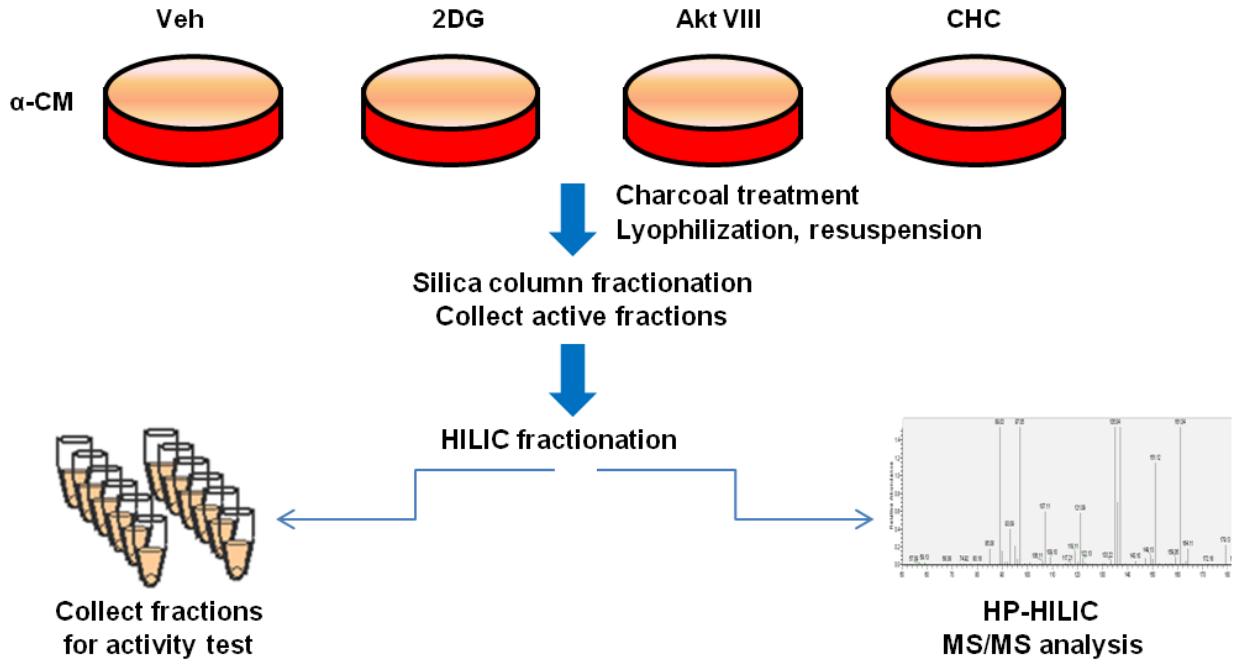


Figure 2.16: Schematic of unbiased purification of the paracrine factor. α-CMs treated with vehicle (veh) or the indicated inhibitor were incubated with charcoal, lyophilized, and fractionated with an open silica column. Active fractions were further separated by HILIC for activity test and HP-HILIC-MS/MS analysis.

solution, suggesting that the paracrine factor is pretty hydrophilic (Figure 2.17). The active fractions were collected and further fractionated by high-pressure hydrophilic interaction liquid chromatography (HP-HILIC) (Figure 2.18a). Evaluations by mass-spectrometry of an active fraction (#27) from these sequential purifications revealed a peak with molecular weight of 104.1 ([M-H]=103.1), which was not present in parallel, inactive fractions from CM of cells pre-treated with 2DG, Akt inhibitor (Akt VIII), or CHC (Figure 2.18b and c). Among multiple candidates based on the retention time in HILIC column, four isobaric hydroxybutyrates potentially

corresponded to this molecular weight (Figure 2.19). Among them, bioactivity was

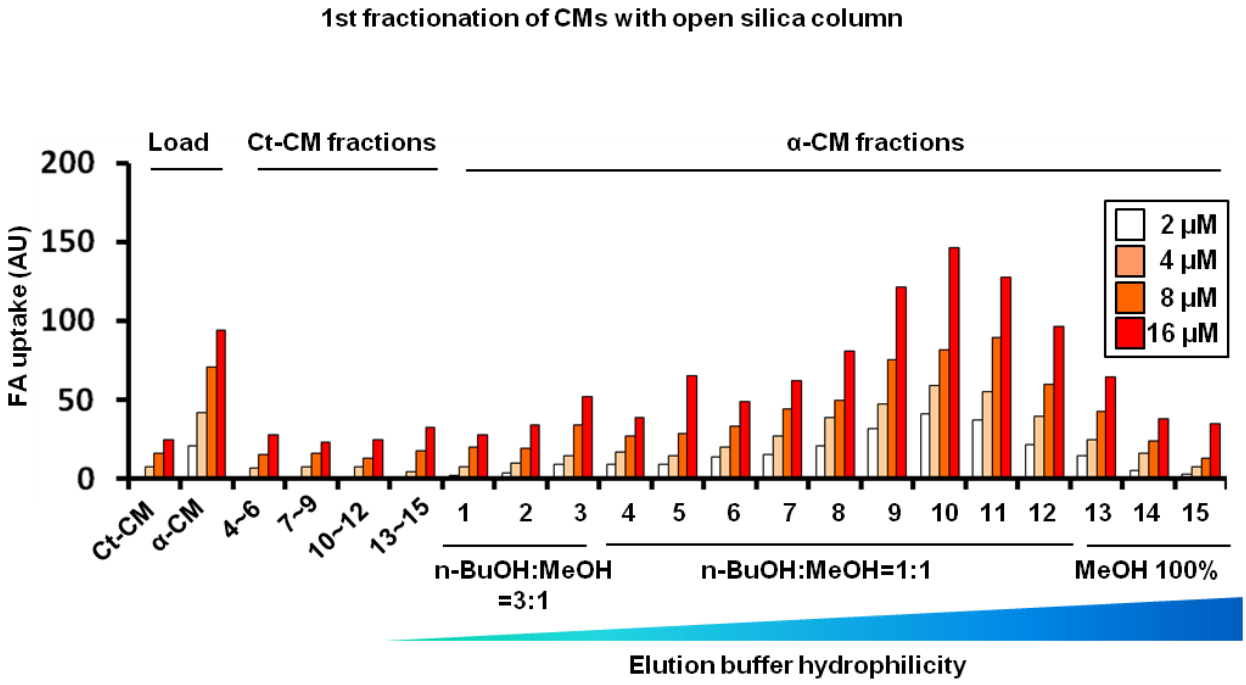


Figure 2.17: Fractionation of CMs and activity test. FA (2-16 μM) uptake by ECs was measured after exposure to Ct-CM or α-CM fractions from an open silica column. Detailed method is described in the Materials and Methods session.

correlated with a molecule with MS/MS fingerprint of 103->73, which is consistent with 3-hydroxyisobutyrate (3-HIB) (Figure 2.20a and b). Further matching of chromatographic properties and MS/MS spectra to synthetic standards unambiguously confirmed this conclusion. Synthetic 3-HIB alone was sufficient to increase FA uptake by HUVECs (Figure 2.20c), confirming its identity as the active component in the fractions.

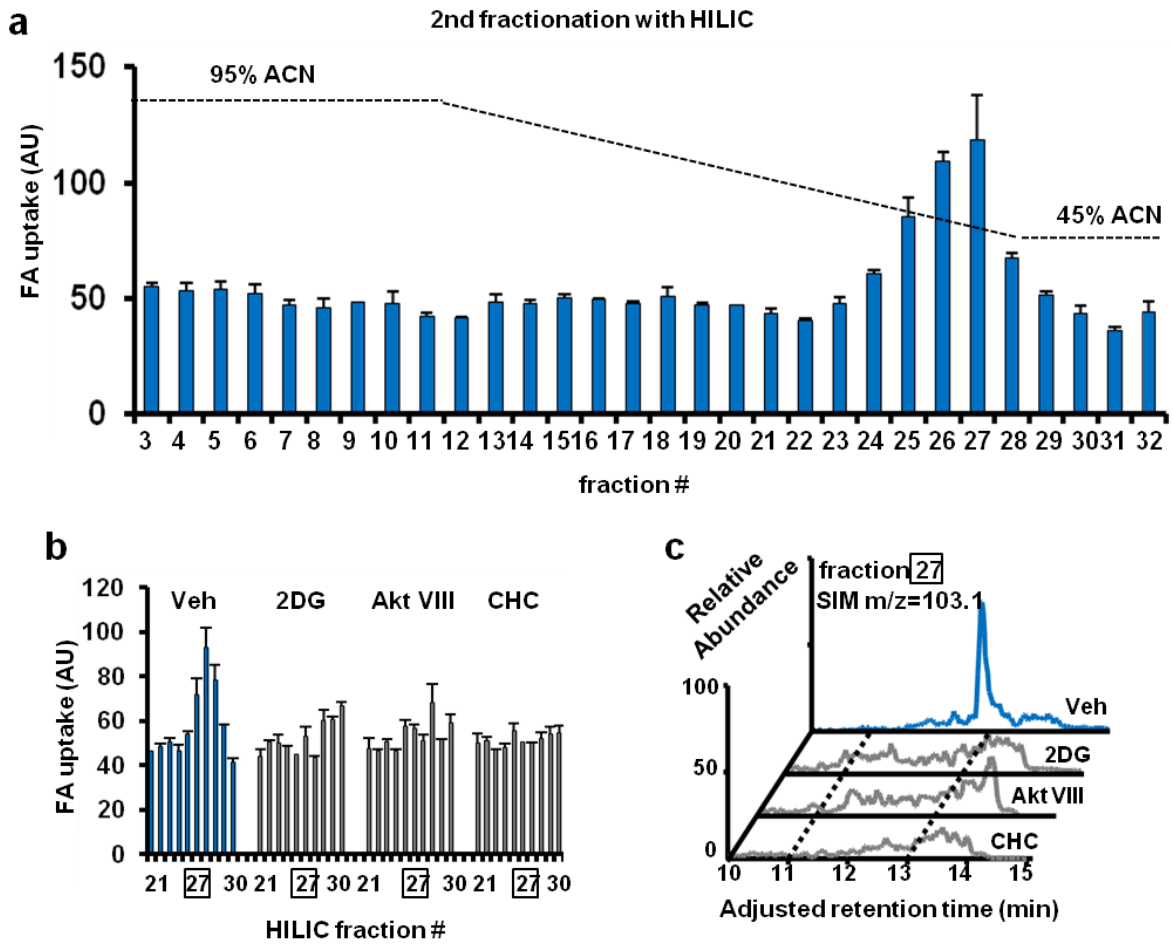


Figure 2.18: Identification of a m/z peak that is unique to match with the activity. a, FA (16 μM) uptake by ECs was measured after exposure to α-CM fractions from an HP-HILIC column. **b**, Fraction 27 after silica column and HILIC fractionation contains the activity, which is not present in CMs from cells treated with the inhibitors. Veh, vehicle. **c**, Identification by mass spectrometry of a molecule with m/z=103.1 that is specific to fraction 27.

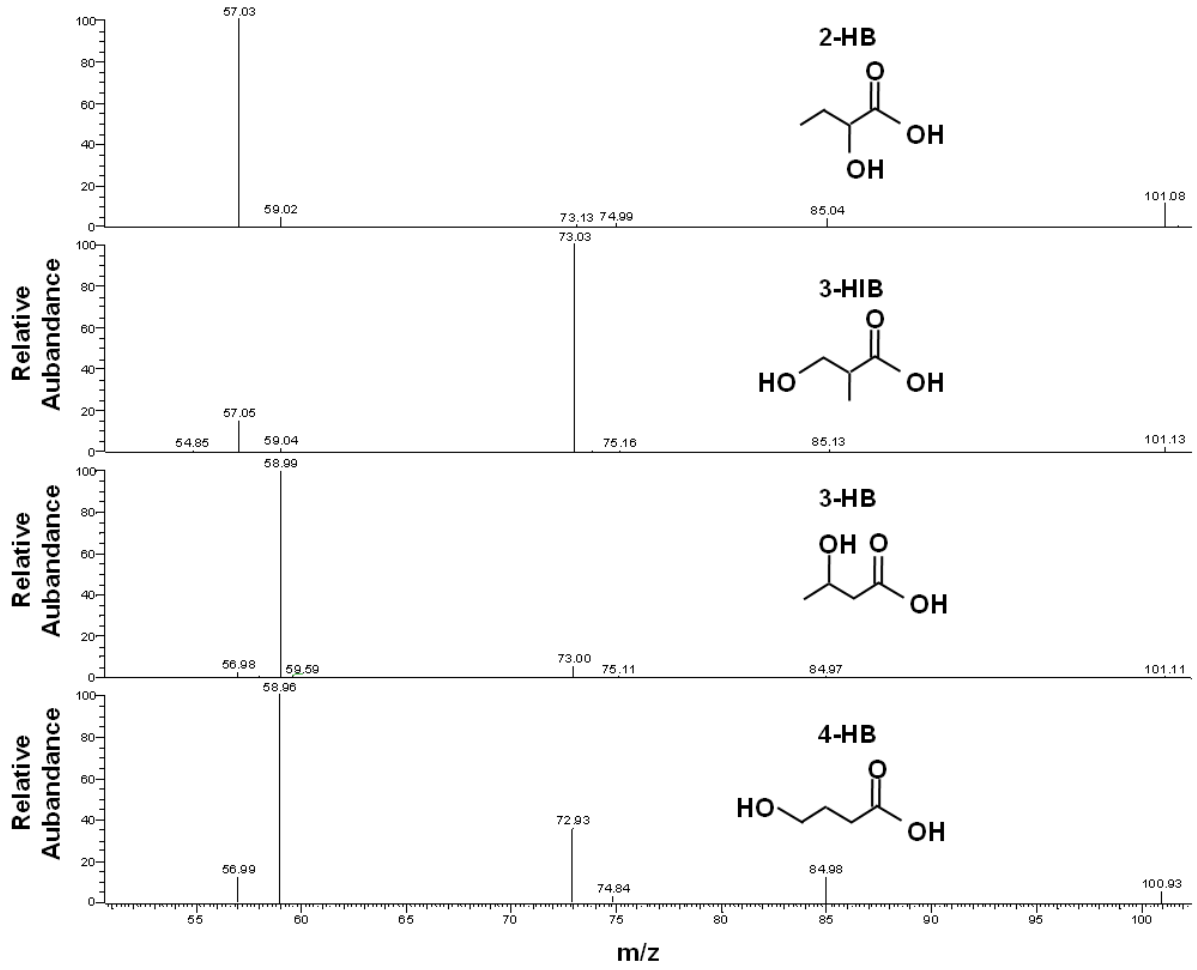


Figure 2.19: MS/MS spectra of four isobaric hydroxybutyrate candidates. Synthetic standards of four isobaric hydroxybutyrates were used to match MS/MS fingerprints.

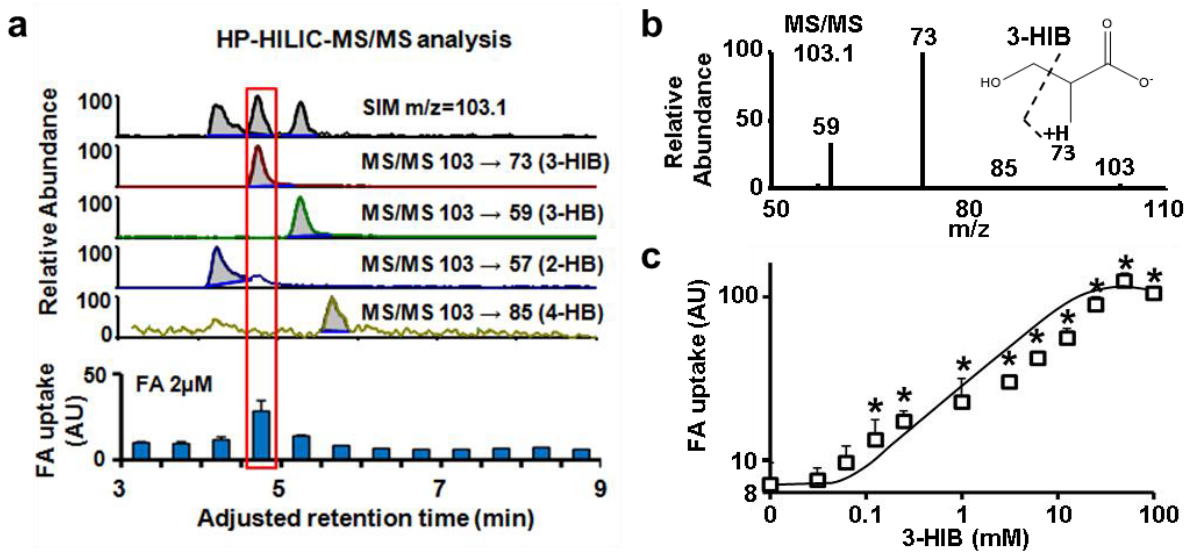


Figure 2.20: Identification of 3-hydroxyisobutyrate (3-HIB) as the paracrine factor in α-CM that stimulates endothelial FA uptake. a-b, Selective ion monitoring (SIM) of HP-HILIC-MS/MS identified the activity overlaid with MS/MS signature of 103->73 (**a**), of which MS/MS spectra matched with 3-HIB (**b**). **c**, 3-HIB alone is sufficient to induce FA uptake. *p<.05 vs. control. Data are mean ± s.d. of at least three biological replicates.

Treatment of 3-HIB also increased fatty acid transport through an endothelial cell monolayer (Figure 2.21a). In contrast, there was no time-dependent increase of Dextran transport after 3-HIB treatment (Figure 2.21b), indicating that the integrity of an endothelial cell monolayer is tight enough to prevent macromolecular transport and that 3-HIB does not induce

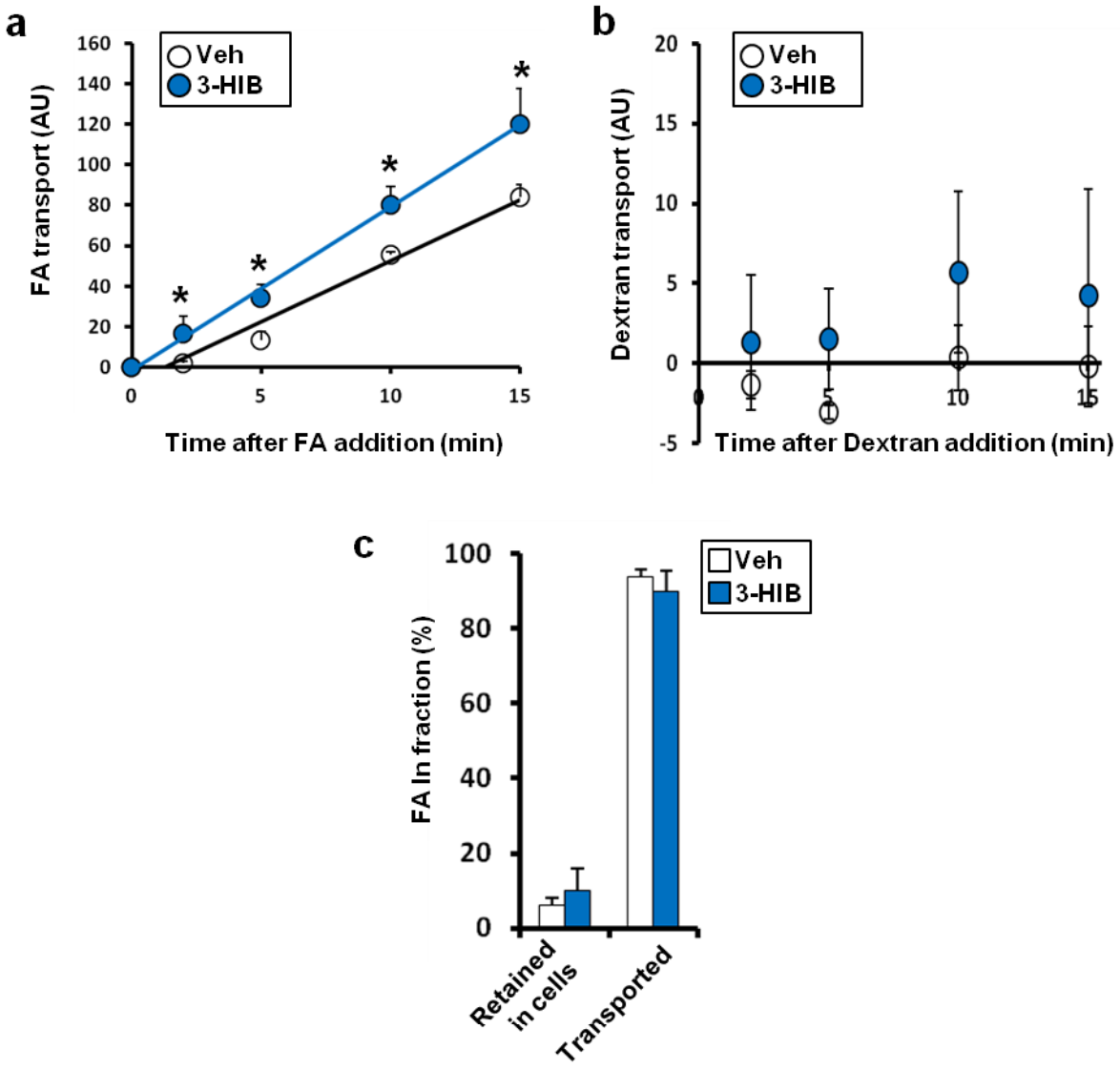


Figure 2.21: 3-HIB increases endothelial FA transport. a-b, FA (**a**, 16 µM) or Dextran Texas-Red (**b**, 50 µg/mL) transport by an EC monolayer was measured after exposure to vehicle (Veh) or 3-HIB for 1 hr. **c**, The amount of FAs retained in or transported by an EC monolayer was measured. *p<.05 vs. control. Data are mean ± s.d. of at least three biological replicates.

endothelial leakiness (Neuhaus et al. 2006). To compare the amount of fatty acids taken up by endothelial cells versus the fraction that is trans-cellularly transported, we have quantified fatty

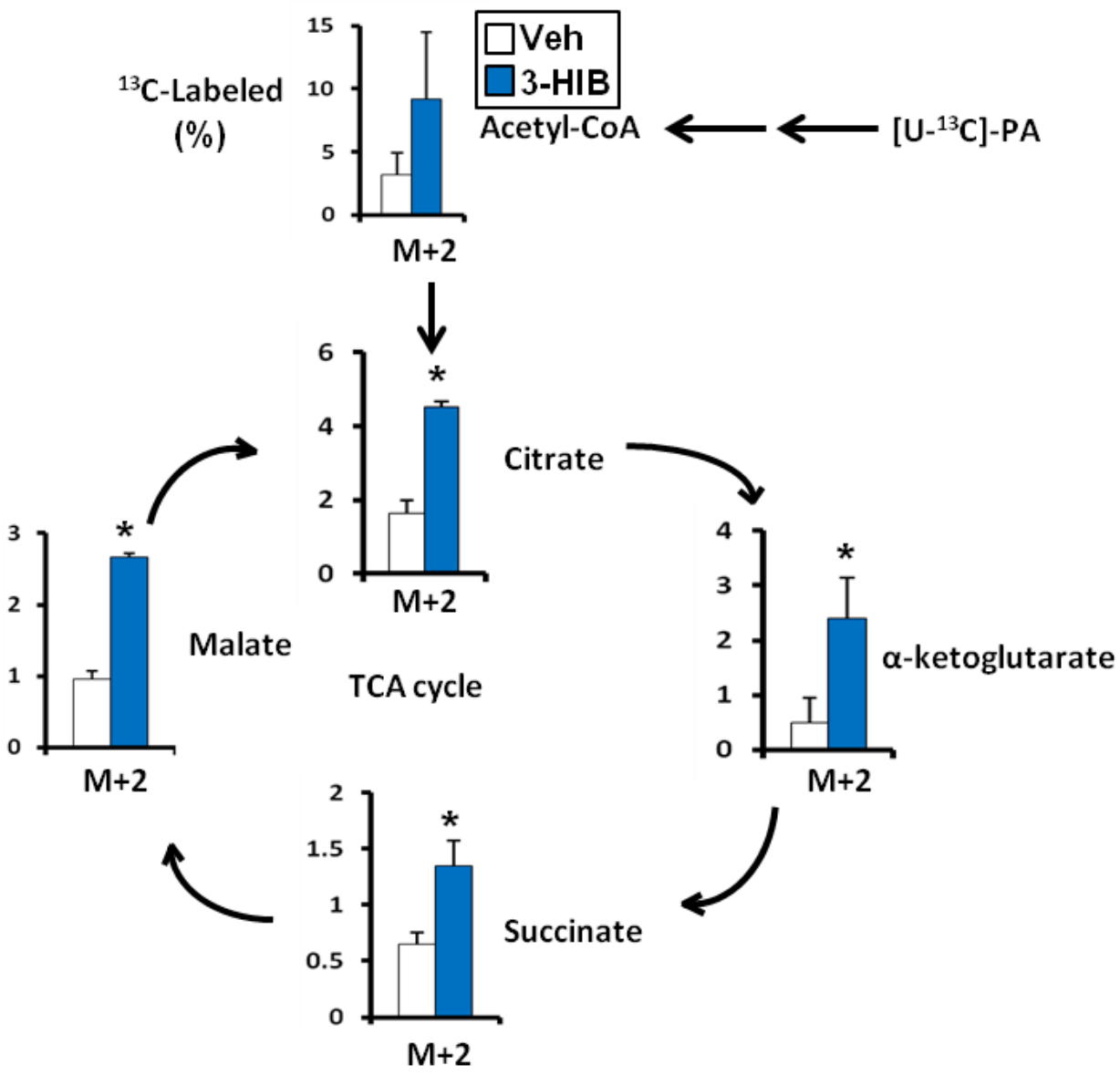


Figure 2.22: C2C12 myotubes metabolize FAs transported by 3-HIB-treated ECs. 13C-metabolic flux analysis of Acetyl-CoA and TCA intermediates in C2C12 myotubes after exposure to the media containing [U-^{13}C]-palmitate (PA) transported by an EC monolayer after treatment with vehicle (Veh) or 3-HIB for 1 hr. M+2 indicates that two carbons are 13C-labeled. *p<.05 vs. control. Data are mean ± s.d. of at least three biological replicates.

acids inside cells and those transported through an endothelial cell monolayer using the transport assay. Less than 10% of fatty acids were retained in cell lysates, while 90% of fatty acids were detected in the bottom of transwells (Figure 2.21c). To measure endothelial fatty acid transport induced by 3-HIB with mass-spectrometry, we performed the trans-endothelial fatty acid transport assay with [U-^{13}C]-palmitate instead of Bodipy-fatty acids, and measured 13C incorporation into the TCA cycle of myotubes exposed to media on the other side of the endothelial monolayer. Briefly, endothelial cells were grown on transwells until they formed a tight monolayer. [U-^{13}C]-palmitate was then added on top of the transwells with or without pre-treatment of endothelial cells with 3-HIB. After 30min, the media from the bottom of the transwells were incubated with C2C12 myotubes for an hour. Metabolites were then isolated from the myotubes and quantified. As shown in new Figure 2.22, the myotubes incubated with media from 3-HIB treated ECs showed a marked induction of 13C-[M+2] labeling of Acetyl-CoA and TCA intermediates. These results indicate that 3-HIB treatment significantly increased FA transport across endothelial cells, which results in increased FA oxidation in muscle cells.

3-HIB is known to be an intermediate of valine catabolism, derived from 3-hydroxyisobutyryl-CoA (HIBC) by HIBC hydrolase (HIBCH), and in turn catabolized by 3-HIB dehydrogenase (HIBADH) to eventually form propionyl-CoA, which can enter the TCA cycle (Figure 2.23a). To test if 3-HIB is indeed derived from valine, C2C12 myotubes were grown in the media containing 13C-labeled valine and mass-spectrometry analysis was performed to detect 13C-labeled 3-HIB. As shown in Figure 2.23b and c, 13C-labeled 3-HIB was detected in α-CM generated with the media containing 13C-valine, while 12C-3-HIB was much more abundant in α-CM generated with the media containing 12C-valine. The trace amount of 13C-

labeled 3-HIB is likely derived from naturally occurring stable isotope of carbon (13C). Some species of bacterial cells can interconvert BCAAs, while mammalian cells are unable to do this and thus entirely depend on intake of all three BCAAs from diet. To test this notion, myotubes were grown in media containing 13C-valine or 13C-leucine with or without isoleucine (in place of using 13C-isoleucine, which is very expensive). As shown in Figure 2.23d, only myotubes

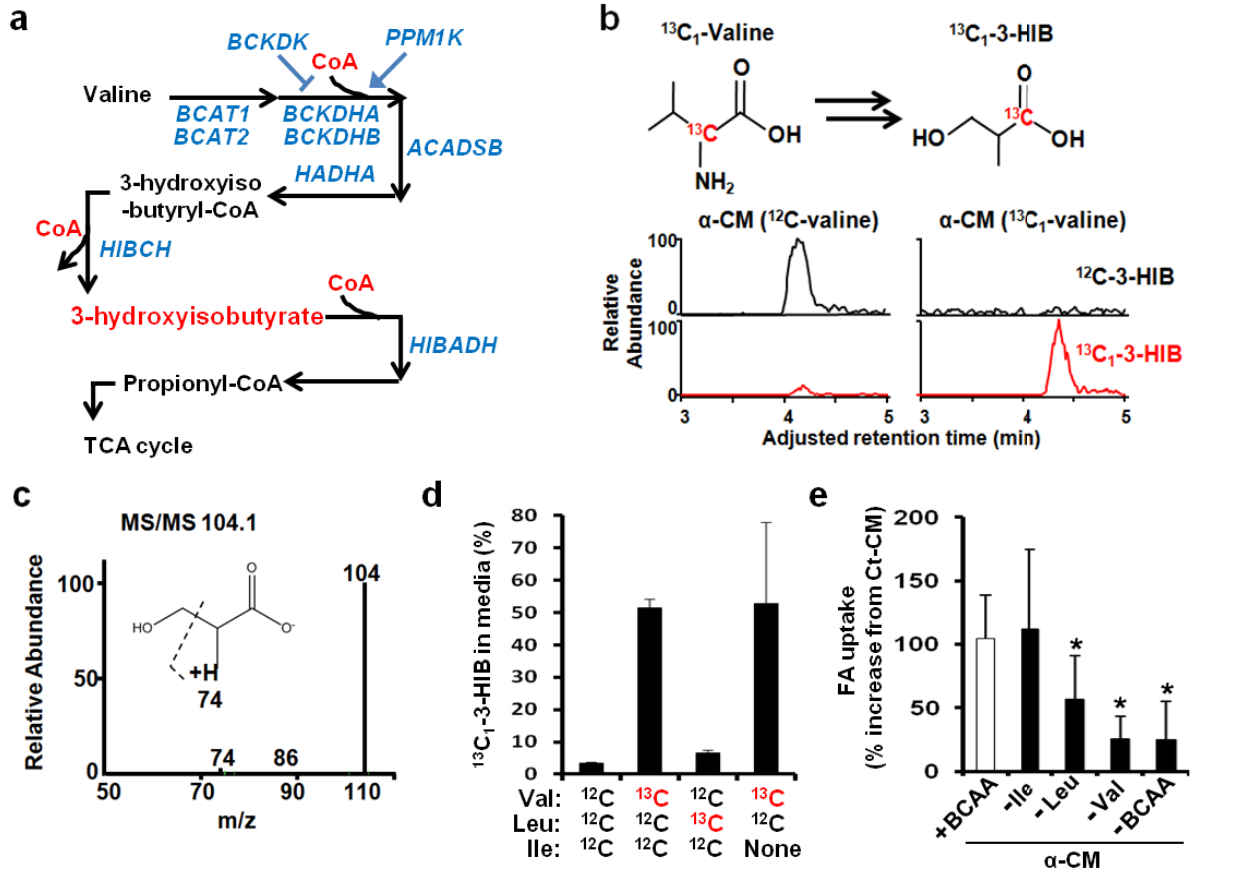


Figure 2.23: 3-HIB is generated from valine catabolism. a, Schematic of valine catabolism. Note that only 3-HIB does not have a CoA residue. **b**, 3-HIB in α-CM is derived from valine. **c**, MS/MS spectra of $^{13}C_1$-3-HIB generated by C2C12 myotubes incubated with $^{13}C_1$-2-Valine. **d**, A comparison of $^{13}C_1$-3-HIB production by C2C12 myotubes incubated with different combinations of ^{12}C- or ^{13}C-labeled BCAAs in the C2C12 differentiation media for 48 hr. Note that only 50% of 3-HIB in media is $^{13}C_1$-3-HIB, indicating that C2C12 myotubes can use endogenous valine and/or proteins to generate 3-HIB in the presence of serum in media. **e**, FA (2 μM) uptake by ECs was measured after exposure to CMs generated with media lacking the indicated BCAA(s). *p<.05 vs. control. Data are mean ± s.d. of at least three biological replicates.

grown with 13C-valine, but not with 13C-leucine, produced 13C-3-HIB. Moreover, the presence of isoleucine did not affect the amount of 13C-3-HIB from 13C-valine, indicating that no unlabeled carbons from isoleucine were contributing. The data thus show that 3-HIB can only be generated from catabolism of valine among BCAAs. Moreover, the FA uptake-inducing capacity of α-CM required the presence of valine in the medium (Figure 2.23e), demonstrating that 3-HIB in α-CM is derived from valine.

PGC-1α induced in myotubes the expression of nearly every enzyme in the pathways of BCAA catabolism (Figure 2.24a). Consistent with these gene expression profiles, PGC-1α overexpressing myotubes increased secretion of 3-HIB (Figure 2.24b), reflecting PGC-1α-induced catabolism of valine. PGC-1β induced the same genes (Figure 2.24c). Conversely, deletion of both PGC-1α and PGC-1β in primary myotubes (double knockout or DKO) repressed the expression of valine catabolic enzymes (Figure 2.25a), while single knockout of PGC-1α did not (Figure 2.25b). We next sought to modulate secretion of 3-HIB into α-CM and measure its effect on endothelial fatty acid uptake. Knockdown of HIBCH by siRNA in the myotubes (Figure 2.26a) strongly inhibited the α-CM-induced uptake of fatty acids in endothelial cells (Figure 2.26c and d). Conversely, knockdown of HIBADH (the 3-HIB degradating enzyme, Figure 2.26b) enhanced the uptake of fatty acids in endothelial cells (Figure 2.26c and d). Similarly, knockdown of HIBADH by siRNA electroporation into mouse skeletal muscle increased triglyceride levels in the muscle (Figure 2.27a and b). Together, these data demonstrate that PGC-1α induces the catabolism of valine to generate 3-HIB, which then acts as a paracrine

factor to stimulate endothelial FA uptake.

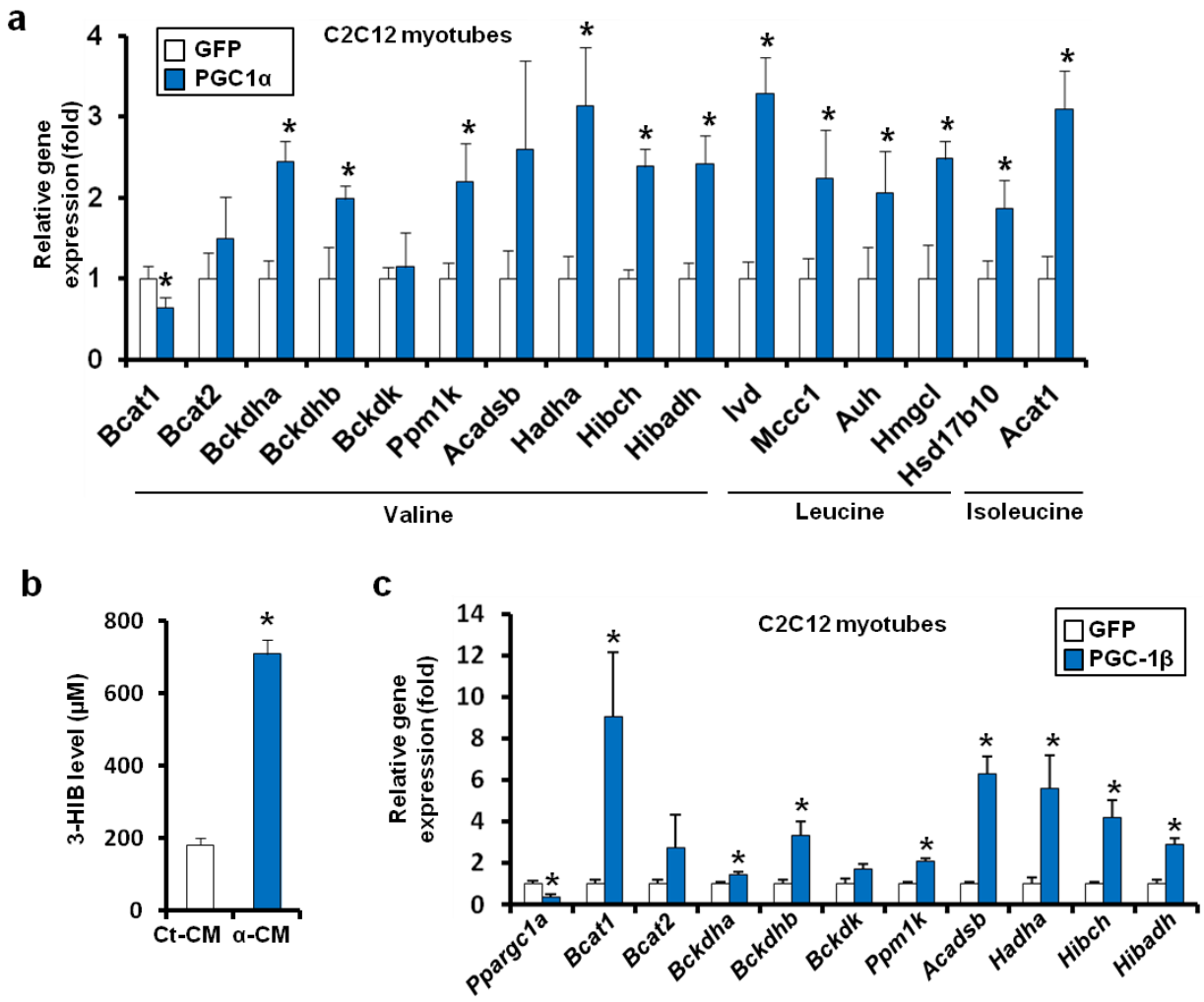


Figure 2.24: PGC-1α and PGC-1β induce expression of BCAA catabolic enzymes in myotubes. a, qPCR analysis of C2C12 myotubes after transfection with adenovirus expressing GFP or PGC-1α for 48 hr. **b**, Quantification of 3-HIB in Ct-CM and α-CM generated from the C2C12 differentiation media for 48 hr. **c**, qPCR analysis of C2C12 myotubes after transfection with adenovirus expressing GFP or PGC-1β for 48 hr. *p<.05 vs. control. Data are mean ± s.d. of at least three biological replicates.

To test if endothelial cells generate 3-HIB to induce fatty acid uptake in an autocrine manner, we measured gene expression of the valine catabolic enzymes in endothelial cells and

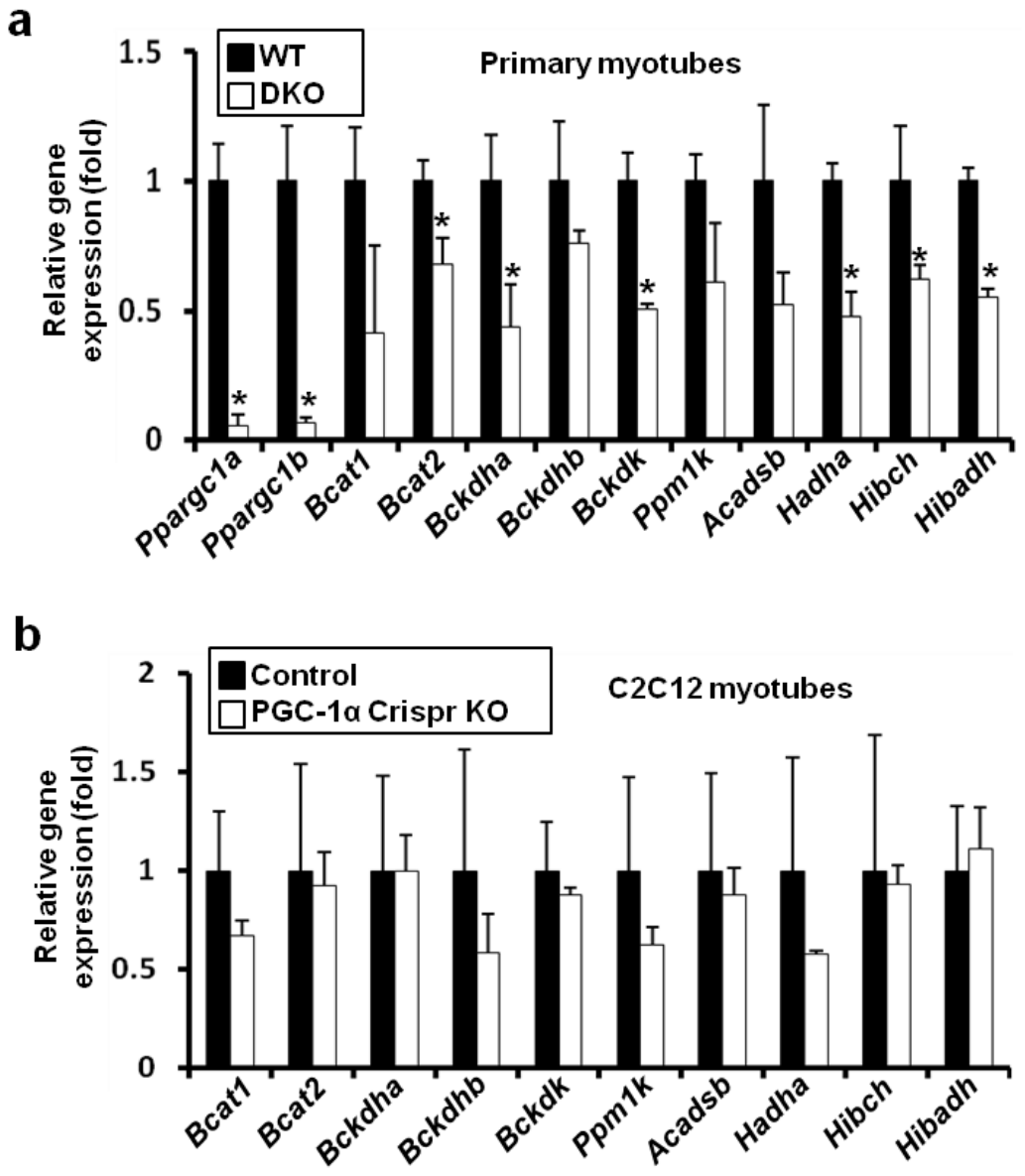


Figure 2.25: Deletion of both PGC-1α and PGC-1β suppresses gene expression of valine catabolic enzymes. a, qPCR analysis of primary myotubes from wild type (WT) or muscle-specific PGC-1α and PGC-1β double knockout (DKO) mice. **b**, qPCR analysis of C2C12 myotubes after transfection with lentivirus expressing Cas9 only (Control) or Cas9 plus a PGC-1α targeting guide RNA (PGC-1α Crispr KO). The transfected cells were selected with puromycin and non-silent indel mutations of PGC-1α were confirmed by genomic DNA sequencing. *p<.05 vs. control. Data are mean ± s.d. of at least three biological replicates.

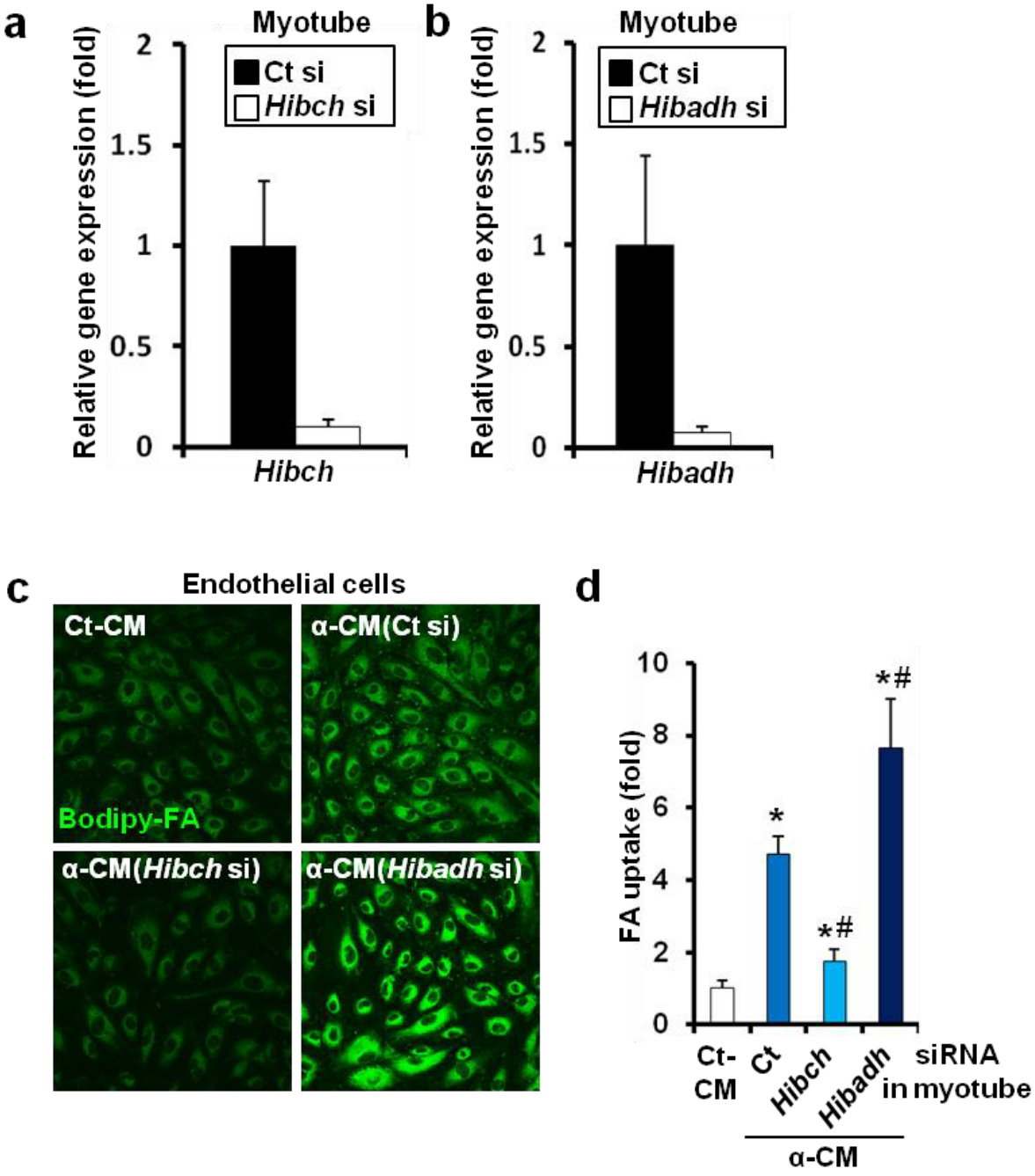


Figure 2.26: Perturbation of 3-HIB production in myotubes affects FA uptake induced by α-CM. a-b, qPCR analysis of C2C12 myotubes after transfection with control or Hibch siRNA (**a**) or Hibadh siRNA (**b**) for 48 hr. **c-d**, Knockdown of Hibch and Hibadh in myotubes decreases and increases the α-CM activity, respectively. Representative images of ECs taking up Bodipy-FA (**c**) and quantification (**d**). *p<.05 vs. control. #p<.05 vs. α-CM. ANOVA was used for **d**. Data are mean ± s.d. of at least three biological replicates.

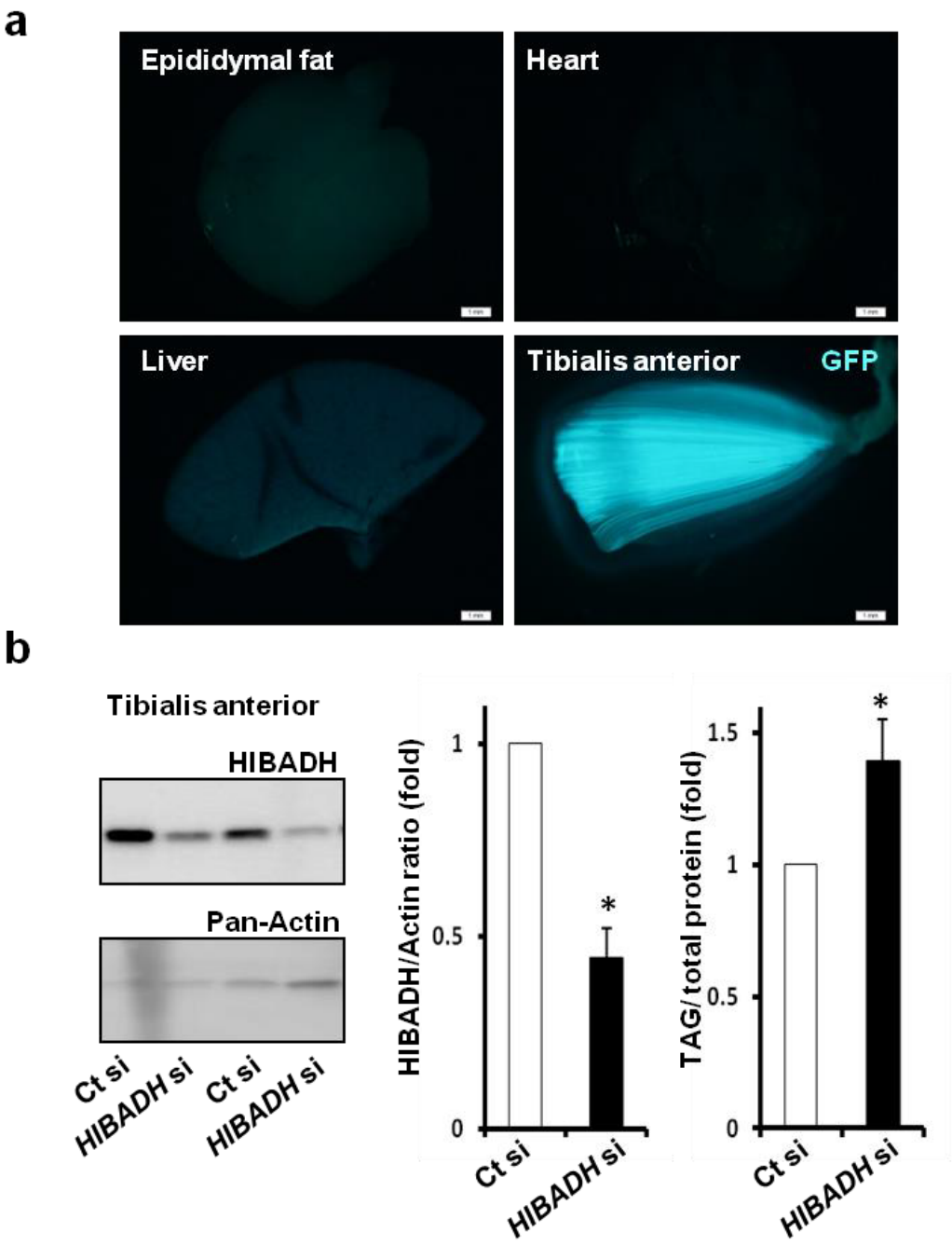


Figure 2.27: Knockdown of HIBADH in mouse skeletal muscle increases triglycerides levels. **a**, Representative fluorescence images of tissues harvested from mice after electroporation of Hibadh siRNA and a GFP plasmid into skeletal muscle. Note that only skeletal muscle shows strong GFP signals, demonstrating tissue-specificity. **b**, Western blot of mouse skeletal muscle after injection of Hibadh siRNA. Representative gel images (left), quantification (middle) and muscle triglyceride (TAG) levels (right). *p<.05 vs. control. Data are mean ± s.d. n=8.

found that they are dramatically lower than those in skeletal muscle (Figure 2.28a). Moreover,

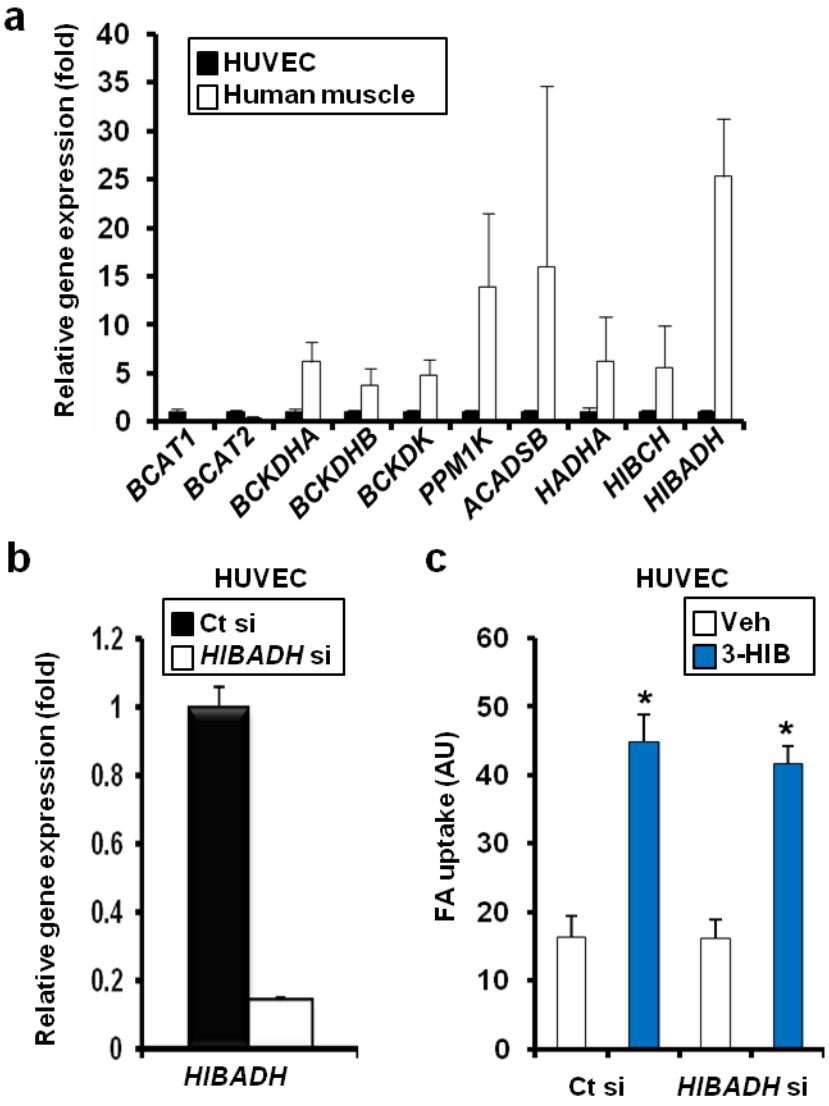


Figure 2.28: Knockdown of HIBADH in HUVECs does not affect FA uptake. a, qPCR analysis of HUVECs and human skeletal muscle biopsies. Note that HUVECs express much lower levels of valine catabolic genes than skeletal muscle does. **b**, qPCR analysis of HUVECs after transfection with control or *HIBADH* siRNA for 48 hr. **c**, FA (2 μM) uptake was measured in HUVECs treated with vehicle (Veh) or 3-HIB for 1 hr after transfection with control or *HIBADH* siRNA for 48 hr. *p<.05 vs. control. Data are mean ± s.d. of at least three biological replicates.

endothelial cells do not make detectable amount of 13C-labeled 3-HIB from 13C-labeled valine provided in the media (data not shown). To test if 3-HIB metabolism in endothelial cells can contribute to fatty acid uptake, we efficiently knocked down HIBADH in endothelial cells (Figure 2.28b). Neither basal nor 3-HIB-mediated fatty acid uptake by endothelial cells was affected (Figure 2.28c). In summary, these data indicate that catabolism of valine or 3-HIB in endothelial cells themselves does not contribute to the regulation of fatty acid trafficking.

Discussion

We here identified a molecular mechanism whereby PGC-1α enables fatty acids to enter muscle from the bloodstream. Building from the previous works demonstrating that PGC-1α drives both myocyte fatty acid consumption and paracrine activation of angiogenesis, we pursued the hypothesis that PGC-1α maximizes delivery of fatty acids to myocytes by enhancing trans-endothelial transport of fatty acids. We used Bodipy-tagged fatty acids and 13C-isotope labeled fatty acids to show that conditioned medium from PGC-1α-expressing C2C12 cells stimulates fatty acid uptake in endothelial cells. The key component in the medium was identified as 3-HIB, a metabolite of valine catabolism, which was sufficient to drive fatty acid uptake and transport by endothelial cells. PGC-1α drives expression of enzymes in this catabolic pathway, and silencing a key enzyme in PGC-1α-expressing C2C12 cells reduced the ability of conditioned medium to drive fatty acid uptake in endothelial cells. These results tie fatty acid and branched-chain amino acid metabolism together in an unexpected fashion.

The observation that Akt inhibition in cell culture blocks the PGC-1α conditioned medium effect is interesting. We believe it is unlikely to be directly a consequence of insulin

signaling, because insulin has a very mild effect on PGC-1α-CM activity (Figure 2.15a), compared to inhibitors (Figure 2.15b), and the insulin treatment required 48 hours (during CM generation), suggesting it is not an acute effect. More likely, we believe this effect stems from inhibition of glycolysis in the following manner: the first step of BCAA catabolism is trans-amination, which requires the NH2 acceptor, alpha-keto glutarate (Figure 2.29a), and the supply

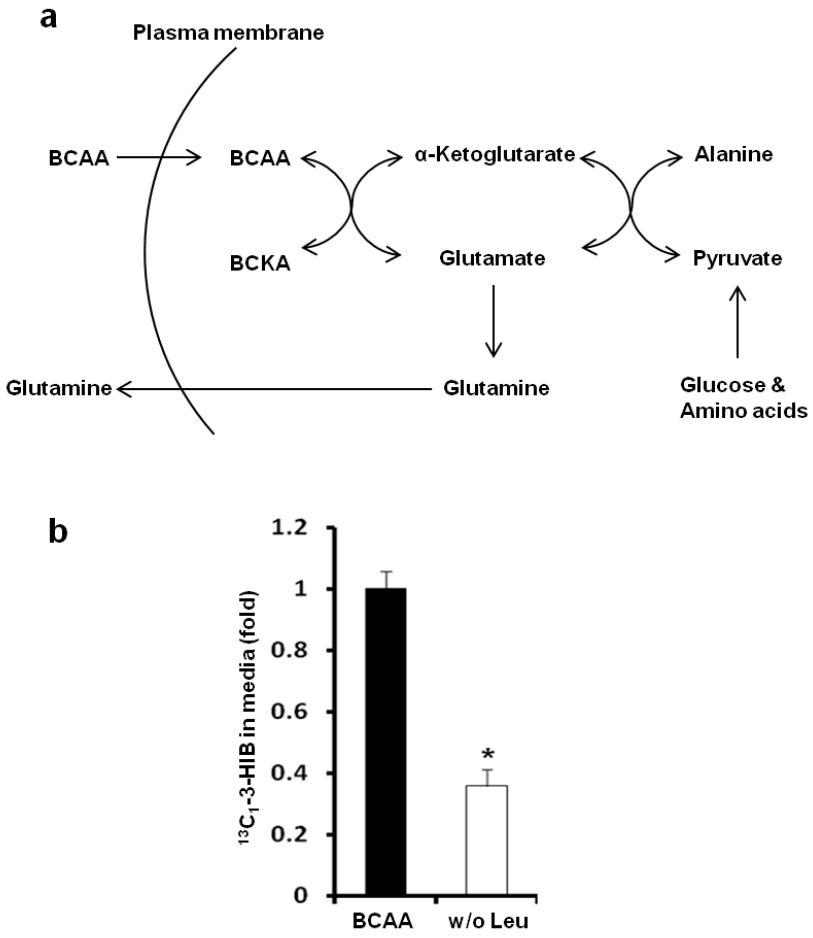


Figure 2.29: BCAA catabolism requires glucose supply. a, Schematic of BCAA catabolism coupled with other metabolism pathways. Pyruvate derived from glucose or amino acids is a nitrogen acceptor of glutamate, which is a nitrogen acceptor of BCAA. BCKA, branched chain alpha-keto acid. **b**, Removal of leucine from the media decreases 3-HIB production.

of which depends on pyruvate, which is mostly derived from glycolysis. Thus, inhibition of glycolysis blocks BCAA transamination in isolated muscle and it is reversed by pyruvate

supplementation (Wu GY and Thompson JR. 1988). In support of this notion, addition of pyruvate partially restored the activity of PGC-1α-CM even in the presence of 2DG or Akt inhibitor (Figure 2.15d). However, pyruvate did not restore CHC-inhibited activity (Figure 2.15d), consistent with a different mechanism underlying the CHC effect (i.e. transport of 3-HIB out of the cell).

We generated PGC-1α-CM with media depleted of either all or each individual BCAA for 30 hours (longer time points were not possible, because they led to atrophic myotubes). As shown in Figure 2.23e, both BCAA-free and valine-free media abrogated the production of the active inducer of fatty acid uptake by endothelial cells. In contrast, removing isoleucine had no impact on fatty acid uptake (Figure 2.23d). Interestingly, leucine-free media showed mild but significant reduction of fatty acid uptake activity (Figure 2.23e), which we suspect occurs because alpha-keto isocaproate, the first product of leucine breakdown, is the most powerful known allosteric enhancer of BCKDH activity, and thus of all BCAA catabolism (Paxton R and Harris RA. 1984; Brosnan JT and Brosnan M. 2006). Therefore, complete removal of leucine from the media likely suppresses valine catabolism as well. To test this hypothesis, we have measured oxidation of 13C-valine in myotubes with or without leucine in the media. Leucine exclusion significantly decreased 13C-3-HIB production (Figure 2.29b), while isoleucine exclusion did not (Figure 2.23d). This is consistent with the notion that leucine-derived alpha-keto isocaproate, the most potent activator of BCKDH among branched chain alpha-keto acids (Paxton R and Harris RA. 1984), is important for myotubes to generate 3-HIB.

The functional redundancy of PGC-1α and PGC-1β has been well established (Rowe GC and Arany Z. 2014). However, it was not known whether PGC-1s have compensatory function in the regulation of BCAA catabolism as well. PGC-1α knockout C2C12 myotubes were generated by the Crispr-Cas9 system and indel mutations were confirmed by single cell cloning and sequencing (data not shown). In spite of this complete knockout of PGC-1α, the conditioned media generated from these knockout myotubes showed a very mild decrease in fatty acid transport activity (Figure 2.9b). Consistent with this, gene expression levels of valine catabolic enzymes were not significantly downregulated by the loss of PGC-1α (Figure 2.25b). This observation is likely explained by a clear redundancy between PGC-1α and PGC-1β, including the ability of PGC-1β to induce valine catabolism genes (Figure 2.24c). Consistent with this point, deletion of both PGC-1α and PGC-1β in muscle cells did show reduced gene expression of valine catabolism genes (Figure 2.25a). As a consequence, endothelial cells treated with CM from double knockout cells (DKO-CM) showed reduced FA-transport (Figure 2.9a).

Similarly, we found *in vivo* that muscle-specific DKO mice have lower expression of valine catabolism genes in muscle and increased insulin sensitivity, in contrast to higher expression of valine catabolism genes and reduced insulin sensitivity in muscle-specific PGC-1β transgenic mice (see Chapter 3). Therefore, it seems obvious that muscle cells use a dual system that involves both PGC-1α and PGC-1β to coordinate valine catabolism for communication with endothelial cells via 3-HIB. It is of importance to elucidate what physiological cues (e.g. fasting and exercise) can regulate PGC-1α and PGC-1β separately for the process.

Another good example of redundancy we have found here is VEGF-B and 3-HIB. Our data clearly show that PGC-1α induces both secreted factors - VEGF-B (Figure 2.10a) and 3-HIB (Figure 2.24b). Why does evolution develop these seemingly redundant mechanisms?

First, redundancy of biological functions is quite common, especially if the process involved is critical for cell survival and function. For example, proper fatty acid supply is crucial for metabolically active muscle cells to continue the contraction process, in particular for cardiomyocytes in the heart for beating and muscle cells in the diaphragm for breathing.

In addition, there is a clear difference between VEGF-B-dependent and 3-HIB-dependent endothelial fatty acid uptake – the speed of action. VEGF-B requires at least 24 hours to induce any increase of endothelial fatty acid uptake because it needs induction of FATP3 and FATP4 gene expression. On the other hand, our time-course experiments show that 3-HIB-dependent endothelial fatty acid uptake is much faster – it occurs within 15 min after 3-HIB treatment. Thus, it is unlikely that the 3-HIB-dependent pathway involves regulation of gene expression. Rather, post-translational mechanisms are more consistent with this rapid process. Fatty acid transport proteins that could be involved in the 3-HIB-dependent pathway will be discussed in Chapter 3. Therefore, it seems that the VEGF-B-dependent pathway is a slow and persistent process, while the 3-HIB-dependent pathway is a fast and transient process.

Collectively, muscle cells may use at least two different mechanisms to efficiently regulate endothelial fatty acid transport in different conditions. An important question that remains to be answered is: blocking which pathway (or both) would be an effective therapeutic strategy to prevent lipotoxicity-induced insulin resistance.

It is quite interesting that PGC-1α employs a metabolite to regulate endothelial fatty acid uptake. This is not the only case where PGC-1α utilizes a metabolite to execute its biological functions. For example, a metabolite called BAIBA (beta-amino isobutyric acid) was shown to be increased by PGC-1α overexpression in muscle, which then stimulates 'browning' of white fat cells, a process of increased thermogenesis upon cold exposure (Roberts LD et al. 2014). What are the potential benefits for cells to use a metabolite as a signaling molecule, instead of a protein?

First, generation of a metabolite can be more energy-efficient. Proteins should be made through multiple steps that involve transcription, translation and perhaps post-translational modifications as well. On the other hand, metabolites can be relatively easily made by enzymes once the substrate is given and they are secreted much faster than proteins.

Second, metabolites are fairly small so that they can diffuse more rapidly and over a longer distance compared to bulky proteins that can be trapped by extracellular matrix. As already discussed, endothelial fatty acid uptake by 3-HIB is very rapid, and at least in certain conditions, this speed of action achieved by 3-HIB could be beneficial for cells instead of using VEGF-B.

Third, metabolites are usually more abundant (in terms of molarity because of their small molecular weight) and resistant to heat and degradation by intracellular/extracellular proteases, thereby having a relatively longer half-life (unless it has a strong reactive moiety).

Finally, single metabolite can link two distinct biological functions through complex networks of cellular metabolism pathways. 3-HIB can be a good example. Muscle cells have three major nutrient sources to generate energy – glucose, fatty acids and proteins. Glucose is rapidly depleted upon fasting or exercise. Then, muscle cells require fatty acids or proteins for

energy. However, protein catabolism must be the last option because degradation of their own proteins can be detrimental for muscle cells. In this regard, muscle protein breakdown induced by prolonged fasting or extensive exercise can accomplish two urgent objectives – one is to generate energy for survival, another is to generate 3-HIB as an SOS signal for rapid supply of fatty acids, the best alternative energy source. Therefore, 3-HIB can be used to link BCAA metabolism to fatty acid metabolism, and this metabolic interlock is also connected to glucose metabolism, a main topic of Chapter 3.

Materials and Methods

FA uptake assay. Confluent HUVECs (passage 2-8) were transferred from a 10 cm dish to a gelatin-coated 96 well black clear bottom plate (Corning #3603) with empty corner wells for no-cell controls. After overnight incubation, the cells were serum-starved with EBM2 containing EGM supplements (Lonza #CC-3162) for at least 8 hours. The cells were then treated with CMs or 3-HIB (2.5 mM) for an hour and briefly washed with DMEM. Then, Bodipy-FA (Molecular Probes #D3823) pre-incubated with FA-free BSA (2:1 molar ratio) in DMEM for 10 min in a 37°C water bath was added to the cells for 5 min at 37°C. The Bodipy-FA/BSA solution was then completely aspirated and the cells were washed with 0.5% BSA in PBS for 1.5 min twice (50 μL/well). To quench extracellular fluorescence, 0.4% trypan blue (MP biomedicals #1691049) was added (50 μL/well) and intracellular fluorescence was measured immediately (bottom-read) with a microplate reader (excitation 488 nm, emission 515 nm, cut-off 495 nm, SpectraMax M5, Molecular Probes). Readings from wells without Bodipy addition were used to subtract background signals. The cells were then quickly washed twice with PBS (50 μL/well) and incubated with 44 μM resazurin (#R7017, Sigma) in DMEM (50 μL/well) containing 10% FBS for 2 hours. The resazurin fluorescence was then measured with a microplate reader (excitation 530 nm, emission 590 nm, cut-off 550 nm) and used to normalize Bodipy signals to cell number. Bodipy FL C16 (#D3821) and Bodipy FL C5 (#D3834) were purchased from Molecular Probes. Oleic acid-BSA was purchased from Sigma (#O3008). To block VEGFB signaling in ECs, cells were pre-treated with 1 μM SU11248 (sc-220178, Santa Cruz) for 10 min before CM treatment, or CMs were pre-incubated with 1 μg/mL sFlt1 (#14-923, Calbiochem) for 6 hours at 4°C with shaking before being treated to ECs. For the trypsin treatment, CMs were

pre-incubated with 30 μg/ml trypsin (Gibco) for 3 hours at 37°C, then incubated with 500 μg/mL soy bean trypsin inhibitor (17075-029, Gibco) before being treated to the cells.

FA transport assay. Isolation of primary rat brain ECs was performed as described previously (Abbott NJ et al. 1992). Cells were counted and seeded (5 x 104 cells/well) on a 0.4 μm transwell (Corning #07-200-147), then grown for 4 days until they formed compact monolayer. Meanwhile, C2C12 was differentiated into myotubes in 24 well plate for 4 days (see below). The brain ECs in a transwell were then incubated with CMs or 3-HIB (2.5 mM) for an hour and the transwell was inserted into the 24 well plate in which C2C12 myotubes were grown. Bodipy-FA/BSA or [U-13C]-palmitate/BSA in CMs (80 μL) with or without Dextran Texas-Red (70 kDa, Molecular Probes #D1830) was then added to the top chamber of the transwell. CMs containing only BSA (520 μL) were added to the bottom chamber of transwell. After each time point, 10 μL of media was taken from the bottom transwell to measure the Bodipy-FA and Dextran Texas-Red fluorescence. To measure [U-13C]-palmitate metabolism in C2C12 myotubes, media from the bottom transwell were collected after 30 min of the transport assay and incubated with C2C12 myotubes for an hour. Metabolites were then isolated from the C2C12 myotubes and quantified (UPenn Metabolomics Core, Princeton). Trans-endothelial electrical resistance (TEER) was measured as described previously (Xie Z et al. 2012).

Preparation of CMs. C2C12 cells were grown in 10 cm dishes until 90% confluency and differentiated into myotubes with 5 μg/mL insulin plus 5 μg/mL transferrin (Sigma) in DMEM for 2 days, followed by 2% horse serum in DMEM (C2C12 differentiation media) for additional 2 days. The cells were then infected with an adenovirus expressing GFP, PGC-1α or PGC-1β.

Two days after infection, the cells were washed twice with PBS to remove the adenovirus and incubated with 12 mL DMEM (with or without 2% horse serum) for 2 days. 2DG (5 mM), Akt VIII (5 μM) or CHC (5 mM) was added if necessary. CMs were then collected, centrifuged at 13,000 g for 10 min at 4°C, aliquoted and stored at -80°C for future use. To generate PGC-1α-expressing C2C12 cell lines, cells were infected with retrovirus expressing PGC-1αor an empty-vector control. Two days after infection, the infected cells were selected with 2.5 μg/mL puromycin for 2 days. To generate VEGFB CM, a VEGFB construct was obtained from the hORFeome Database and cloned into the Gateway pcDNA-DEST40 vector (Invitrogen) and transfected into HEK293T cells. Fifteen hours after transfection, the cells were washed once with PBS and incubated with DMEM for 2 days before collection. The control CM was generated with GFP construct.

Cell culture. HUVECs, human umbilical cord blood-derived endothelial colony-forming cells (hECFCs), primary rat brain endothelial cells, primary mouse heart and muscle endothelial cells were grown in EBM2 containing EGM supplements with 20% FBS. C2C12 and all other cell lines (ATCC) were grown in DMEM with 10% FBS. Isolation of primary mouse endothelial cells and myoblasts was performed as described previously (Sawada N et al. 2008; Rowe GC et al. 2013). Pericyte-like cells were differentiated from 10T1/2 with TGF-β for 4 days as described previously (Darland DC and D'Amore PA. 2001). For the siRNA transfection, control siRNA (SIC001), FATP3 siRNA (SASI_Hs01_00100092), FATP4 siRNA (SASI_Hs01_00047530), FLK1 siRNA (SASI_Hs01_00073461), CD36 esiRNA (EHU089321), HIBADH siRNA (SASI_Hs01_00061462), Hibch siRNA (SASI_Mm02_00341755), Hibadh siRNA (SASI_Mm01_00120340) or Vegfb siRNA (SASI_Mm01_00114251, all from Sigma) was

mixed with Lipofectamine RNAi Max (Invitrogen) in Opti-MEM (Sigma) for 20 min before being treated to cells.

Bodipy and immunofluorescence staining. ECs were grown on fibronectin-coated cover glass. The cells were then washed with PBS once and fixed with 4% formaldehyde in PBS for 20 min at room temperature. The cells were then washed with washing buffer (0.1% Triton X-100 in PBS) three times for 30 min in total, incubated in blocking buffer (5% BSA in washing buffer) for an hour, and incubated with 1 μg/ml Bodipy (Molecular Probes) in blocking buffer with or without a primary antibody (1:100 dilution) overnight at 4°C. The cells were then washed with washing buffer 3 times for 30 min in total, incubated with a secondary antibody (1:1000 dilution in blocking buffer) for 3 h at room temperature. The cells were then washed with washing buffer 6 times for an hour in total, and mounted with DAPI mounting media (Molecular Probes #P36931). Images were then taken with a confocal microscopy.

Chromatography. Silica was baked to remove moisture and mixed to n-BuOH:MeOH = 3:1 for packing. CMs were treated with charcoal, lyophilized and resuspended in the same solvent. The column was eluted with three 5 mL of n-BuOH:MeOH = 3:1, 1:1 mixture and 100% methanol. Each fraction was dried and resuspended in media for the activity test. For HILIC separation, active fractions were resuspended in-phase and injected to HPLC (Dionex LC20 with GP50 quad pump and AD25 single wavelength UV detector) equipped with an HILIC column (Agilent HILIC plus, 4.6 mm x 100 mm x 3.5 μm). Ammonium acetate buffer (10 mM adjusted to pH 4.0) in water/acetonitrile mix was used as eluent, initially at water:acetonitrile = 5:95 for 5 min, ramped to 55:45 over 8 min and held for 2 min. Thirty fractions were collected every 30 sec.

Tandem Mass spectrometry for structural identification. HP-HILIC (Waters BEH amide, 2.1 mm x 100 mm x 2.5 μm, equipped with HP1100 quad pump HPLC) coupled with tandem mass spectrometers (Thermo Scientific LTQ XL for structural identification and pathway analysis of 3-HIB, or Thermo Scientific Q Exactive orbitrap for high-sensitivity quantitation of in vitro, in vivo and patient samples) was used. Ammonium formate buffer (2 mM adjusted at pH 9.0) in water/acetonitrile mix was used as eluent, initially at water:acetonitrile=10:90 for 4 min, ramped to 40:60 over 3 min and held for 5 min for washing and reconditioned for 12 mins. Selective ion monitoring (SIM)/parallel reaction monitoring (PRM) at 103.1 (hydroxybutyrate (HB) isomers), 106.1 (d3-2HB standard) and 109.1 (d6-4HB standard) were carried out for MS/MS spectra acquisition. Quantification of each HB species was carried out with specific Q1→Q3 transition fingerprint (2-HB: 103→57, 3-HB:103→59, 3-HIB:103→73, 4-HB:103→85). $^{13}C_1$-2-Valine was purchased from Sigma (#604917). $^{13}C_2$-1,2-Leucine was purchased from Cambridge Isotope Laboratories (#CLM-3524). d3-2-HB was purchased from CDN Isotopes (#D-7002) and d6-4-HB was purchased from Cerilliant (#G-006).

References

Abbott NJ, Hughes CC, Revest PA, Greenwood J. (1992). Development and characterization of a rat brain capillary endothelial culture: towards an in vitro blood-brain barrier. J Cell Sci 103, 23-37.

Brosnan JT, Brosnan ME. (2006). Branched-chain amino acids: enzyme and substrate regulation. J Nutr. 136:207S-11S.

Darland DC, D'Amore PA. (2001). TGF beta is required for the formation of capillary-like structures in three-dimensional cocultures of 10T1/2 and endothelial cells. Angiogenesis 4,11-20.

DiRusso CC, Li H, Darwis D, Watkins PA, Berger J, Black PN. (2005). Comparative biochemical studies of the murine fatty acid transport proteins (FATP) expressed in yeast. J Biol Chem. 280:16829-37.

Dubikovskaya E, Chudnovskiy R, Karateev G, Park HM, Stahl A. (2014). Measurement of long-chain fatty acid uptake into adipocytes. Methods Enzymol. 538:107-34.

Gimeno RE, Ortegon AM, Patel S, Punreddy S, Ge P, Sun Y, Lodish HF, Stahl A. (2003). Characterization of a heart-specific fatty acid transport protein. J Biol Chem. 278:16039-44.

Hagberg CE, Falkevall A, Wang X, Larsson E, Huusko J, Nilsson I, van Meeteren LA, Samen E, Lu L, Vanwildemeersch M, Klar J, Genove G, Pietras K, Stone-Elander S, Claesson-Welsh L, Yla-Herttuala S, Lindahl P, Eriksson U. (2010). Vascular endothelial growth factor B controls endothelial fatty acid uptake. Nature. 464:917-21.

Hagberg CE, Mehlem A, Falkevall A, Muhl L, Fam BC, Ortsater H, Scotney P, Nyqvist D, Samen E, Lu L, Stone-Elander S, Proietto J, Andrikopoulos S, Sjoholm A, Nash A, Eriksson U. (2012). Targeting VEGF-B as a novel treatment for insulin resistance and type 2 diabetes. Nature. 490:426-30.

Kuda O, Pietka TA, Demianova Z, Kudova E, Cvacka J, Kopecky J, Abumrad NA. (2013). Sulfo-N-succinimidyl oleate (SSO) inhibits fatty acid uptake and signaling for intracellular calcium via binding CD36 lysine 164: SSO also inhibits oxidized low density lipoprotein uptake by macrophages. J Biol Chem. 288:15547-55.

Li H, Black PN, Chokshi A, Sandoval-Alvarez A, Vatsyayan R, Sealls W, DiRusso CC. (2008). High-throughput screening for fatty acid uptake inhibitors in humanized yeast identifies atypical antipsychotic drugs that cause dyslipidemias. J Lipid Res. 49:230-44.

Matter K, Balda MS. (2003). Functional analysis of tight junctions. Methods. 30:228-34.

Nellis MM, Doering CB, Kasinski A, Danner DJ. (2002). Insulin increases branched-chain alpha-ketoacid dehydrogenase kinase expression in Clone 9 rat cells. Am J Physiol Endocrinol Metab. 283:E853-60.

Neuhaus W, Trzeciak J, Lauer R, Lachmann B, Noe CR. APTS-labeled dextran ladder: a novel tool to characterize cell layer tightness. (2006). J Pharm Biomed Anal. 40:1035-9.

Newgard CB. (2012). Interplay between lipids and branched-chain amino acids in development of insulin resistance. Cell Metab. 15:606-14.

Overmyer KA, Evans CR, Qi NR, Minogue CE, Carson JJ, Chermside-Scabbo CJ, Koch LG, Britton SL, Pagliarini DJ, Coon JJ, Burant CF. (2015). Maximal oxidative capacity during exercise is associated with skeletal muscle fuel selection and dynamic changes in mitochondrial protein acetylation. Cell Metab. 21:468-78.

Paxton R, Harris RA. (1984). Regulation of branched-chain alpha-ketoacid dehydrogenase kinase. Arch Biochem Biophys. 231:48-57.

Pechlivanis A, Kostidis S, Saraslanidis P, Petridou A, Tsalis G, Mougios V, Gika HG, Mikros E, Theodoridis GA. (2010). (1)H NMR-based metabonomic investigation of the effect of two different exercise sessions on the metabolic fingerprint of human urine. J Proteome Res. 9:6405-16.

Rambold AS, Cohen S, Lippincott-Schwartz J. (2015). Fatty acid trafficking in starved cells: regulation by lipid droplet lipolysis, autophagy, and mitochondrial fusion dynamics. Dev Cell. 32:678-92.

Roberts LD, Bostrom P, O'Sullivan JF, Schinzel RT, Lewis GD, Dejam A, Lee YK, Palma MJ, Calhoun S, Georgiadi A, Chen MH, Ramachandran VS, Larson MG, Bouchard C, Rankinen T, Souza AL, Clish CB, Wang TJ, Estall JL, Soukas AA, Cowan CA, Spiegelman BM, Gerszten RE. (2014). β-Aminoisobutyric acid induces browning of white fat and hepatic β-oxidation and is inversely correlated with cardiometabolic risk factors. Cell Metab. 19:96-108.

Rowe GC, Arany Z. (2014). Genetic models of PGC-1 and glucose metabolism and homeostasis. Rev Endocr Metab Disord. 15:21-9.

Rowe GC, Patten IS, Zsengeller ZK, El-Khoury R, Okutsu M, Bampoh S, Koulisis N, Farrell C, Hirshman MF, Yan Z, Goodyear LJ, Rustin P, Arany Z. (2013). Disconnecting mitochondrial content from respiratory chain capacity in PGC-1-deficient skeletal muscle. Cell Rep. 3:1449-56.

Sawada N, Salomone S, Kim HH, Kwiatkowski DJ, Liao JK. (2008). Regulation of endothelial nitric oxide synthase and postnatal angiogenesis by Rac1. Circ Res. 103:360-8.

Shimomura Y, Murakami T, Nakai N, Nagasaki M, Harris RA. (2004). Exercise promotes BCAA catabolism: effects of BCAA supplementation on skeletal muscle during exercise. J Nutr. 134:1583S-1587S.

Shin AC, Fasshauer M, Filatova N, Grundell LA, Zielinski E, Zhou JY, Scherer T, Lindtner C, White PJ, Lapworth AL, Ilkayeva O, Knippschild U, Wolf AM, Scheja L, Grove KL, Smith RD,

Qian WJ, Lynch CJ, Newgard CB, Buettner C. (2014). Brain insulin lowers circulating BCAA levels by inducing hepatic BCAA catabolism. Cell Metab. 20:898-909.

Shulman GI. (2014). Ectopic fat in insulin resistance, dyslipidemia, and cardiometabolic disease. N Engl J Med. 371:1131-41.

Torres N, Lopez G, De Santiago S, Hutson SM, Tovar AR. (1998). Dietary protein level regulates expression of the mitochondrial branched-chain aminotransferase in rats. J Nutr. 128:1368-75.

Wu GY, Thompson JR. (1988). The effect of ketone bodies on alanine and glutamine metabolism in isolated skeletal muscle from the fasted chick. Biochem J. 255:139-44.

Xie Z, Ghosh CC, Patel R, Iwaki S, Gaskins D, Nelson C, Jones N, Greipp PR, Parikh SM, Druey KM. (2012). Vascular endothelial hyperpermeability induces the clinical symptoms of Clarkson disease (the systemic capillary leak syndrome). Blood. 119:4321-32.

Chapter 3:

Role of 3-HIB in glucose homeostasis

Attributions: Cholsoon Jang performed all experiments for this section unless otherwise noted. Soumya Ullas (Longwood Small Animal Imaging Facility) conducted the bioluminescence imaging experiments. Dr. Sungwhan Oh performed all the mass spectrometry analysis. Dr. Glenn Rowe performed glucose tolerance test for PGC-1β transgenic mice and PGC-1α / PGC-1β double knockout mice. Dr. Qingwei Chu and Dr. Joseph Baur performed hyperinsulinemic-euglycemic clamp studies. Dr. Saikumari Krishnaiah and Dr. Aalim Weljie performed lipidomics analysis.

Abstract

Aberrant accumulation of fats in muscle cells is known to trigger lipotoxicity-induced insulin resistance. Our data indicate that muscle-derived 3-HIB, a catabolism product of the BCAA valine, increases endothelial fatty acid transport and thereby increases fatty acid flux into muscle cells. PGC-1 co-activators regulate this process in muscle cells through induction of valine catabolic genes. In endothelial cells, we found that FATP3 and FATP4 play major roles in mediating 3-HIB-dependent fatty acid uptake. To further understand the role of PGC-1s and 3-HIB in fatty acid transport *in vivo*, we used transgenic mice expressing PGC-1α or PGC-1β in skeletal muscle and measured lipid trafficking and glucose homeostasis. We found that increased 3-HIB levels in skeletal muscle are sufficient to stimulate fatty acid uptake and induce insulin resistance in muscle. Providing animals with 3-HIB in drinking water, or inducing 3-HIB levels in skeletal muscle by over-expressing PGC-1α, stimulates muscle to take up fatty acids, leading to muscle lipid accumulation, and systemic glucose intolerance. Importantly, 3-HIB levels are also elevated in muscle from *db*/*db* mice and muscle biopsies from patients with type II diabetes. These data thus unveil a novel mechanism that regulates trans-endothelial flux of fatty acids, revealing 3-HIB as a new bioactive signaling metabolite that links the regulation of fatty acid flux to BCAA catabolism and provides a mechanistic explanation for how increased BCAA catabolic flux can cause diabetes.

Introduction

Protein-mediated endothelial fatty acid transport

Accumulating evidence has demonstrated that there are facilitated fatty acid transport mechanisms mediated by a variety of proteins localized in the plasma membrane as well as intracellular organelles (Mehrotra D et al. 2014) (Figure 3.1). How these proteins are regulated is

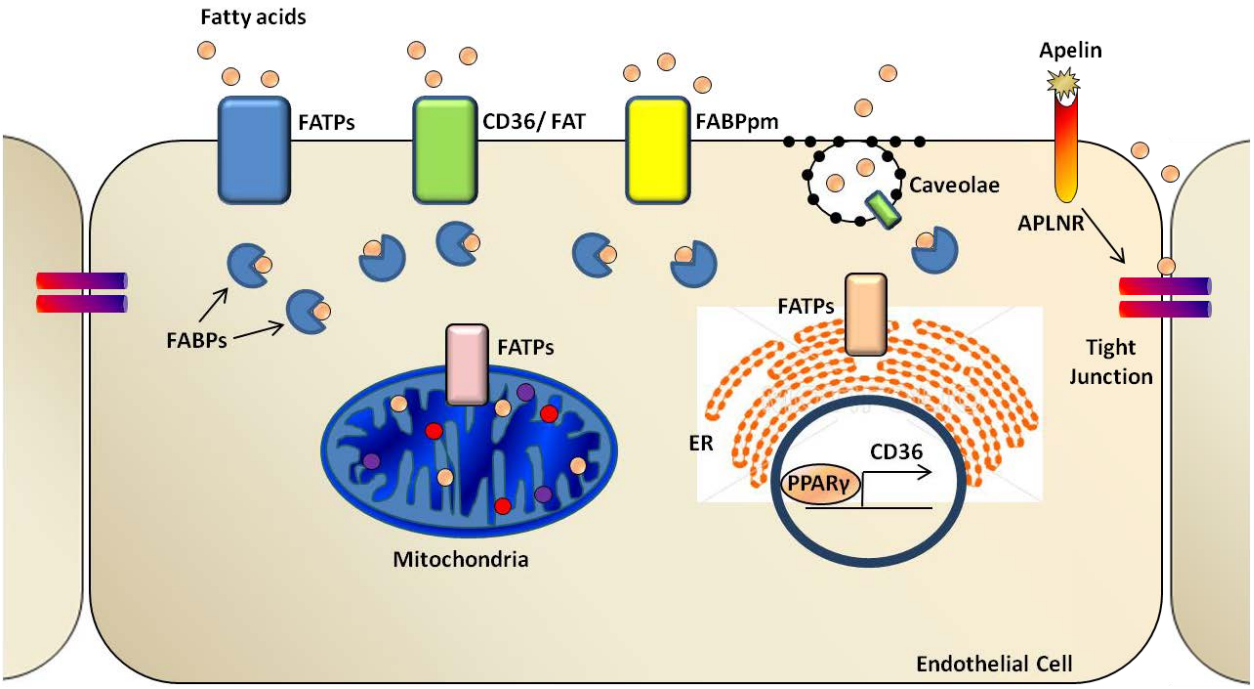


Figure 3.1: Protein-mediated fatty acid transport in ECs. A variety of proteins have been shown to facilitate FA transport in ECs. They localize in the plasma membrane, mitochondria, ER and cytoplasm. Caveolae are specialized lipid raft vesicles, which also regulate FA uptake. A transcription factor PPARγ induces CD36 gene expression. Apelin binds to its receptor APLNR and regulates vascular permeability by controlling tight junctions. All these proteins seem to cooperate with each other to coordinate endothelial FA transport.

poorly understood. The biggest family of proteins involved in fatty acid transport is FATPs. Six members of FATPs are expressed differently in different tissues. In endothelial cells, FATP3 and FATP4 are most highly expressed. Recent studies have suggested that VEGF-B-dependent

signaling pathway regulates gene expression of FATP3 and FATP4 in endothelial cells (Hagberg CE et al. 2010). Another layer of regulatory mechanism of FATPs is modulation of their intracellular localization. FATP1 is highly expressed in adipocytes and insulin is known to induce rapid translocation of FATP1 from intracellular vesicles to the plasma membrane (Stahl A et al. 2002), reminiscent of GLUT4 translocation by insulin (Rowland AF et al. 211). The subcellular localization of FATP3 is still debatable (Pei Z et al. 2004; DiRusso CC et al. 2005) and its regulation is unknown. Subcellular localization of FATP4 is also controversial – it involves mitochondria, endoplasmic reticulum (ER), peroxisomes, and the plasma membrane (Milger K et al. 2006; Krammer J et al. 2011; Hillebrand M et al. 2012). It was suggested that FATP4 in the ER facilitates acylation of intracellular fatty acids through its acyl-CoA synthetase activity, thereby inducing gradient-dependent uptake of extracellular fatty acids in cooperation with CD36 in the plasma membrane (Digel M et al. 2011). CD36 (or FAT) is the most well-studied fatty acid transporter. A transcription factor PPARγ regulates CD36 gene expression with many other genes related to fatty acid oxidation (Motojima K et al. 1998). Endothelial specific knockout of PPARγ reduced CD36 expression in endothelial cells, which in turn reduced fatty acid transport into underlying tissues (Goto K et al. 2013). This mechanism partly explains improved insulin sensitivity in the EC-specific PPARγ knockout mice on a high-fat diet (Kanda T et al. 2009). CD36 is also acutely regulated by membrane translocation via insulin and AMP-activated protein kinase (AMPK), a cellular energy-sensing molecule that is activated by exercise in skeletal muscle (Luiken JJ et al. 2002; Chabowski A et al. 2006). Fatty acid binding proteins (FABPs) are also known to be induced by exercise (Kiens B et al. 1997). They are localized in cytosol except plasma membrane FABP (FABPpm) (Figure 3.1). Since unbound free fatty acids are water-insoluble and acidic, FABPs play crucial roles in cytosol to keep fatty acids

soluble and pH-neutral by direct binding (like the albumin in blood) (Makowski L and Hotamisligil GS. 2004). How cytosolic FABPs can regulate uptake of extracellular fatty acids is poorly understood. Knockout of capillary endothelial FABP4 and FABP5 resulted in reduced fatty acid transport into the heart, making it dependent more on glucose than fatty acids (Iso T et al. 2013). There are other mechanisms of fatty acid uptake that are potentially important in endothelial cells (Figure 3.1). Caveolae is a special type of lipid raft invaginations of the plasma membrane, especially abundant in endothelial cells and adipocytes (Scherer PE et al. 1994). Caveolin-1 (Cav-1) is a major component of these vesicles and it seems to play important roles in fatty acid uptake (Ring A et al. 2006). It appears that proper functions of CD36 (but not FATPs) are dependent on its localization in caveolae. Inhibition of caveolae formation by cholesterol depletion or genetic knockout of Cav-1 blocked fatty acid uptake by CD36 (Pohl J et al. 2005; Le Lay S and Kurzchalia TV. 2005). Finally, a small peptide called Apelin and its G-protein-coupled receptor (GPCR) APLNR have been identified to regulate fatty acid transport (Figure 3.1). They are known to increase fatty acid transport by adjusting vascular permeability (Novakova V et al. 2015). Both Apelin and APLNR are highly expressed in endothelial cells. Apelin, in particular, is predominantly expressed in vascular networks in Apelin-lacZ reporter mouse (Sheikh AY et al. 2008), suggesting that there is an autocrine mechanism. An important question to answer is: which of these known fatty acid transport mechanisms are crucial for 3-HIB-mediated fatty acid transport.

BCAA catabolism and diabetes

Since the strong correlation has been discovered between high BCAA levels in blood and high risk of type II diabetes (Wang TJ et al. 2011; Wurtz P et al. 2012; McCormack SE, et al.

2013), research has focused on the molecular mechanism of how BCAAs can cause insulin resistance. It is still controversial whether high BCAAs or high BCAA catabolism induces insulin resistance. A recent study using an unbiased metabolomics profiling of obese versus lean people has discovered that BCAA-related metabolites are the most significantly different metabolites between two groups, supporting a correlation between increased catabolism of BCAAs and insulin resistance (Newgard CB et al. 2009). To test a causal relationship between BCAA catabolism and insulin resistance, the authors fed rats with a high-BCAA diet with or without a high-fat diet. High-fat diet is a well-established method to induce insulin resistance in rodents through induction of lipotoxicity in skeletal muscle. Surprisingly, the rats fed with a high-BCAA, high-fat-diet showed much higher lipid accumulation with more severe insulin resistance than the rats fed with just a high fat diet. The authors found that these rats showed highly active mTOR signaling in skeletal muscle (Newgard CB et al. 2009). Treatment of rapamycin, an mTOR inhibitor, partially rescued the insulin resistance phenotype of these rats, which led the authors to conclude that high BCAA-mediated mTOR activation may induce insulin resistance. However, rats fed with only high BCAA diet did not show strong mTOR activation or insulin resistance (Newgard CB et al. 2009). Thus, BCAAs alone do not seem to activate mTOR sufficiently to cause insulin resistance. Importantly, a new study has demonstrated that mTOR activation is not the cause of muscle insulin resistance (Smith GI et al. 2015). They found that ingestion of whey proteins or leucine, the strongest mTOR-activating BCAA, can both increase plasma leucine concentrations and mTOR activation in muscle at a similar level. However, only ingestion of whey proteins induces insulin resistance. Thus, there must be an mTOR-independent pathway that is triggered by BCAAs (or their catabolism products), which can provoke aberrant accumulation of fatty acid species in skeletal muscle.

BCAAs are three amino acids – leucine, isoleucine and valine. However, it is unclear that which of three (or all three) is sufficient and/or necessary to trigger insulin resistance. Animal feeding experiments with each of BCAAs give some hints to answer this question. For instance, mice fed with leucine-containing drinking water showed improved glucose homeostasis upon a high-fat diet (Zhang Y et al. 2007). These mice have reduced weight gain, increased resting energy expenditure, and reduced plasma cholesterol levels. On the other hand, feeding of leucine with a low-fat diet did not show any changes in body weight and glucose homeostasis (Noatsch A et al. 2011), again suggesting that dietary fat is an important factor to determine the effect of BCAA feeding. Supplementation of excess isoleucine in drinking water also did not cause insulin resistance but rather improved glucose homeostasis upon a high-fat diet (Nishimura J et al. 2010). It is surprising that there is no study so far that investigated the effect of a high-valine diet in animals. Since only a high-BCAA diet (but not a high-leucine or a high-isolucine diet) could recapitulate insulin resistance phenotypes of humans, it is very likely that excess valine (or its metabolites) is the major cause of insulin resistance triggered by high BCAAs. Or, it is possible that interaction between three BCAAs is necessary to induce insulin resistance (e.g. positive feedback activation of BCAA catabolism by alpha-keto acids drived from BCAAs).

Results

To identify fatty acid transport mechanisms underlying the 3-HIB-mediated fatty acid transport, we first knocked downed in HUVECs a number of fatty acid transport proteins

expressed in endothelial cells, including FATP3, FATP4 and CD36 (Figure 3.2a and c).

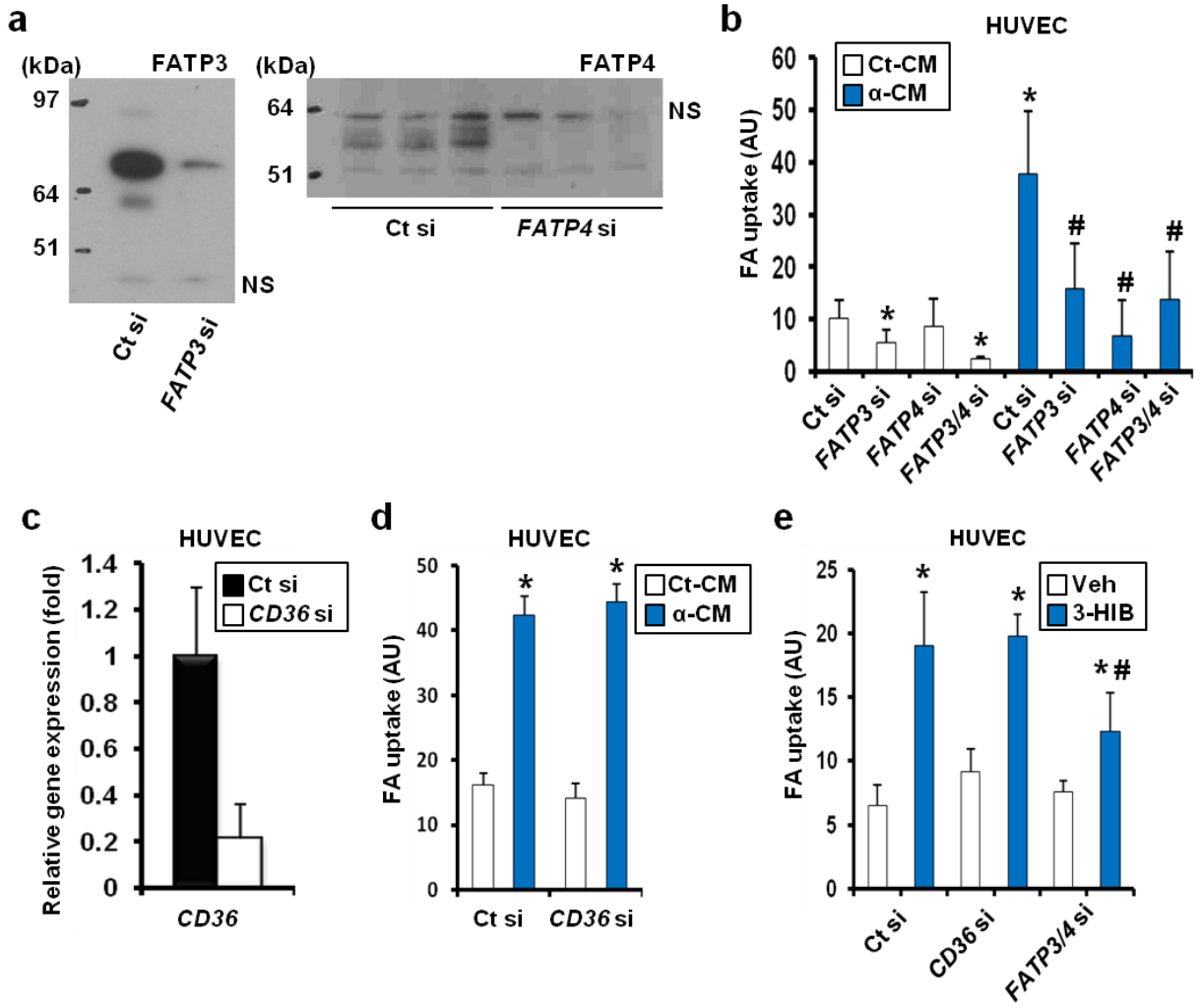


Figure 3.2: FATPs but not CD36 mediate endothelial FA uptake by α-CM or 3-HIB. a, Western blot analysis of HUVECs after transfection with control, FATP3 siRNA (left) or FATP4 siRNA (right) for 48 hr. NS, non-specific bands. **b**, FA uptake was measured in HUVECs treated with Ct-CM or α-CM for 1 hr after transfection with the indicated siRNA(s) for 48 hr. **c**, qPCR analysis of HUVECs after transfection with control or CD36 siRNA for 48 hr. **d**, FA uptake was measured in HUVECs treated with Ct-CM or α-CM for 1 hr after transfection with control or CD36 siRNA for 48 hr. **e**, FA uptake was measured in HUVECs treated with vehicle (Veh) or 3-HIB for 1 hr after transfection with the indicated siRNA for 48 hr. *p<.05 vs. control. #p<.05 vs. α-CM. Data are mean ± s.d. of at least three biological replicates.

Knockdown of FATP3 or FATP4, but not CD36, in HUVECs suppressed fatty acid uptake in response to either α-CM or 3-HIB (Figure 3.2b, d, and e), indicating that FATP3 and 4 are

required for fatty acid uptake in response to 3-HIB, but that CD36 is dispensable. Similarly, primary endothelial cells isolated from FATP4 knockout mice showed reduced fatty acid uptake by α-CM or 3-HIB (Figure 3.3a and c), while primary endothelial cells isolated from CD36 knockout mice exhibited mildly reduced baseline fatty acid uptake that remained inducible by 3-HIB (Figure 3.3b and d). Next, we measured gene expression of these fatty acid transporters as

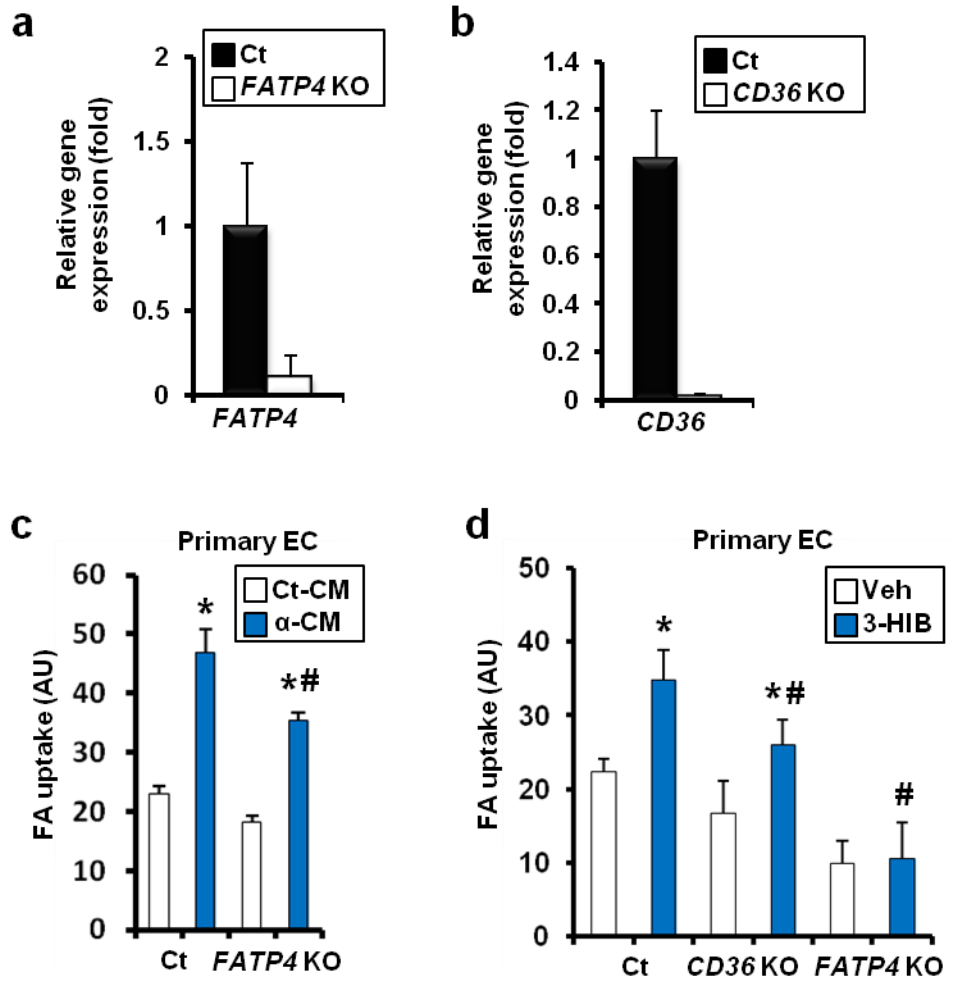


Figure 3.3: Fatty acid transport proteins mediate endothelial FA uptake by α-CM or 3-HIB. **a-b**, qPCR analysis of primary ECs isolated from FATP4 knockout mice (**a**) or CD36 knockout mice (**b**). **c-d**, FA uptake was measured in primary ECs isolated from FATP4 or CD36 knockout mice after exposure to Ct-CM or α-CM (**c**) or 3-HIB (**d**) for 1 hr. *p<.05 vs. control. #p<.05 vs. α-CM. Data are mean ± s.d. of at least three biological replicates.

well as potential regulators of fatty acid transport (PPARγ, Apelin) in endothelial cells after treatment with α-CM or 3-HIB. However, no significant change was observed in either gene (Figure 3.4a and b) or protein (Figure 3.5a and b) levels, suggesting that FATP3/4 function must

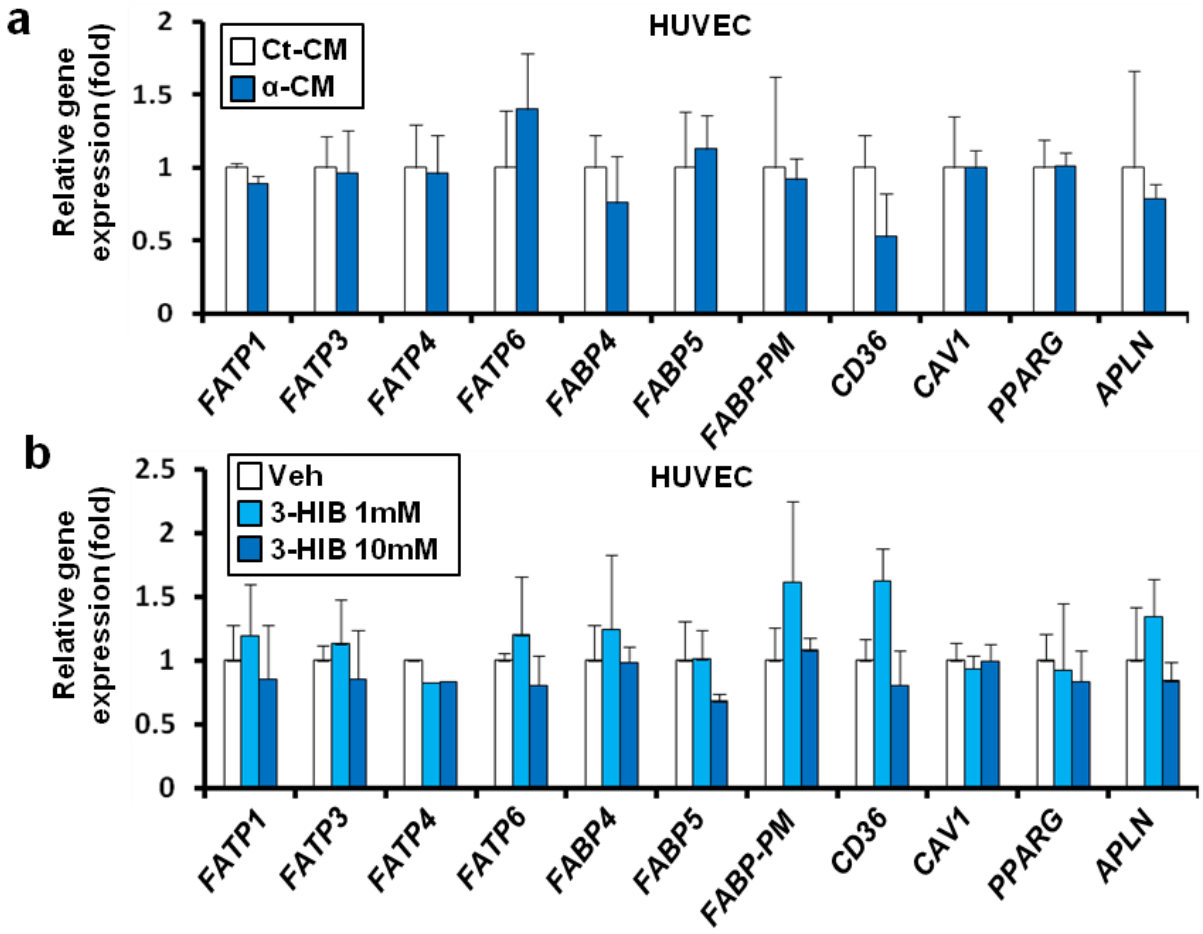


Figure 3.4: α-CM or 3-HIB does not affect expression of fatty acid transport-related genes. **a-b**, qPCR analysis of HUVECs after exposure to CMs (**a**) or 3-HIB (**b**) for 1 hr.

be affected by post-translational mechanisms. This conclusion is also consistent with our observation that only 15 min of α-CM treatment is sufficient to increase fatty acid uptake (Figure 2.7b), a speed of action best explained by post-translational mechanisms. Interestingly, these

observations also indicate that 3-HIB and VEGFB signaling converge on a common final

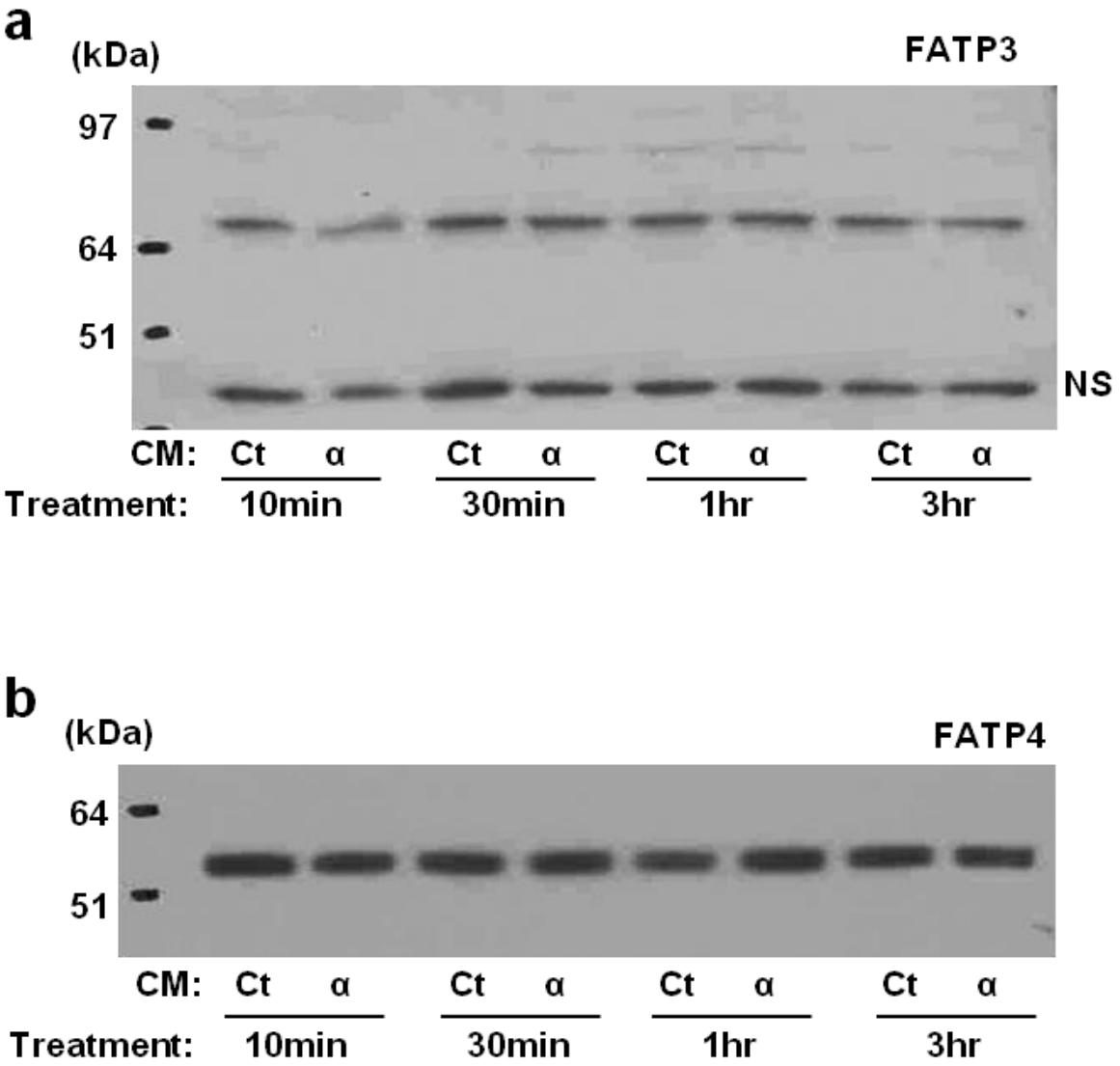


Figure 3.5: α-CM does not affect protein levels of FATP3 and FATP4. a-b, Western blot analysis of FATP3 (**a**) and FATP4 (**b**) in HUVECs after exposure to CMs for the indicated time. NS, non-specific bands.

effector pathway, FATP3/4, but via different transcriptional (VEGFB) versus post-translational (3-HIB) mechanisms.

Mice that transgenically overexpress PGC-1α or PGC-1β in skeletal muscle (MCKα and MCKβ mice) have been described (Lin J et al. 2002; Arany Z et al. 2007). The majority of genes that mediate valine catabolism are induced in the muscle of these mice (Figure 3.6a and c). The concentration of secreted 3-HIB is increased in skeletal muscle of MCKα mice (Figure 3.6b), which is consistent with increased gene expression of valine catabolic enzymes.

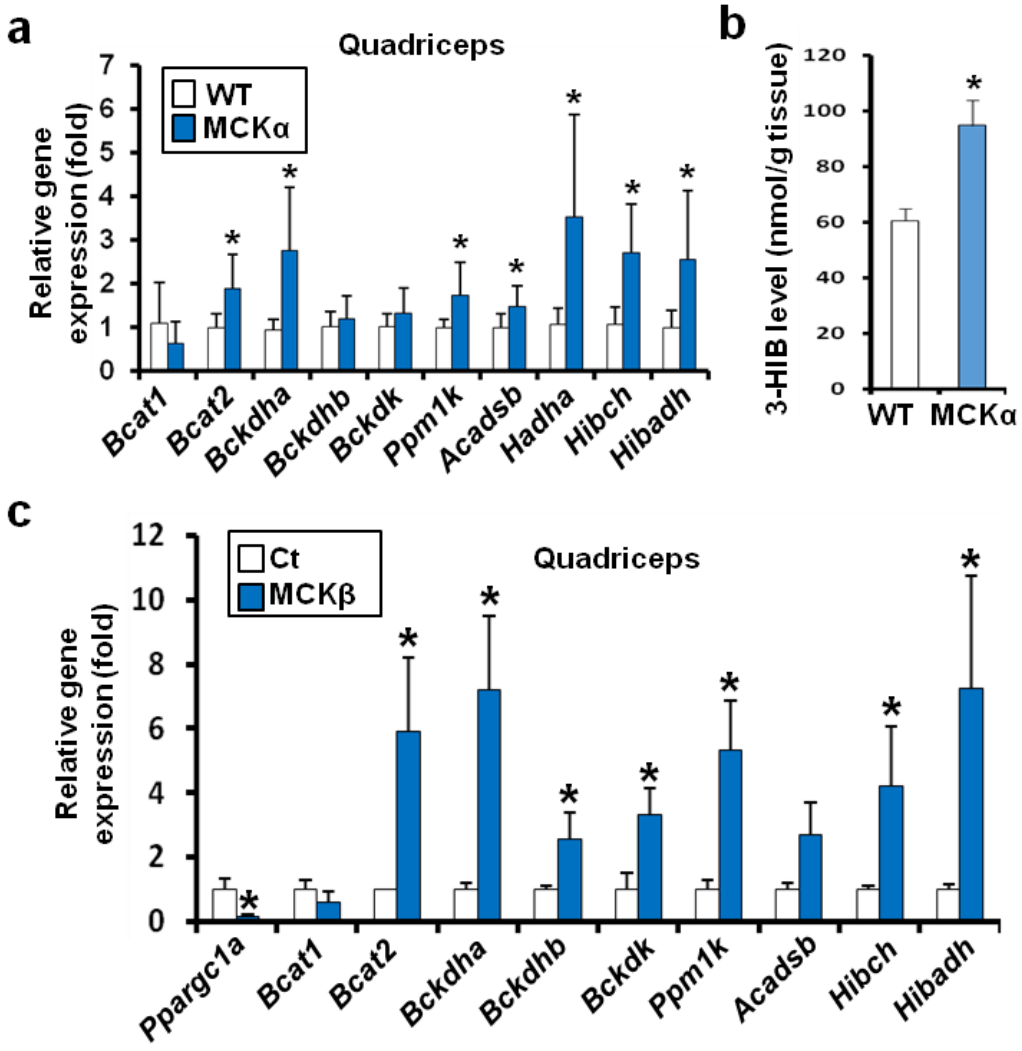


Figure 3.6: PGC-1α and PGC-1β in muscle regulate valine catabolic enzyme expression. a-b, PGC-1α in skeletal muscle induces many genes of valine catabolism (**a**, n=6) and increases 3-HIB levels (**b**, n=3). **c**, qPCR analysis of quadriceps skeletal muscle from control (Ct) or muscle-specific PGC-1β transgenic mice (MCKβ). *p<.05 vs. control. Data are mean ± s.d. (**a** and **c**) or ± s.e. (**b**).

On the other hand, these genes are highly repressed in mice lacking both PGC-1α and PGC-1β (double knockout or DKO mice) in skeletal muscle (Figure 3.7). To measure in real time and

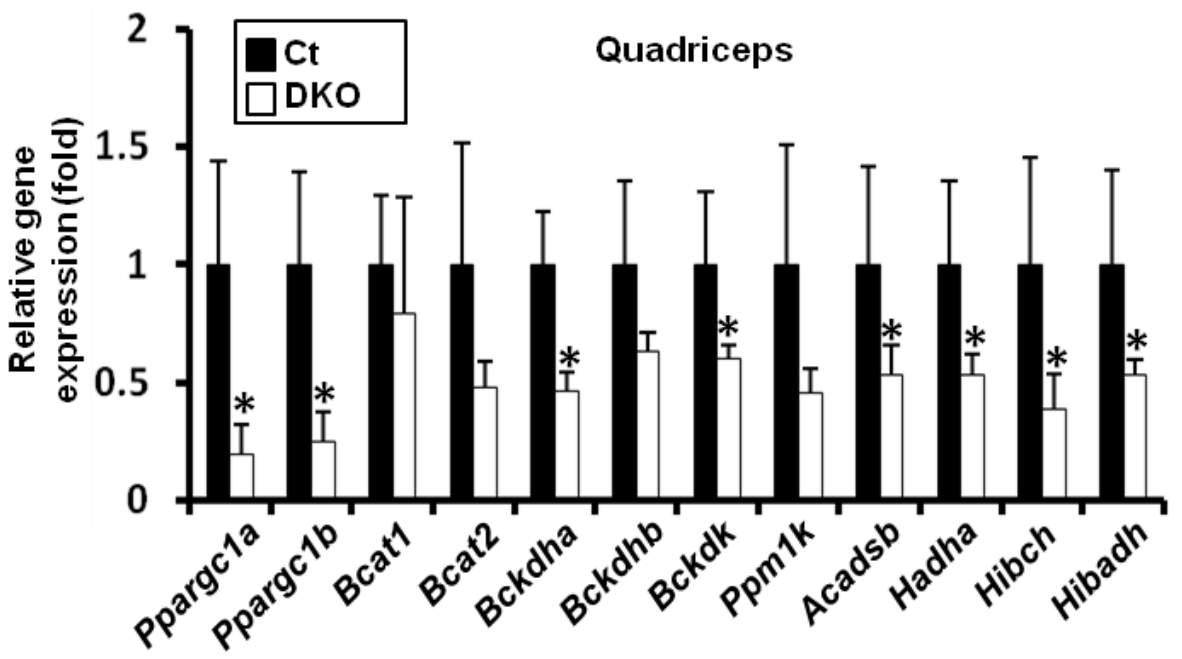


Figure 3.7: PGC-1α and PGC-1β cooperate to regulate valine catabolic enzyme expression. qPCR analysis of quadriceps skeletal muscle from control (Ct) or muscle-specific PGC-1α and PGC-1β double knockout mice (DKO). *p<.05 vs. control. Data are mean ± s.d. n=4.

noninvasively the uptake of fatty acids into skeletal muscle in MCKα mice, we employed a recently developed technique, in which mice ubiquitously expressing the luciferase enzyme are injected with luciferin substrate covalently linked to long chain fatty acids by a disulfide bond (Luc-S-S-FA) (Henkin AH et al. 2012). Upon entry of this substrate into cells, the disulfide bond is reduced by intracellular glutathione, and free luciferin is liberated to be consumed by luciferase, thus allowing for quantification via luminometry of fatty acid uptake *in vivo* (Figure 3.8a). Administration of Luc-S-S-FA to MCKα/Luciferase double transgenic mice demonstrated a dramatic increase in FA uptake in skeletal muscle, compared to single transgenic mice with luciferase alone (Figure 3.8b). These findings are thus consistent with the seemingly paradoxical

observation that MCKα mice accumulate excess lipid species in skeletal muscle, leading to lipotoxicity and insulin resistance (Choi CS et al. 2008). Since MCKβ mice similarly show

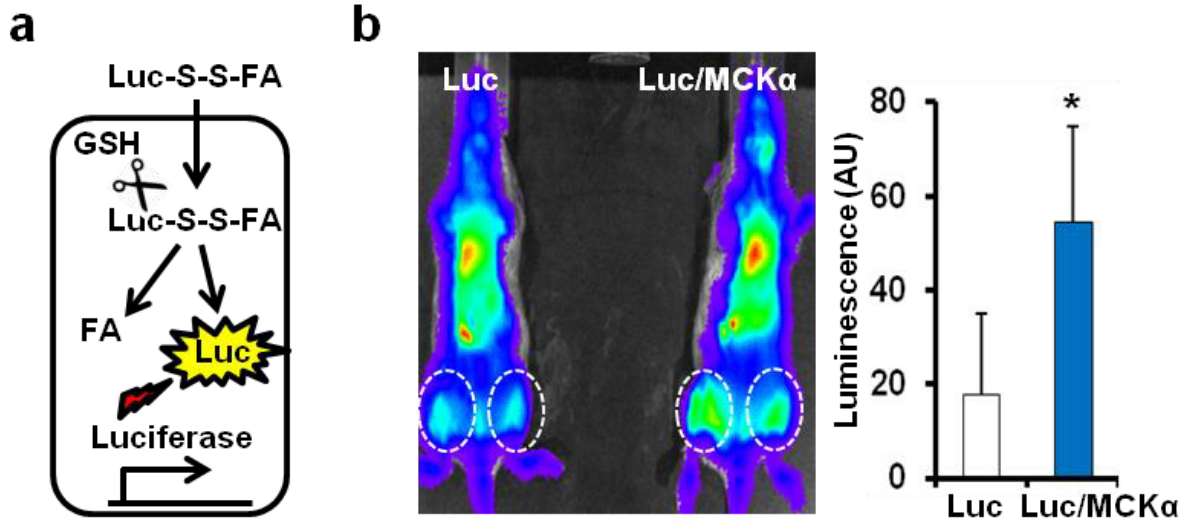


Figure 3.8: PGC-1α expression in muscle induces fatty acid uptake *in vivo*. a, Schematic of *in vivo* FA uptake assay. GSH, glutathione. **b**, Representative images (left) and quantification (right) of FA uptake in Luciferase (Luc) and Luc/MCKα double transgenic mice (n=4). *p<.05 vs. control. Data are mean ± s.d.

increased gene expression of valine catabolic enzymes, we have tested glucose homeostasis in MCKβ and DKO mice using intraperitoneal glucose tolerance test (IPGTT). Similar glucose intolerance was observed in MCKβ mice (Figure 3.9a). Conversely, glucose tolerance was improved in DKO mice (Figure 3.9b). Collectively, these data indicate that both PGC-1 co-activators control valine catabolism in muscle, which is important for the regulation of fatty acid trafficking into muscle and consequently glucose homeostasis.

To test if 3-HIB alone is sufficient to cause fatty acid accumulation *in vivo*, we provided 3-HIB in the food paste to Luciferase transgenic mice for 1.5 hours, which led to efficient

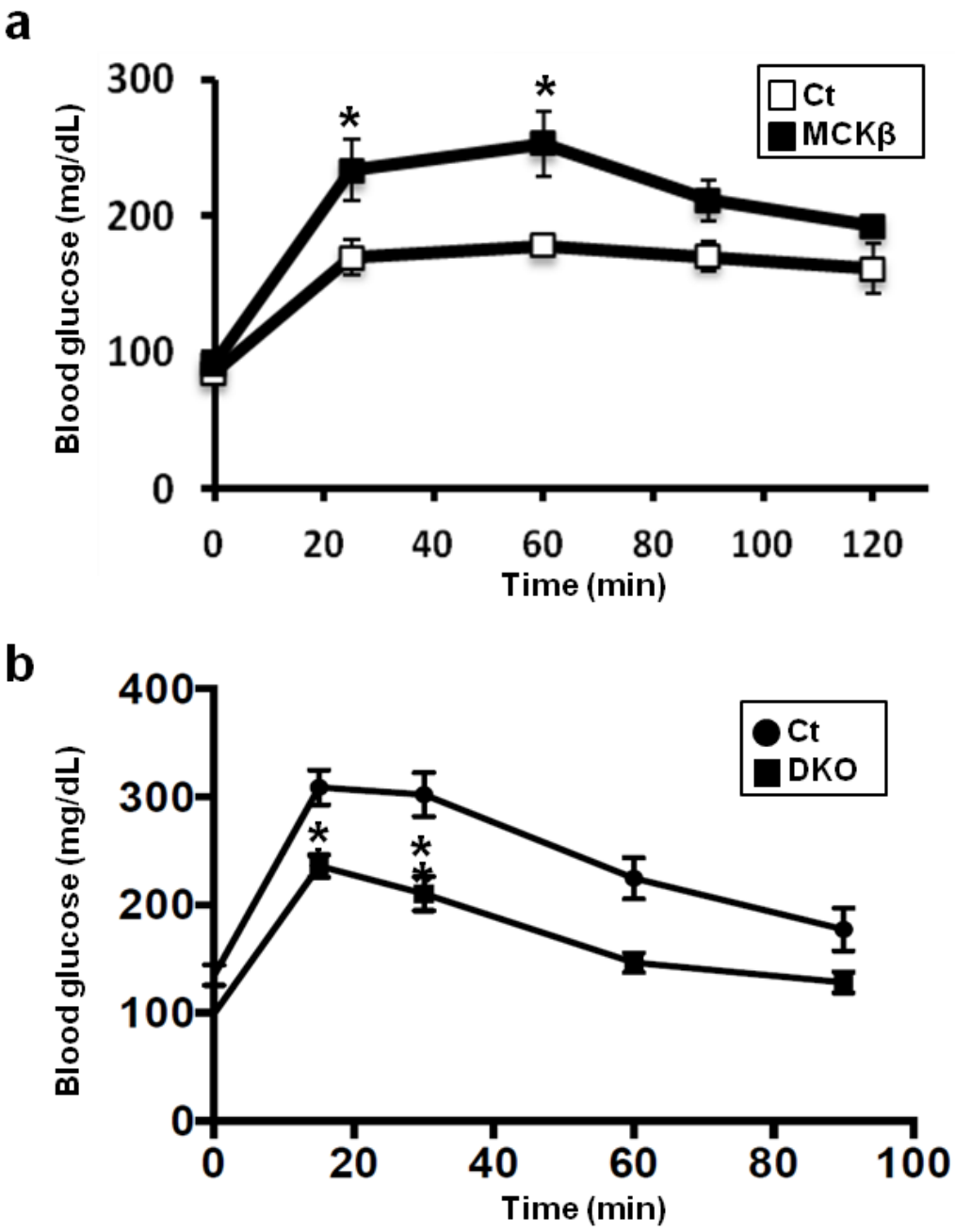


Figure 3.9: PGC-1α and PGC-1β in muscle regulate glucose tolerance. a-b, Glucose tolerance tests of MCKβ (**a**, n=5) and DKO mice (**b**, n=8). *p<.05 vs. control. Data are mean ±s.e.

accumulation of 3-HIB in the serum and skeletal muscle (Figure 3.10a). Imaging by luminometry after injection of the Luc-S-S-FA showed that 3-HIB feeding dramatically increased uptake of FAs into the heart and thigh (Figure 3.10b-d). To test if 3-HIB provision

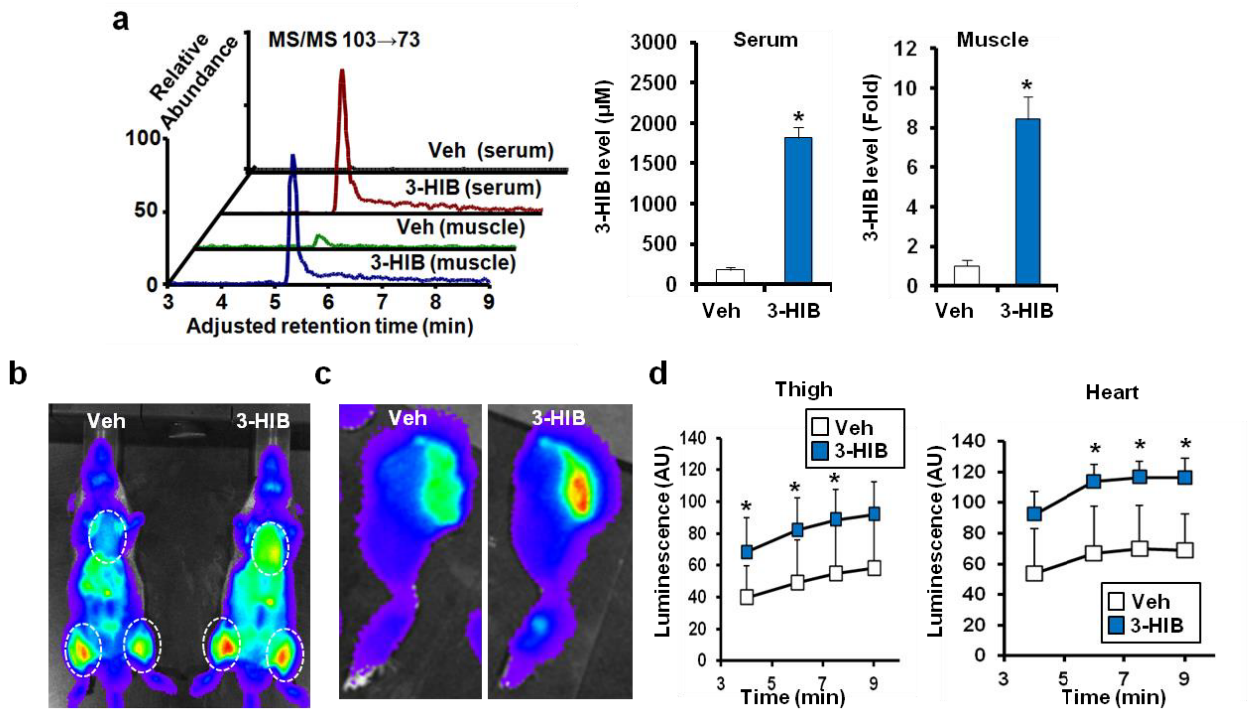


Figure 3.10: Acute feeding of mice with 3-HIB stimulates FA uptake by heart and thigh. a, Provision of vehicle (Veh) or 3-HIB in the food paste for 1.5 hr increased 3-HIB levels in serum (n=2, 3) and muscle (n=4, 6). **b-d**, Representative luminometry images of mice (**b**) and thigh muscle after removal of the skin (**c**) and quantification of luminescence (**d**, n=4). *p<.05 vs. control. Data are mean ± s.e.

affects vascular permeability/perfusion *in vivo*, we have injected Evans Blue (EB) intravenously and quantified EB leakage into muscle (Han ED et al. 2002). Mice fed with 3-HIB did not show any increase in EB penetrance into muscle compared to mice fed with vehicle (Figure 3.11a), demonstrating that 3-HIB feeding does not alter endothelial cell permeability *in vivo*. Histological sections of muscle isolated from mice fed with 3-HIB for 2 weeks showed no

obvious morphological differences between control and 3-HIB fed groups (Figure 3.11b). These

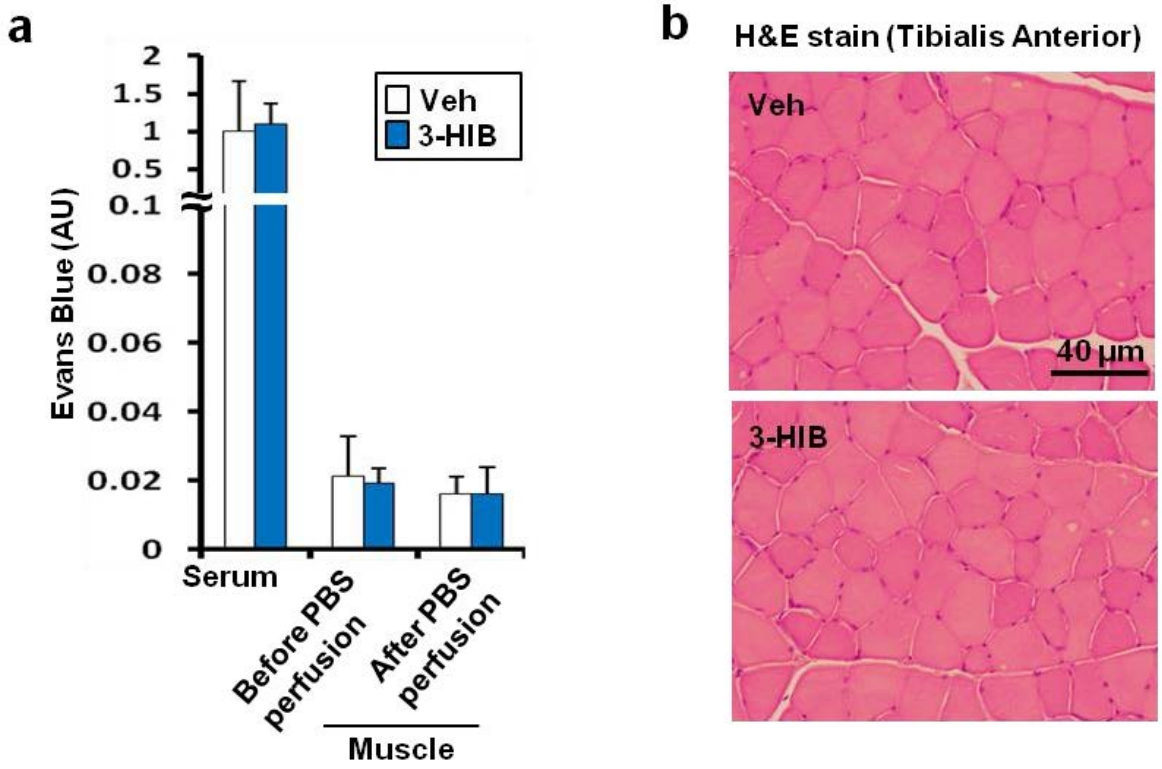


Figure 3.11: Acute feeding of mice with 3-HIB does not affect vessel permeability or damage muscle. a, Quantification of Evans Blue in serum and skeletal muscle before or after PBS perfusion of the mice fed with vehicle (Veh) or 3-HIB (n=3) for 1.5 hours. **b**, Representative images of hematoxylin and eosin staining of muscle cross sections of the mice fed with vehicle (Veh) or 3-HIB for two weeks.

results indicate that increased levels of 3-HIB in muscle induces fatty acid entry into muscle without damaging blood vessels or myocytes.

We next sought to investigate a long-term effect of 3-HIB feeding on muscle lipid and whole body glucose homeostasis. No difference in body weight gain was observed between vehicle- and 3-HIB-fed mice after feeding for two weeks, suggesting that 3-HIB feeding is not toxic (Figure 3.12a). Then, we performed lipidomics analysis with skeletal muscle isolated from

these mice. Surprisingly, there was significant excess accumulation of triglycerides (TAG)

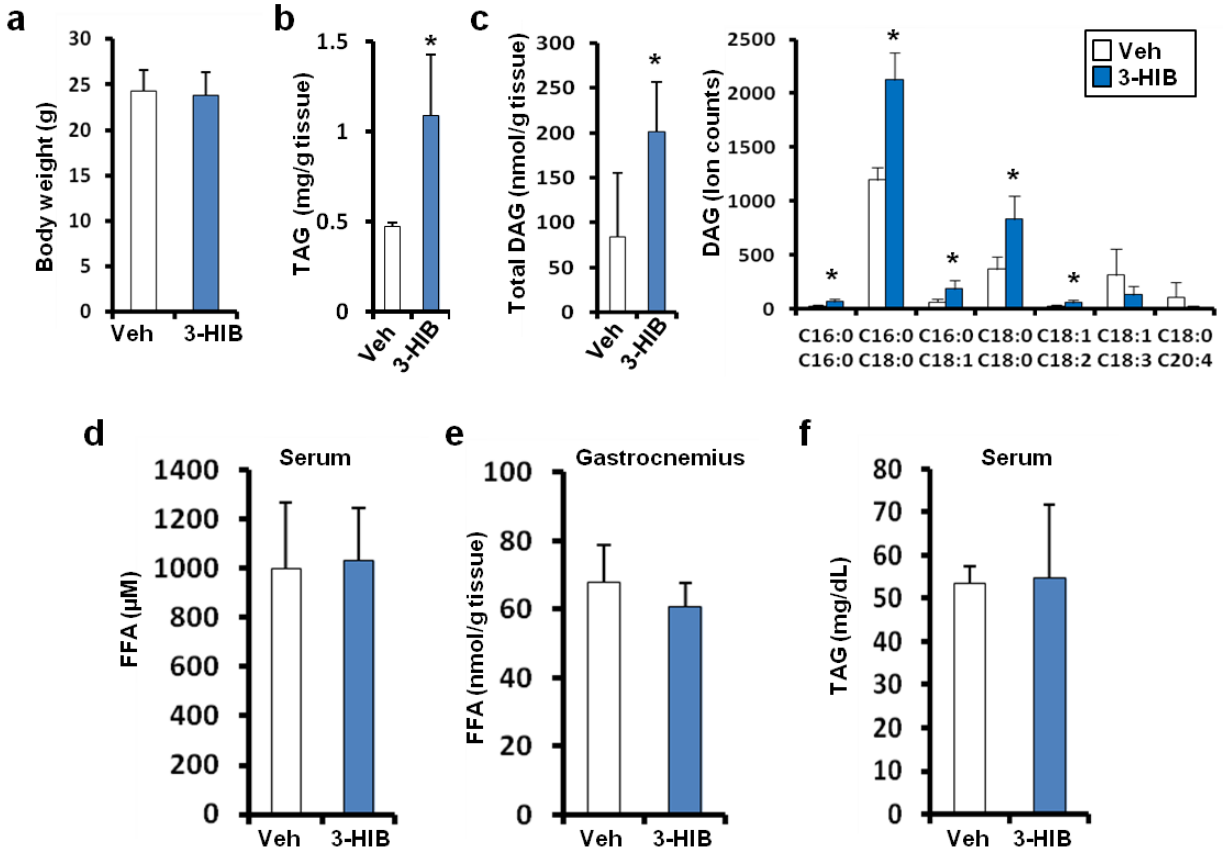


Figure 3.12: Effect of two-week 3-HIB feeding on FA metabolism. a, Provision of vehicle (Veh) or 3-HIB in the drinking water for 2 weeks does not show any significant change in body weight. **b-c**, 3-HIB provision increases TAG (**b**, n=3) and DAG (**c**, n=4) in skeletal muscle. **d-f**, 3-HIB provision does not affect levels of free FA (FFA) in serum (**d**) or in skeletal muscle (**e**), or TAG levels in serum (**f**). *p<.05 vs. control. Data are mean ± s.d. (n=4).

and diglycerides (DAG) species in skeletal muscle in 3-HIB-fed mice (Figure 3.12b and c), despite the absence of any increase in plasma fatty acids or TAG levels (Figure 3.12d-f). Increased accumulation of DAG species is known to stimulate plasma membrane translocation of PKC (Szendroedi J et al. 2014). The plasma membrane localization of PKC is important for its activation, which inhibits insulin signaling by phosphorylating insulin receptor substrate-1 (IRS-1) (Yu C et al. 2012). Therefore, we performed subcellular fractionation experiments to examine

the localization of PKCθ in 3-HIB-fed mouse muscle. As shown in Figure 3.13a and b, the plasma membrane localization of PKCθ was increased in muscle from 3-HIB fed mice. In addition, phosphorylation of Akt was blunted in mice treated with 3-HIB (Figure 3.14a),

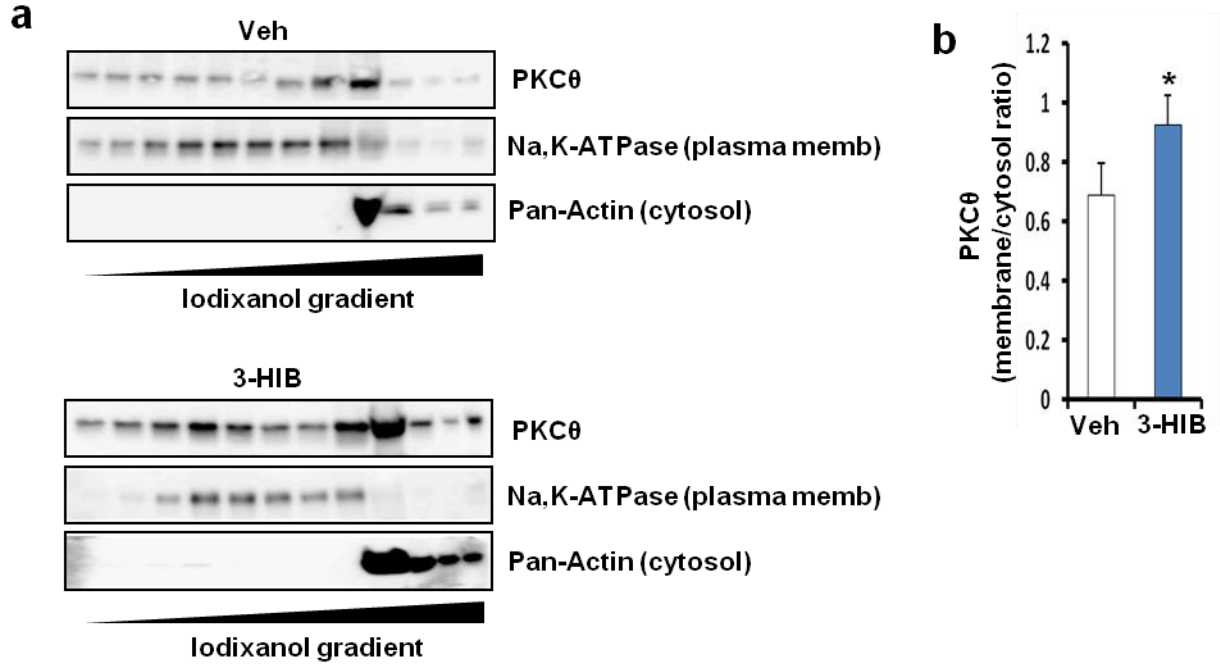


Figure 3.13: 3-HIB induces PKCθ membrane translocation in muscle. a, Western blot analysis of quadriceps skeletal muscle from the mice fed with vehicle (Veh) or 3-HIB after subcellular fractionation using an iodixanol gradient. **b**, Quantification of PKCθ membrane translocation (n=4).*p<.05 vs. control. Data are mean ± s.d.

consistent with the inhibition of insulin signaling by DAG and activated PKCθ. These results show that prolonged feeding of mice with 3-HIB can cause lipotoxicity phenotypes in skeletal muscle. Finally, the mice fed with 3-HIB for two weeks revealed a diminished ability to clear a glucose load from the blood, as revealed by IPGTT experiments (Figure 3.14b). Since IPGTT measures systemic glucose homeostasis (including gluconeogenesis in the liver and glucose uptake by other organs such as adipose tissues, brain, and kidney) instead of muscle glucose

uptake, we have performed hyperinsulinemic-euglycemic clamp on mice provided with 3-HIB

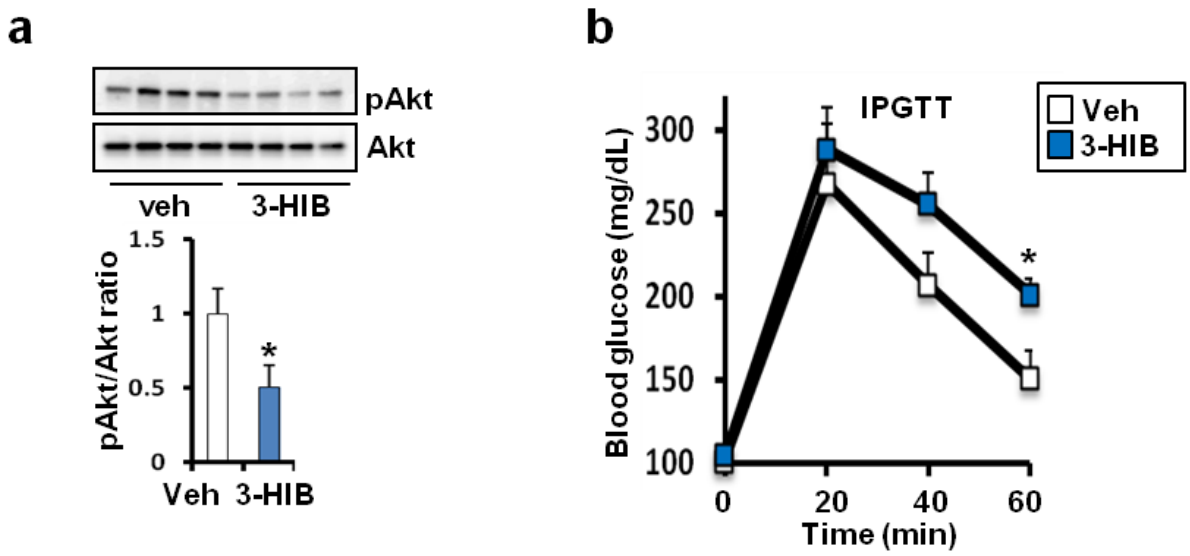


Figure 3.14: 3-HIB reduces Akt signaling and induces glucose intolerance. a, Western blot analysis of quadriceps skeletal muscle from the mice fed with vehicle (Veh) or 3-HIB. Gel images (top) and quantification (bottom, n=4). **b**, Intraperitoneal glucose tolerance test (IPGTT) of the mice fed with vehicle (Veh) or 3-HIB (n=8). *p<.05 vs. control. Data are mean ± s.e.

in drinking water for two weeks, compared to vehicle-fed controls. As shown, 3-HIB-fed mice had significantly lower glucose infusion rates, as well as a strong trend towards lower muscle glucose uptake (Figure 3.15a-c). 3-HIB thus causes systemic and muscle insulin resistance. Neither hepatic gluconeogenesis gene expression nor glucose output was significantly different (Figure 3.15d and e), suggesting that 3-HIB has little impact on hepatic function. Together, these data demonstrate that paracrine secretion of 3-HIB, an intermediate of BCAA catabolism, induces FA uptake *in vivo*, and causes excess accumulation of incompletely esterified lipids in skeletal muscle, blunted Akt signaling, and glucose intolerance.

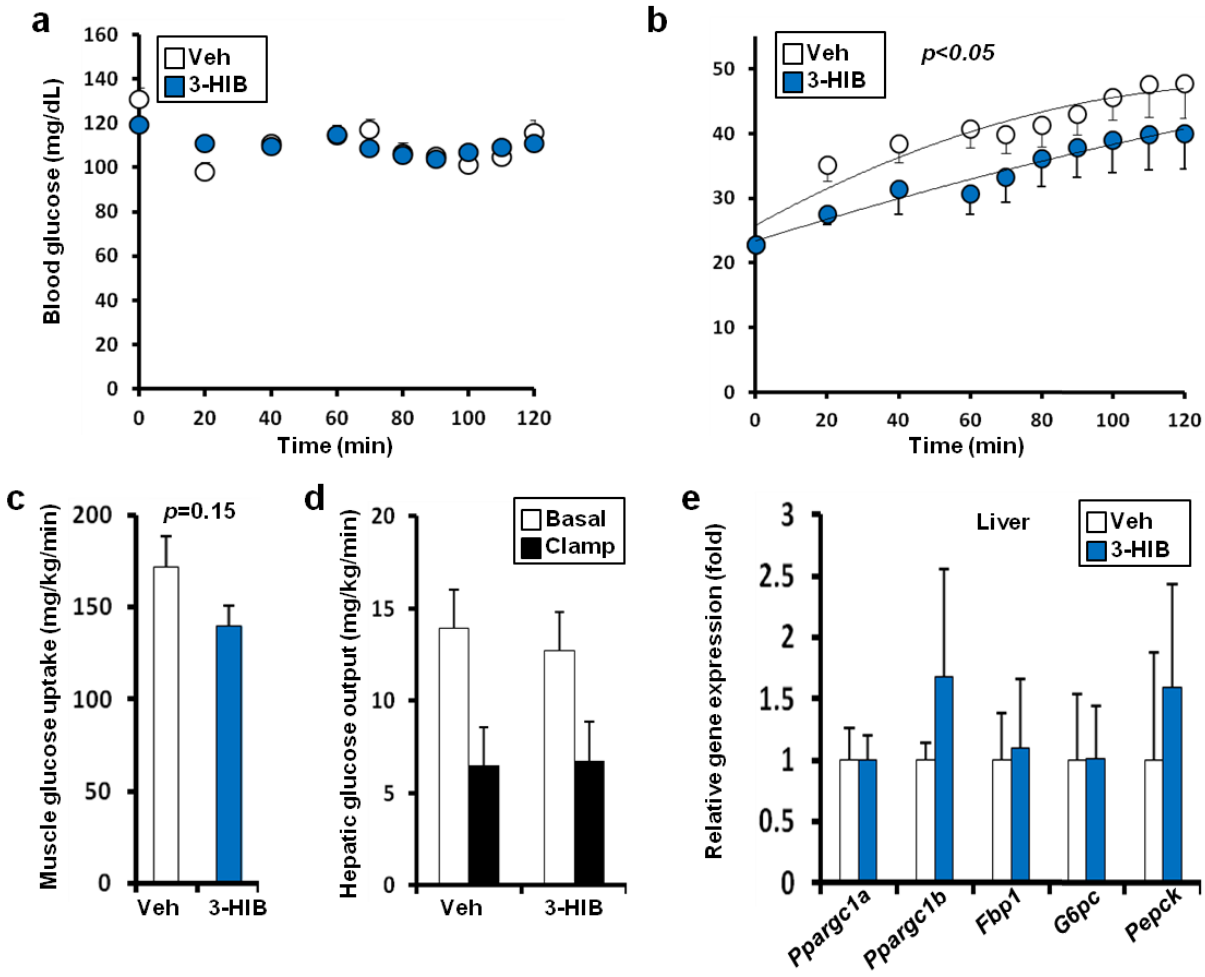


Figure 3.15: Mice fed with 3-HIB for 2 weeks show systemic insulin resistance. a-d, Blood glucose levels (**a**), glucose infusion rate (**b**), skeletal muscle glucose uptake (**c**), and hepatic glucose output (**d**) were measured by the hyperinsulinemic-euglycemic clamp on the mice fed with vehicle (Veh) or 3-HIB for 2 weeks. **e**, qPCR analysis of the liver from the mice fed with vehicle (Veh) or 3-HIB for 2 weeks. p<.05 by ANOVA analysis in **b**. Data are mean ± s.e. (n=8).

BCAA levels in blood are fluctuating during the fed-fast cycle, and catabolism of BCAA is dependent on energy status of skeletal muscle (Lynch CJ and Adams SH. 2014). To examine if the physiological levels of 3-HIB are also fluctuating during the fed-fast cycle, we measured plasma and skeletal muscle levels of 3-HIB in mice in the fasting, postprandial, and insulin-stimulated conditions. Fasted mice (for 16 hours) showed 2.5-fold higher 3-HIB levels in muscle

and plasma, compared to postprandial mice (2 hours after refeeding), and 3.3-fold higher compared to *ad lib* mice (Figure 3.16a and b). This observation is consistent with increased

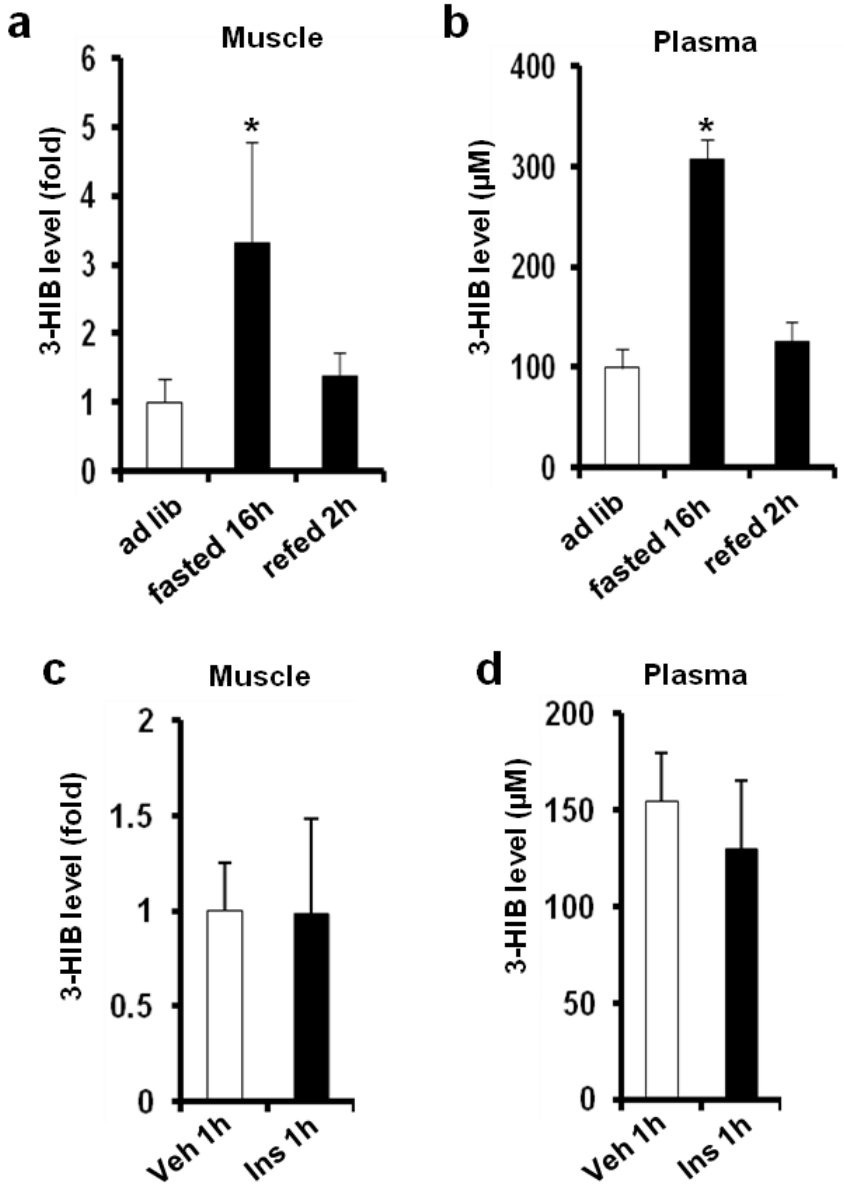


Figure 3.16: Fasting increases muscle and plasma levels of 3-HIB. a-b, Quantification of 3-HIB in muscle (**a**) and plasma (**b**) of the mice fasted for 16 hr or refed for 2 hr after fasting. **c-d**, Quantification of 3-HIB in muscle (**c**) and plasma (**d**) of the mice injected with insulin (0.5U/kg) for 1 hr after fasting for 3 hr. *p<.05 vs. control. Data are mean ± s.d. (n=5).

catabolism of protein and amino acids in skeletal muscle during prolonged fasting, and with the notion that 3-HIB acts as a signal to increase fatty acid import in the context of insufficient nutrients. Similarly, 3-HIB was increased 5-fold in serum of humans fasted for 72 hours (Avogaro A and Bier DM. 1989). On the other hand, stimulation of mice with physiological levels of insulin (0.5 U/kg injection for 1 hour after fasting for 3 hours) did not significantly affect plasma or muscle 3-HIB levels (Figure 3.16c and d), consistent with the idea that insulin does not acutely affect the process.

Discussion

Valine is one of three branched-chain amino acids (BCAAs), all three of which are essential dietary components. BCAAs are abundant, comprising up to 30% of muscle protein. Catabolic flux of the three BCAAs is tightly regulated, and skeletal muscle is one of the key sites of BCAA catabolism, unlike that of other amino acids, which primarily occurs in the liver. Interestingly, all intermediate products of catabolism of all three branched-chain α-keto acids are trapped inside the cell by covalent linkage to Co-enzyme A (CoA), with the single exception of 3-HIB (Figure 2.1). 3-HIB is thus ideally suited to act as a secreted reporter of BCAA catabolic flux in muscle. Excess BCAA catabolic flux has recently been implicated in the progression to diabetes both in rodents and human (Wang TJ et al. 2007; Newgard CB. 2012). Data from the Framingham Heart Study, for example, show that elevated BCAAs in blood precede the onset of diabetes by decades (Wang TJ et al. 2007). A mechanistic explanation for these observations has been lacking. Our data indicate that increased catabolic flux of BCAAs can cause the secretion of 3-HIB from muscle, leading to excess trans-endothelial FA import into muscle, accumulation of lipotoxic incompletely esterified intermediates like DAG, and blunted insulin signaling. Consistent with this notion, we found highly increased levels of 3-HIB in skeletal muscle from

db/*db* mice (Figure 3.17a) and muscle biopsies from diabetic patients (Figure 3.17b). Elevated 3-

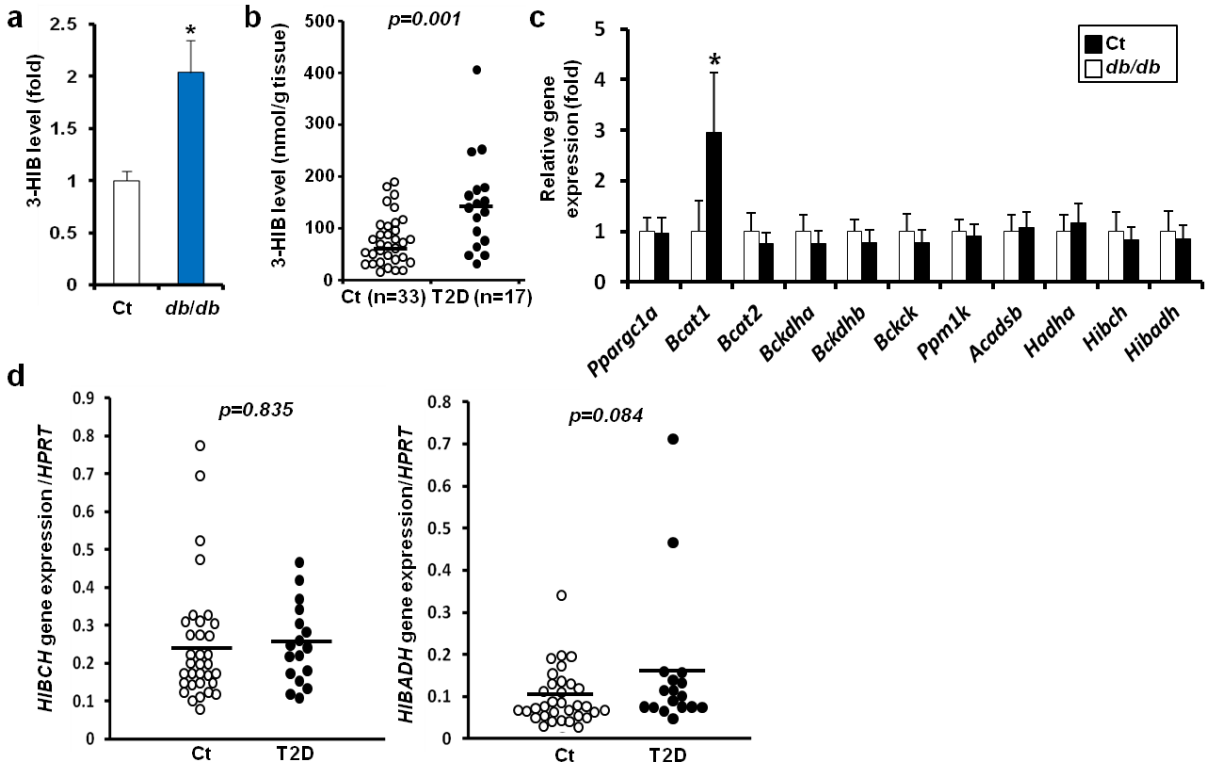


Figure 3.17: 3-HIB is increased in muscle of *db*/*db* mice and human diabetic patients. a-b, Quantification of 3-HIB in muscle from *db*/*db* mice (**a**, n=8) or muscle biopsies from type II diabetic (T2D) patients (**b**). **c-d**, qPCR analysis of muscle from db/db mice (**c**, n=8) or muscle biopsies from T2D patients (**d**). *p<.05 vs. control. Data are mean ± s.d.

HIB in serum of diabetic patients has also been reported (Avogaro A and Bier DM. 1989; Giesbertz P et al. 2015). Patients with severe 3-HIB aciduria and significant neurological sequelae have also been described (Sasaki M et al. 2001), but their glucose homeostasis has not been reported. These increases in 3-HIB levels are unlikely to be explained by altered gene expression, because HIBCH and HIBADH mRNA expression in muscle was not significantly different in *db*/*db* mice or type 2 diabetic patients (Figure 3.17c and d). It is possible that post-transcriptional regulation is involved – e.g. reduced HIBADH protein levels in type 2 diabetic rat muscle, as noted previously (Mullen E and Ohlendieck K. 2010). Interestingly, a recent analysis

of gene expression omnibus (GEO) database and small nucleotide polymorphisms (SNPs) associated with type II diabetes identified HIBADH as one of two genes that are both differentially expressed in type II diabetes (Chen J et al. 2013; Deng WJ et al. 2010) and have diabetes-associated SNPs. Two SNPs were identified close to the genomic region of HIBADH. Whether these SNP alleles affect expression of HIBADH requires more investigation such as expression quantitative trait loci (eQTLs). In summary, our mouse and human data demonstrate that 3-HIB levels are strongly induced in muscle of subjects with type II diabetes.

We found that fasting increases 3-HIB levels both in blood and skeletal muscle, similar to the diabetic condition. Then, why 3-HIB does not trigger insulin resistance in skeletal muscle upon fasting? High 3-HIB levels under normal conditions likely reflect active catabolism in muscle (e.g. fasting or exercise) and we propose that increased 3-HIB contributes to better fatty acid trafficking into muscle in these physiological conditions. Consistent with the induction of PGC-1α upon exercise, it has been incidentally noted that 3-HIB levels are increased after exercise in mouse muscle (Overmyer KA et al. 2015) and human urine (Pechlivanis A et al. 2010). Increased levels of 3-HIB during fasting or exercise do not trigger pathological insulin resistance because fasting or exercised muscle consumes the fat that is delivered, and thus fat accumulation or lipotoxicity does not happen. On the other hand, increased 3-HIB levels in muscle can be a pathological driver of insulin resistance if it occurs in the context of excess supply of dietary fat and/or reduced consumption of fatty acids (e.g. the fed, sedentary state). Combination of these factors (higher dietary fat, higher muscle 3-HIB also in part due to higher BCAA consumption, combined with lower muscle fat oxidation due to sedentary behavior and uninterrupted feeding) conspire to aberrant fat accumulation in muscle, lipotoxicity, and

eventually insulin resistance. In other words, lipid delivery desynchronized with consumption leads to lipotoxicity. Consistent with this idea, the PGC-1α transgenic animals, which are insulin resistant at baseline, become even more insulin sensitive than controls after an exercise regimen.

It has been suggested that BCAA catabolism is accomplished through a metabolite shuttle between the liver and muscle. We confirmed that liver cells express almost no BCATs, supporting the notion that transamination of BCAAs primarily happens in muscle (Figure 3.18a). We also compared gene expression of BCKDH subunits between the liver and various subtypes of muscle. Both BCKDH-A and BCKDH -B levels in muscle are comparable to those in the liver (Figure 3.18b).

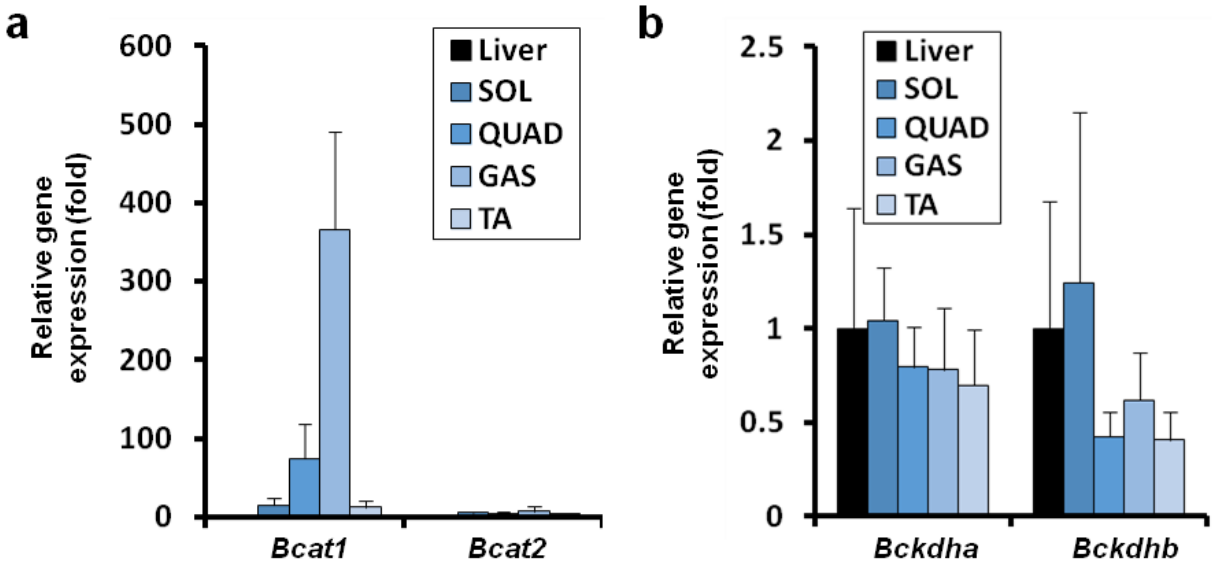


Figure 3.18: Comparison of BCAT and BCKDH gene expression between the liver and muscle subtypes. a-b, qPCR analysis of the liver and various subtypes of skeletal muscle. SOL, soleus; QUAD, quadriceps; GAS, gastrocnemius; TA, tibialis anterior. n=5.

Nevertheless, it is controversial which organ (liver or muscle) is the major site for further catabolism of alpha-keto acids generated by BCAT activity in muscle. The absolute BCKDH

activity is much higher (about 200 fold) in the liver than muscle in rats because of low BCKDK inhibitory activity in the liver (Suryawan A et al. 1998). Surprisingly, this is not the case in human and monkey - the absolute BCKDH activity is only slightly lower (only 3 fold) in muscle than that in the liver in human (Suryawan A et al. 1998). A key point to be noted is that humans do not have a storage mechanism for excess BCAA (unlike fats in adipose tissue), which therefore must be catabolized somewhere. Whole-body muscle mass greatly exceeds that of the liver, and thus the capacity of muscle BCAA catabolism in humans is dramatically higher relative to the liver than in rodents (muscle:liver is 29:60% in mouse, versus 66:9% in human (Suryawan A et al. 1998). Consistent with this, it has been reported that skeletal muscle contributes considerably to whole body BCKDH activity (Brosnan JT and Brosnan M. 2006). It is interesting why there is such a difference in BCKDH activity between rodents and humans. Nonetheless, we found very similar concentrations of 3-HIB in skeletal muscle from mice and human (Figure 3.6b and 3.17b), conclusively demonstrating that catabolism of valine is occurring in skeletal muscle. Thus, catabolism in human muscle is critical even if the capacity is lower than rodents.

More importantly, in diabetic patients, BCKDH expression and/or activity is severely abrogated in the liver and adipose tissue but not in muscle (She P et al. 2007; Kuzuya T et al. 2008; Lynch CJ and Adams SH. 2014). Therefore, the contribution of skeletal muscle to whole body BCKDH activity is most likely significantly induced in type II diabetes, and circulating alpha-keto acids will be shuttled back to muscle and further catabolized in muscle, resulting in increased 3-HIB production in muscle. This notion is consistent with our new finding that 3-HIB levels are higher in muscles from *db*/*db* mice and type II diabetes patients (Figure 3.17a and b).

We found that FATP3 and FATP4, but not CD36, play major roles in mediating 3-HIB-dependent fatty acid uptake in ECs. On the other hand, treatment of SSO, which mainly blocks CD36 (Kuda O et al 2013), efficiently blocks endothelial fatty acid transport induced by α-CM (Figure 2.8c). SSO is a membrane-impermeable sulfo-N-hydroxysuccinimidyl (NHS) ester of oleate. Its NHS moiety can react with primary or secondary amines (nucleophiles) to yield stable amide or imide bond. Therefore, in principle, any primary amino-terminal and ϵ-amino groups in lysine side chains of proteins that bind to fatty acids on the plasma membrane or proteins in the lipid rafts can be the target of SSO, including CD36 (Pohl J et al. 2005; Kuda O et al. 2013). Consistent with this notion, SSO blocks fatty acid incorporation into triglycerides in CD36 knockout cells as much as it does in wild type cells, questioning the specificity of the inhibitor (Holloway GP et al. 2009; Drahota Z et al. 2010; Nicholls HT et al. 2011). Thus, SSO likely blocks endothelial FA transport through inhibition of both CD36 and other, yet poorly defined, fatty acid transporter proteins, perhaps including FATP3 and/or 4.

Materials & Methods

Quantitative RT-PCR (qPCR). mRNA was isolated using a TurboCapture mRNA kit (Qiagen) and reverse-transcribed with an RT kit (Applied Biosystems) according to the manufacturers' protocols. Primers used for qPCR are below.

Mouse Bcat1 forward	CCCATCGTACCTCTTTCACCC
Mouse Bcat1 reverse	GGGAGCGTGGGAATACGTG
Mouse Bcat2 forward	CTCATCCTGCGCTTCCAG
Mouse Bcat2 reverse	TCACACCCGAAACATCCAATC
Mouse Bckdha forward	ATCTACCGTGTCATGGACCG
Mouse Bckdha reverse	ATGGTGTTGAGCAGCGTCAT
Mouse Bckdhb forward	AGCTATTGCGGAAATCCAGTTT
Mouse Bckdhb reverse	ACAGTTGAAAAGATCACCTGAGC
Mouse Bckdk forward	ACATCAGCCACCGATACACAC
Mouse Bckdk reverse	GAGGCGAACTGAGGGCTTC
Mouse Ppm1k forward	ATGTTATCAGCGGCCTTCATTAC
Mouse Ppm1k reverse	GTGGAGAAGTAGCAGGCAGG
Mouse Acadsb forward	TGGGTCGAAGATGTGGATCAG
Mouse Acadsb reverse	TCGGTCTACTAAGAAGCAGGTG
Mouse Hadha forward	TGCATTTGCCGCAGCTTTAC
Mouse Hadha reverse	GTTGGCCCAGATTTCGTTCA
Mouse Hibch forward	GTGGAGGCGTCATAACGCTC

Mouse Hibch reverse	AGGAATGTGTCAGGGTCTTGT
Mouse Hibadh forward	GCAGCGGTGTGTTCTAGGTC
Mouse Hibadh reverse	ACACGTCATAGAGGATGAGTGG
Mouse Vegfa forward	CTGTAACGATGAAGCCCTGGAG
Mouse Vegfa reverse	TGGTGAGGTTTGATCCGCAT
Mouse Vegfb forward	GGTTGCCATACCCCACCACC
Mouse Vegfb reverse	CCTTGGCAATGGAGGAAGCG
Mouse Flt1 forward	CCTGCATGATTCCTGATTGGA
Mouse Flt1 reverse	GCCTAAGCTCACCTGCGG
Mouse Flk1 forward	GACTTGGTTCATCAGGCTAG
Mouse Flk1 reverse	GACGCTGTTAAGCTGCTACAC
Mouse Ppargc1a forward	AGCCGTGACCACTGACAACGAG
Mouse Ppargc1a reverse	GCTGCATGGTTCTGAGTGCTAAG
Mouse Ppargc1b forward	CTCCAGGCAGGTTCAACCC
Mouse Ppargc1b reverse	GGGCCAGAAGTTCCCTTAGG
Mouse Fbp1 forward	TATGGTGGAAAGGGACGGGAA
Mouse Fbp1 reverse	CCTCTGGTGATACTCAAGGATGG
Mouse G6pc forward	TGCAAGGGAGAACTCAGCAA
Mouse G6pc reverse	GGACCAAGGAAGCCACAATG
Mouse Pepck forward	TTGAACTGACAGACTCGCCCT
Mouse Pepck reverse	TGCCCATCCGAGTCATGA
Mouse Ivd forward	GGACGGCGAGTTTCCAGTT
Mouse Ivd reverse	CCACAGGCAATATCGAGTGGG

Mouse Mccc1 forward	GGGTGATACGAACAGCCAAAA
Mouse Mccc1 reverse	GGGTGATACGAACAGCCAAAA
Mouse Auh forward	TGCTCGGGATTAACAGAGCTT
Mouse Auh reverse	TCCACCGCTTTTGATAACATCTT
Mouse Hmgcl forward	GGTCTCCCCGGCTAAAGTTG
Mouse Hmgcl reverse	GCCAGAGCTTGACCATAGGTAT
Mouse Hsd17b10 forward	GCTTGGTCGCGGTAGTAACTG
Mouse Hsd17b10 reverse	TGGGGCAAATATGCAGCTTTC
Mouse Acat1 forward	CAGGAAGTAAGATGCCTGGAAC
Mouse Acat1 reverse	TTCACCCCCTTGGATGACATT
Human FATP1 forward	TCTATGGGGTGGCTGTTCCA
Human FATP1 reverse	TCAAACCCTCTCGCTGCA
Human FATP3 forward	AGAGACCTTCAAACAGCAGAAAG
Human FATP3 reverse	GTCCAGAACGTACAGTGGGT
Human FATP4 forward	AGGCAAAGGTGCGACAGTG
Human FATP4 reverse	CCAGTGGGTATCTGTGCCC
Human FATP6 forward	ACAACCTCGGAAACCTTTCATC
Human FATP6 reverse	CCCCTTTTTCAGAGAGGAATGG
Human FABP4 forward	AGCACCATAACCTTAGATGGGG
Human FABP4 reverse	CGTGGAAGTGACGCCTTTCA
Human FABP5 forward	TTGGTTCAGCATCAGGAGTG
Human FABP5 reverse	GATCCGAGTACAGGTGACATTG

Human FABP-PM forward	ATTTGGACAAGGAATACCTGCC
Human FABP-PM reverse	GCCACTCTTCAAGACTTCGC
Human CD36 forward	GCCAAGGAAAATGTAACCCAGG
Human CD36 reverse	GCCTCTGTTCCAACTGATAGTGA
Human CAV1 forward	CATCCCGATGGCACTCATCTG
Human CAV1 reverse	CACGGCTGATGCACTGAATCT
Human PPARG forward	ACCAAAGTGCAATCAAAGTGGA
Human PPARG reverse	AGGCTTATTGTAGAGCTGAGTCT
Human APLN forward	GTCTCCTCCATAGATTGGTCTGC
Human APLN reverse	GGAATCATCCAAACTACAGCCAG
Human FLK1 forward	GGCCCAATAATCAGAGTGGCA
Human FLK1 reverse	TGTCATTTCCGATCACTTTTGGA
Human BCAT1 forward	AGCCCTGCTCTTTGTACTCTT
Human BCAT1 reverse	CCAGGCTCTTACATACTTGGGA
Human BCAT2 forward	CGCTCCTGTTCGTCATTCTCT
Human BCAT2 reverse	CCCACCTAACTTGTAGTTGCC
Human BCKDHA forward	CTACAAGAGCATGACACTGCTT
Human BCKDHA reverse	CCCTCCTCACCATAGTTGGTC
Human BCKDHB forward	TGGAGTCTTTAGATGCACTGTTG
Human BCKDHB reverse	CGCAATTCCGATTCCAAATCCAA
Human BCKDK forward	GACTTCCCTCCGATCAAGGAC
Human BCKDK reverse	CTCTCACGTAGGCCCTCTG
Human PPM1K forward	ATAACCGCATTGATGAGCCAA

Human PPM1K reverse	CGCACCCCACATTTTCCAAG
Human ACADSB forward	GATGGCAAATGTAGACCCTACC
Human ACADSB reverse	AAGGCCCGGAGTATCACGA
Human HADHA forward	CTGCCCAAAATGGTGGGTGT
Human HADHA reverse	GGAGGTTTTAGTCCTGGTCCC
Human HIBCH forward	TGGTTCTTGCCAGAAACCTTATG
Human HIBCH reverse	GTAGCCACTCGAAATTGCCCA
Human HIBADH forward	TGCTGCCCACCAGTATCAATG
Human HIBADH reverse	GCAGGATCAATAGTGCTGGAATC

Subcellular fractionation. All procedures were performed on ice. Fresh or frozen muscle (~150 mg) was minced with scissors and homogenized with a Dounce homogenizer (Corning, PYREX 2ml, 30 strokes) in 1.3 mL homogenization buffer (0.1 M sucrose, 10 mM EDTA, 46 mM KCl, 5 mM NaN3, 100 mM Tris-HCl pH 7.4 and protease inhibitors). The samples were then centrifuged at 4,000 g for 10 min at 4 °C to precipitate nuclear fractions and cell debris. The supernatant (1 mL) was then collected and mixed with 0.33 mL Opti-Prep (Sigma D1556, 60% iodixanol) to make a 15% iodixanol solution. Then, 1.33 mL of 40% iodixanol gradient solution containing 0.1 M sucrose, 10mM EDTA, 46mM KCl, 5mM NaN3, 10 mM Tris-HCl pH 7.4 and protease inhibitor, was added into a 4 mL ultracentrifuge tube and the sample was carefully added on top of the gradient solution. Then, 1.33 mL of 5% iodixanol gradient solution containing 0.1 M sucrose, 10 mM EDTA, 46 mM KCl, 5 mM NaN3, 10 mM Tris-HCl pH 7.4 and protease inhibitor, was carefully added on top of the sample. After ultracentrifugation at 80,000 g for 16 hours at 4°C, fractions (250 μL) were collected from the top. Then each fraction

was mixed with 6X SDS sample loading buffer, boiled for 5 min at 95°C, and loaded to 4-20% gradient SDS-PAGE gels for Western blot.

Lipidomics. Liquid chromatography-mass spectrometry (LC-MS) grade acetonitrile (ACN), isopropanol (IPA), methanol, and chloroform were purchased from Fisher Scientific (New Jersey, USA). Diglyceride standard mix (d5-DAG, LM-6004) was purchased from Avanti Polar Lipids (USA) and leucine enkephalin from Sigma Aldrich (USA). To extract lipids, vehicle or 3-HIB-fed mouse muscle samples were pulverized in liquid nitrogen and lipids were extracted from muscle powders (50 mg) with a methanol-chloroform (2:1) mixture (300 µL), lysed by mechanical disruption (Tissue laser from QIAGEN, USA) with 25 pulses/sec for 2 min and sonicated for an additional 15 min. Chloroform and water were added (100 µL each) and vortexed. Organic and aqueous layers were separated by centrifugation for 7 min at 13,300 rpm at 4°C. The d5-DAG internal standard mix was added to the organic layer and samples were dried under N2 gas. The dried lipid samples were redissolved in a mixture of 60% solvent A (40% H2O, 60% ACN, 10 mM Ammonium formate) and 40% solvent B (90% IPA, 10% ACN, 10 mM Ammonium formate). The samples were centrifuged at 13,300rpm for 5 min to remove fine particulates. The supernatant was transferred to a glass vial for ultra-performance liquid chromatography combined with qTOF Xevo G2S (Waters) detector for high through put LC-MS lipidomics. For UPLC QTOF MS based data acquisition for untargeted lipidomics profiling, each 10 µL sample was injected on to a reverse-phase column (XSELECTTM CSHTM C18 2.5 µm 2.1x100 mm) using an Aquity H-class UPLC system (Waters Corporation, USA). Each sample was chromatographed for 9 min at a flow rate of 0.5 mL/min. The UPLC gradient consisted of 75% A and 25% B for 0.5 min, a quick ramp of 50% A and 50% B for 0.5 min, 25% A and 75%

B for 4 min followed by a ramp of 10% A and 90% B for 2 min, and finally a ramp to 1% A and 99% B for 2 min. The column eluent was introduced directly into the mass spectrometer. MS was performed with a positive ion sensitive mode with a Capillary voltage of 3000 V and Sampling Cone voltage of 40°C. The desolvation gas flow was set to 800 L/hr and the temperature was set to 450°C. The source temperature was set at 80°C. Accurate mass was maintained by introduction of a lock-spray interface of leucine-enkephalin (556.2771 m/z) at a concentration of 0.5 ng/μL in 50% aqueous acetonitrile and a rate of 5 μL/min. Data was acquired in centroid MSe mode from 50-1200 m/z mass ranges for both MS (low energy) and MSe (high energy) modes. Low energy or fragmented data were collected without collision energy, while high energy or fragmented data were collected by using collision energy ramp from 15-40 eV. The entire set of triplicate sample injections was bracketed with a test mix of standard metabolites at the beginning and at the end of the run to evaluate instrument performance with respect to sensitivity and mass accuracy. The sample queue was randomized to remove bias. Lipid analysis and identifications were performed using Progenesis software (Waters Corporation, USA). Endogenous DG(16:0/16:0) - m/z 551.50 Da, DG(16:0/18:0) - 596.54 Da, DG(16:0/18:1) – 577.51 Da, DG(18:0/18:0)- 607.56 Da, DG(18:1/18:2)-601.51 Da, DG(18:1/18:3)-1234.07, DG(18:0/20:4)-689.51 Da fragmentation was confirmed by DDA and TOF-MS MS methods along with MSe.

Animal Models. All animal experiments were performed according to procedures approved by the Institutional Animal Care and Use Committee. For 3-HIB feeding, 12-week-old C57BL/6 male mice (Jackson Lab) were fed with 3-HIB (Sigma 36105) in drinking water (300 mg/kg/day) for 2 weeks. Free FAs (Cayman), TAG (Cayman) and DAG (Mybiosourse) kits were used

according to manufacturer's protocols. For glucose tolerance test, 8-week-old male mice were fasted for 16 hours, weighed, and a baseline blood glucose level was measured using a glucometer. Each mouse was intraperitoneally injected with sterilized 10% w/v D-glucose (10 μL/g body weight), then blood glucose was measured at each time point. Flt flox/flox and Flk flox/flox mice were kindly shared by Genentech. FATP4 KO and CD36 KO mice were kindly provided by Dr. Jeffrey H. Miner (Washington University School of Medicine) and Dr. Jack Lawler (Harvard Medical School), respectively. Hyperinsulinemic euglycemic clamp studies were performed as described previously (Titchenell PM et al. 2015). Luciferase-transgenic mice were purchased from Jackson Lab (#008450). Luc-S-S-FA was purchased from INTRACE MEDICAL SA. To measure in vivo FA uptake, 10-week-old female Luciferase-TG or Luciferase/MCKalpha double transgenic mice were fasted for 16 hours, then ad lib fed with food paste mixed with 30 mM 3-HIB in water for 1.5 hours. The mice were then anesthetized and intravenously injected with 20 μM Luc-S-S-FA in warm 100 μL PBS containing 10 μM FA-free BSA. Luminescence was measured immediately after injection of Luc-S-S-FA with Xenogen IVIS-50 Bioluminescence Imaging System at the BIDMC Small Animal Imaging Core. Images and quantifications were performed by personnel blinded to the treatment or genotypes. To measure vessel leakiness in vivo, the mice were anesthetized and intravenously injected with 50 μL of 2% Evans Blue in PBS. After 5 min, blood was collected and intracardiac perfusion was performed with 100 mL PBS. The skeletal muscle was then isolated, minced with scissors in PBS, homogenized with metal beads, centrifuged at 13,000 g for 10min, and Evans Blue in supernatants was quantified (absorbance at 611 nm) and normalized to total protein concentrations measured by BCA assay (Promega). To perform plasmid and siRNA electroporation into the tibialis anterior muscle, 8-week-old mice were anesthetized with

isofuran, hair was then removed from legs, and a small incision was made on the skin to expose the muscle. Then, 25 μg of CMV-EGFP plasmid (Addgene) with 5 μg of control or HIBADH siRNA in 25 μL sterilized saline was slowly injected into the muscle with an insulin syringe. The skin incision was then sutured and electropersation was applied by touching the two pin electrodes around the injection site (Voltage, 50 V/cm; pulse duration, 100 ms; frequency of pulses, 1 Hz). A train of total 8 pulses (4 pulses first, then additional 4 pulses after switching electrode position) was delivered. The left leg was injected with control siRNA and the right leg was injected with HIBADH siRNA. After 9 days of recovery, the injected muscle was isolated and GFP-positive muscle fibers (5-10 mg) were collected to measure TAG and protein concentrations.

Human samples. The cohort of skeletal muscle biopsy samples was described previously (Forman DE et al. 2014). Human studies were approved by the institutional review board (IRB).

Reagents. Anti-Pan-Actin (#4968), Anti-ERK1/2 (#9102), anti-pERK1/2 Thr 202/Tyr204 (#9101), anti-Akt (#4685), anti-pAkt Ser473 (#9271 all from Cell Signaling), anti-FATP3 (Proteintech 12943-1-AP), anti-FATP4 (Abnova H00010999-M01), anti-PKCθ (BD Transduction lab 610089), anti-Na,K ATPase A1 (Novus Biologicals NB300-146SS) and anti-HIBADH (Proteintech 13466-1-AP) antibodies were used for Western blot. Anti-Occludin-1 (Abcam ab31721) and anti-Calnexin (Thermo MA3-27) antibodies were used for immunostaining. Mitotracker® Red CMXRos (Cell Signaling 9082S) was used for mitochondria staining. Sulfo-N-succinimidyl Oleate (sc-208408) was purchased from Santa Cruz. Akt VIII (#124018) was purchased from Calbiochem. 2-deoxyglucose (#D8375) and activated charcoal

(#C4386) were purchased from Sigma. CHC (#5029) was purchased from Tocris. Recombinant VEGFA (#293-VE-010) and VEGFB (#767-VE-010) were purchased from R&D systems. Human insulin (Humulin R U-100) was purchased from Harvard Drug Group (#821501). Membrane filters (MWCO 3 kDa #Z677094), Calcimycin (#C9275), 2,4-Dinitrophenol (#D198501) and other chemicals were purchased from Sigma unless otherwise stated.

Statistics. P-values were calculated using the two-tailed Student's t-test. For statistical comparisons between study groups, ANOVA was used followed by Bonferroni post hoc testing. $P<0.05$ was considered statistically significant. Data are displayed as mean ± standard deviation or standard error (as indicated). All cell culture experiments included at least 3 biological replicates. All animal cohorts included at least 3 animals in each study group (as indicated in each case). Animals were randomized to treatment groups.

References

Arany Z, Lebrasseur N, Morris C, Smith E, Yang W, Ma Y, Chin S, Spiegelman BM. (2007). The transcriptional coactivator PGC-1β drives the formation of oxidative type IIX fibers in skeletal muscle. Cell Metab. 5:35-46.

Avogaro A, Bier DM. (1989). Contribution of 3-hydroxyisobutyrate to the measurement of 3-hydroxybutyrate in human plasma: comparison of enzymatic and gas-liquid chromatography-mass spectrometry assays in normal and in diabetic subjects. J Lipid Res. 30:1811-7.

Brosnan JT, Brosnan ME. (2006). Branched-chain amino acids: enzyme and substrate regulation. J Nutr. 136:207S-11S.

Chabowski A, Momken I, Coort SL, Calles-Escandon J, Tandon NN, Glatz JF, Luiken JJ, Bonen A. (2006). Prolonged AMPK activation increases the expression of fatty acid transporters in cardiac myocytes and perfused hearts. Mol Cell Biochem. 288:201-12.

Choi CS, Befroy DE, Codella R, Kim S, Reznick RM, Hwang YJ, Liu ZX, Lee HY, Distefano A, Samuel VT, Zhang D, Cline GW, Handschin C, Lin J, Petersen KF, Spiegelman BM, Shulman GI. (2008). Paradoxical effects of increased expression of PGC-1α on muscle mitochondrial function and insulin-stimulated muscle glucose metabolism. Proc Natl Acad Sci U S A. 105:19926-31.

Deng WJ, Nie S, Dai J, Wu JR, Zeng R. (2010). Proteome, phosphoproteome, and hydroxyproteome of liver mitochondria in diabetic rats at early pathogenic stages. Mol Cell Proteomics. 9:100-16

Digel M, Staffer S, Ehehalt F, Stremmel W, Ehehalt R, Fullekrug J. (2011). FATP4 contributes as an enzyme to the basal and insulin-mediated fatty acid uptake of C2C12 muscle cells. Am J Physiol Endocrinol Metab. 301:E785-96.

DiRusso CC, Li H, Darwis D, Watkins PA, Berger J, Black PN. (2005). Comparative biochemical studies of the murine fatty acid transport proteins (FATP) expressed in yeast. J Biol Chem. 280:16829-37.

Drahota Z, Vrbacky M, Nuskova H, Kazdova L, Zidek V, Landa V, Pravenec M, Houstek J. (2010). Succinimidyl oleate, established inhibitor of CD36/FAT translocase inhibits complex III of mitochondrial respiratory chain. Biochem Biophys Res Commun. 391:1348-51.

Forman DE, Daniels KM, Cahalin LP, Zavin A, Allsup K, Cao P, Santhanam M, Joseph J, Arena R, Lazzari A, Schulze PC, Lecker SH. (2014). Analysis of skeletal muscle gene expression patterns and the impact of functional capacity in patients with systolic heart failure.J Card Fail. 20:422-30.

Giesbertz P, Padberg I, Rein D, Ecker J, Hofle AS, Spanier B, Daniel H. (2015). Metabolite profiling in plasma and tissues of ob/ob and db/db mice identifies novel markers of obesity and type 2 diabetes. Diabetologia. 58:2133-43.

Goto K, Iso T, Hanaoka H, Yamaguchi A, Suga T, Hattori A, Irie Y, Shinagawa Y, Matsui H, Syamsunarno MR, Matsui M, Haque A, Arai M, Kunimoto F, Yokoyama T, Endo K, Gonzalez FJ, Kurabayashi M. (2013). Peroxisome proliferator-activated receptor-γ in capillary endothelia promotes fatty acid uptake by heart during long-term fasting. J Am Heart Assoc. 2:e004861.

Hagberg CE, Falkevall A, Wang X, Larsson E, Huusko J, Nilsson I, van Meeteren LA, Samen E, Lu L, Vanwildemeersch M, Klar J, Genove G, Pietras K, Stone-Elander S, Claesson-Welsh L, Yla-Herttuala S, Lindahl P, Eriksson U. (2010). Vascular endothelial growth factor B controls endothelial fatty acid uptake. Nature. 464:917-21.

Han ED, MacFarlane RC, Mulligan AN, Scafidi J, Davis AE 3rd. (2002). Increased vascular permeability in C1 inhibitor-deficient mice mediated by the bradykinin type 2 receptor. J Clin Invest. 1057-63.

Henkin AH, Cohen AS, Dubikovskaya EA, Park HM, Nikitin GF, Auzias MG, Kazantzis M, Bertozzi CR, Stahl A. (2012). Real-time noninvasive imaging of fatty acid uptake in vivo. ACS Chem Biol. 7:1884-91.

Hillebrand M, Gersting SW, Lotz-Havla AS, Schafer A, Rosewich H, Valerius O, Muntau AC, Gartner J. (2012). Identification of a new fatty acid synthesis-transport machinery at the peroxisomal membrane. J Biol Chem. 287:210-21.

Holloway GP, Jain SS, Bezaire V, Han XX, Glatz JF, Luiken JJ, Harper ME, Bonen A. (2009). FAT/CD36-null mice reveal that mitochondrial FAT/CD36 is required to upregulate mitochondrial fatty acid oxidation in contracting muscle. Am J Physiol Regul Integr Comp Physiol. 297:R960-7.

Iso T, Maeda K, Hanaoka H, Suga T, Goto K, Syamsunarno MR, Hishiki T, Nagahata Y, Matsui H, Arai M, Yamaguchi A, Abumrad NA, Sano M, Suematsu M, Endo K, Hotamisligil GS, Kurabayashi M. (2013). Capillary endothelial fatty acid binding proteins 4 and 5 play a critical role in fatty acid uptake in heart and skeletal muscle. Arterioscler Thromb Vasc Biol. 33:2549-57.

Kanda T, Brown JD, Orasanu G, Vogel S, Gonzalez FJ, Sartoretto J, Michel T, Plutzky J. (2009). PPARgamma in the endothelium regulates metabolic responses to high-fat diet in mice. J Clin Invest. 119:110-24.

Kiens B, Kristiansen S, Jensen P, Richter EA, Turcotte LP. (1997). Membrane associated fatty acid binding protein (FABPpm) in human skeletal muscle is increased by endurance training. Biochem Biophys Res Commun. 231:463-5.

Krammer J, Digel M, Ehehalt F, Stremmel W, Fullekrug J, Ehehalt R. (2011). Overexpression of CD36 and acyl-CoA synthetases FATP2, FATP4 and ACSL1 increases fatty acid uptake in human hepatoma cells. Int J Med Sci. 8:599-614.

Kuda O, Pietka TA, Demianova Z, Kudova E, Cvacka J, Kopecky J, Abumrad NA. (2013). Sulfo-N-succinimidyl oleate (SSO) inhibits fatty acid uptake and signaling for intracellular calcium via binding CD36 lysine 164: SSO also inhibits oxidized low density lipoprotein uptake by macrophages. J Biol Chem. 288:15547-55.

Kuzuya T, Katano Y, Nakano I, Hirooka Y, Itoh A, Ishigami M, Hayashi K, Honda T, Goto H, Fujita Y, Shikano R, Muramatsu Y, Bajotto G, Tamura T, Tamura N, Shimomura Y. (2008). Regulation of branched-chain amino acid catabolism in rat models for spontaneous type 2 diabetes mellitus. Biochem Biophys Res Commun. 373:94-8.

Le Lay S, Kurzchalia TV. (2005). Getting rid of caveolins: phenotypes of caveolin-deficient animals. Biochim Biophys Acta. 1746:322-33.

Lin J, Wu H, Tarr PT, Zhang CY, Wu Z, Boss O, Michael LF, Puigserver P, Isotani E, Olson EN, Lowell BB, Bassel-Duby R, Spiegelman BM. (2002). Transcriptional co-activator PGC-1 alpha drives the formation of slow-twitch muscle fibres. Nature. 418:797-801

Luiken JJ, Koonen DP, Willems J, Zorzano A, Becker C, Fischer Y, Tandon NN, Van Der Vusse GJ, Bonen A, Glatz JF. (2002). Insulin stimulates long-chain fatty acid utilization by rat cardiac myocytes through cellular redistribution of FAT/CD36. Diabetes. 51:3113-9.

Lynch CJ, Adams SH. (2014). Branched-chain amino acids in metabolic signalling and insulin resistance. Nat Rev Endocrinol. 10:723-36.

Makowski L, Hotamisligil GS. (2004). Fatty acid binding proteins--the evolutionary crossroads of inflammatory and metabolic responses. J Nutr. 134:2464-8.

Mehrotra D, Wu J, Papangeli I, Chun HJ. (2014). Endothelium as a gatekeeper of fatty acid transport. Trends Endocrinol Metab. 25:99-106.

Milger K, Herrmann T, Becker C, Gotthardt D, Zickwolf J, Ehehalt R, Watkins PA, Stremmel W, Fullekrug J. (2006). Cellular uptake of fatty acids driven by the ER-localized acyl-CoA synthetase FATP4. J Cell Sci. 119:4678-88.

Motojima K, Passilly P, Peters JM, Gonzalez FJ, Latruffe N. (1998). Expression of putative fatty acid transporter genes are regulated by peroxisome proliferator-activated receptor alpha and gamma activators in a tissue- and inducer-specific manner. J Biol Chem. 273:16710-4.
Mullen E, Ohlendieck K. (2010). Proteomic profiling of non-obese type 2 diabetic skeletal muscle. Int J Mol Med. 25:445-58.

Newgard CB, An J, Bain JR, Muehlbauer MJ, Stevens RD, Lien LF, Haqq AM, Shah SH, Arlotto M, Slentz CA, Rochon J, Gallup D, Ilkayeva O, Wenner BR, Yancy WS Jr, Eisenson H, Musante G, Surwit RS, Millington DS, Butler MD, Svetkey LP. (2009). A branched-chain amino acid-related metabolic signature that differentiates obese and lean humans and contributes to insulin resistance. Cell Metab. 9:311-26.

Newgard CB. (2012). Interplay between lipids and branched-chain amino acids in development of insulin resistance. Cell Metab. 15:606-14.

Nicholls HT, Kowalski G, Kennedy DJ, Risis S, Zaffino LA, Watson N, Kanellakis P, Watt MJ, Bobik A, Bonen A, Febbraio M, Lancaster GI, Febbraio MA. (2011). Hematopoietic cell-restricted deletion of CD36 reduces high-fat diet-induced macrophage infiltration and improves insulin signaling in adipose tissue. Diabetes. 60:1100-10.

Nishimura J, Masaki T, Arakawa M, Seike M, Yoshimatsu H. (2010). Isoleucine prevents the accumulation of tissue triglycerides and upregulates the expression of PPARalpha and uncoupling protein in diet-induced obese mice. J Nutr. 140:496-500.

Noatsch A, Petzke KJ, Millrose MK, Klaus S. (2011). Body weight and energy homeostasis was not affected in C57BL/6 mice fed high whey protein or leucine-supplemented low-fat diets. Eur J Nutr. 50:479-88.

Novakova V, Sandhu GS, Dragomir-Daescu D, Klabusay M. (2015). Apelinergic system in endothelial cells and its role in angiogenesis in myocardial ischemia. Vascul Pharmacol. pii: S1537-189.

Overmyer KA, Evans CR, Qi NR, Minogue CE, Carson JJ, Chermside-Scabbo CJ, Koch LG, Britton SL, Pagliarini DJ, Coon JJ, Burant CF. (2015). Maximal oxidative capacity during exercise is associated with skeletal muscle fuel selection and dynamic changes in mitochondrial protein acetylation. Cell Metab. 21:468-78.

Pechlivanis A, Kostidis S, Saraslanidis P, Petridou A, Tsalis G, Mougios V, Gika HG, Mikros E, Theodoridis GA. (2010). (1)H NMR-based metabonomic investigation of the effect of two different exercise sessions on the metabolic fingerprint of human urine. J Proteome Res. 9:6405-16.

Pei Z, Fraisl P, Berger J, Jia Z, Forss-Petter S, Watkins PA. (2004). Mouse very long-chain Acyl-CoA synthetase 3/fatty acid transport protein 3 catalyzes fatty acid activation but not fatty acid transport in MA-10 cells. J Biol Chem. 279:54454-62.

Pohl J, Ring A, Korkmaz U, Ehehalt R, Stremmel W. (2005). FAT/CD36-mediated long-chain fatty acid uptake in adipocytes requires plasma membrane rafts. Mol Biol Cell. 16:24-31.

Ring A, Le Lay S, Pohl J, Verkade P, Stremmel W. (2006). Caveolin-1 is required for fatty acid translocase (FAT/CD36) localization and function at the plasma membrane of mouse embryonic fibroblasts. Biochim Biophys Acta. 1761:416-23.

Rowland AF, Fazakerley DJ, James DE. (2011). Mapping insulin/GLUT4 circuitry. Traffic. 12:672-81.

Sasaki M, Iwata H, Sugai K, Fukumizu M, Kimura M, Yamaguchi S. (2001). A severely brain-damaged case of 3-hydroxyisobutyric aciduria. Brain Dev. 23:243-5.

Scherer PE, Lisanti MP, Baldini G, Sargiacomo M, Mastick CC, Lodish HF. (1994). Induction of caveolin during adipogenesis and association of GLUT4 with caveolin-rich vesicles. J Cell Biol. 127:1233-43.

She P, Van Horn C, Reid T, Hutson SM, Cooney RN, Lynch CJ. (2007). Obesity-related elevations in plasma leucine are associated with alterations in enzymes involved in branched-chain amino acid metabolism. Am J Physiol Endocrinol Metab. 293:E1552-63.

Sheikh AY, Chun HJ, Glassford AJ, Kundu RK, Kutschka I, Ardigo D, Hendry SL, Wagner RA, Chen MM, Ali ZA, Yue P, Huynh DT, Connolly AJ, Pelletier MP, Tsao PS, Robbins RC, Quertermous T. (2008). In vivo genetic profiling and cellular localization of apelin reveals a hypoxia-sensitive, endothelial-centered pathway activated in ischemic heart failure. Am J Physiol Heart Circ Physiol. 294:H88-98.

Smith GI, Yoshino J, Stromsdorfer KL, Klein SJ, Magkos F, Reeds DN, Klein S, Mittendorfer B. (2015). Protein ingestion induces muscle insulin resistance independent of leucine-mediated mTOR activation. Diabetes. 64:1555-63.

Stahl A, Evans JG, Pattel S, Hirsch D, Lodish HF. (2002). Insulin causes fatty acid transport protein translocation and enhanced fatty acid uptake in adipocytes. Dev Cell. 2:477-88.

Suryawan A, Hawes JW, Harris RA, Shimomura Y, Jenkins AE, Hutson SM. (1998). A molecular model of human branched-chain amino acid metabolism. Am J Clin Nutr. 68:72-81.

Szendroedi J, Yoshimura T, Phielix E, Koliaki C, Marcucci M, Zhang D, Jelenik T, Muller J, Herder C, Nowotny P, Shulman GI, Roden M. (2014). Role of diacylglycerol activation of PKCtheta in lipid-induced muscle insulin resistance in humans. Proc Natl Acad Sci U S A. 111:9597-602.

Titchenell PM, Chu Q, Monks BR, Birnbaum MJ. (2015). Hepatic insulin signalling is dispensable for suppression of glucose output by insulin in vivo. Nat Commun. 6:7078.

Yu C, Chen Y, Cline GW, Zhang D, Zong H, Wang Y, Bergeron R, Kim JK, Cushman SW, Cooney GJ, Atcheson B, White MF, Kraegen EW, Shulman GI. (2002). Mechanism by which

fatty acids inhibit insulin activation of insulin receptor substrate-1 (IRS-1)-associated phosphatidylinositol 3-kinase activity in muscle. J Biol Chem. 277:50230-6.

Wang TJ, Larson MG, Vasan RS, Cheng S, Rhee EP, McCabe E, Lewis GD, Fox CS, Jacques PF, Fernandez C, O'Donnell CJ, Carr SA, Mootha VK, Florez JC, Souza A, Melander O, Clish CB, Gerszten RE. (2011). Metabolite profiles and the risk of developing diabetes. Nat Med. 17:448-53.

Zhang Y, Guo K, LeBlanc RE, Loh D, Schwartz GJ, Yu YH. (2007). Increasing dietary leucine intake reduces diet-induced obesity and improves glucose and cholesterol metabolism in mice via multimechanisms. 56:1647-54.

Chapter 4: Discussion

3-HIB receptors and downstream signaling

From a therapeutic point of view, it is important to identify 3-HIB receptors and downstream signaling pathways in endothelial cells because they can be the key drug targets to block lipotoxicity. A growing number of receptors have been identified that recognize metabolites as ligands and transduce signaling inside cells. Most of them are the G-protein coupled receptors (GPCRs) that bind to small G proteins (e.g. Gα or Gi) as downstream effectors (Blad CC et al. 2012). For example, several GPCRs have been shown to function as receptors for a small signaling molecule, including sphingosine-1-phosphate, adenosine, short-chain fatty acids and so on. Recently, many of secreted metabolites have been added to the list of GPCR ligands, such as citrate, succinate, lactate, and a ketone body beta-hydroxybutyrate (He W et al. 2004; Sapieha P et al. 2008; Ahmed K et al. 2010; Youm YH et al. 2015). Pertussis toxin is an inhibitor of Gi protein via irreversible ADP-ribosylation of the protein (Mangmool S and Kurose H). Interestingly, we found that pre-treatment of endothelial cells with pertussis toxin substantially blocked fatty acid uptake induced by α-CM (data not shown), suggesting that 3-HIB has a GPCR as its receptor. Therefore, we have tried an siRNA screen that covered the top 100 orphan GPCRs most highly expressed in endothelial cells, since the α-CM effect is quite endothelial cell specific. However, we failed to identify siRNAs that efficiently blocked fatty acid uptake by α-CM (data not shown).

There are many possible reasons why this approach did not work. First, GPCRs are highly redundant and it is very likely that 3-HIB has multiple GPCR receptors. Therefore, knockdown of single GPCR may not exhibit any noticeable changes in fatty acid uptake. Second, it is possible that the GPCR for 3-HIB is not orphan receptors but rather GPCRs with known ligands. We thus have tested GPCRs that have ligands structurally similar to 3-HIB (e.g. lactate,

short-chain fatty acids, beta-hydroxybutyrate, and gamma-hydroxybutyrate) (Andriamampandry C et al. 2007; Ahmed K et al. 2009; Youm YH et al. 2015), but again failed to identify it. Third, it may not be a GPCR at all. It is now apparent that there is a GPCR-independent Gi signaling pathway that pertussis toxin can inhibit (Cismowski MJ and Lanier SM. 2005). For instance, a recent report showed that Gi is localized in Golgi and has a GPCR-independent function (Lo IC et al. 2015). Therefore, it seems that identification of 3-HIB receptors requires more serious efforts. These may involve development of more comprehensive and large-scale loss-of-function screens, or a gain-of-function screen that uses Chinese hamster ovary (CHO) cells with ectopic expression of individual GPCRs. Furthermore, to identify downstream signaling pathways that mediate the 3-HIB effect in ECs, screens using chemical libraries, genome-wide siRNAs or recently-developed Crispr-Cas9 guide RNAs would be useful.

Another potential drug target for the treatment of diabetes is vascular FATP3 and FATP4. Our data demonstrate that FATP3 and FATP4 are mainly responsible for the 3-HIB-mediated fatty acid transport. Interestingly, VEGF-B also depends on these fatty acid transporters, rendering FATP3 and FATP4 as an ideal point of convergence to efficiently block endothelial fatty acid transport. Then, it should be useful to examine the known consequences of FATP3 and/or FATP4 inhibition in animals because one might expect similar symptoms in the patients given with FATP3/4 inhibitors.

It seems that expression of FATP3 is fairly limited to endothelial cells, which is a good feature for a drug target. However, the function of FATP3 as a fatty acid transporter has been controversial (Pei Z et al. 2004; DiRusso CC et al. 2005; Hagberg CE et al. 2010; Hagberg CE et al. 2012). For example, it was shown that knockdown of FATP3 in a mouse testis tumor cell line

(MA-10 cells) decreased acyl-CoA synthase activity but not fatty acid uptake activity (Pei Z et al. 2004). However, the authors used just one cancer cell line, which hardly reflects the real physiological relevance of FATP3 function in fatty acid transport. Moreover, it is possible that their knockdown efficiency was only sufficient to affect enzymatic activity but not fatty acid uptake activity of FATP3. Therefore, more thorough studies using FATP3 knockout in physiologically relevant cell types (e.g. endothelial cells) or in animals are essential. No FATP3 knockout mice have been reported yet.

In contrast to FATP3, expression of FATP4 is much broader and the highest level is observed in gastrointestinal enterocytes (Stahl A et al. 1999). This led a pharmaceutical company to develop specific inhibitors of FATP4 as a potential blocker of fatty acid uptake in the gut to treat obesity (Blackburn C et al. 2006). However, they did not see a significant decrease of intestinal fatty acid uptake after injection of mice with the inhibitor. The authors discussed that a dose or tissue distribution of the inhibitor might not be optimal. FATP4 knockout mice were generated or accidently discovered by two independent groups. One group found an interesting mouse strain that manifested postnatal lethality with a severe skin phenotype. Later, it was identified as a consequence of FATP4 deficiency due to a transposon insertion into one exon of FATP4 (Moulson CL et al. 2003). This group also showed that overexpression of FATP4 specifically in keratinocytes in the skin was sufficient to rescue the lethality and the skin phenotype of the knockout mice (Moulson CL et al. 2007). Another group reported similar phenotypes using conditional knockout mice they generated. Interestingly, they found that knockout of FATP4 in adult mice resulted in only a mild skin phenotype (Herrmann T et al. 2005), suggesting that FATP4 is more important during the early developmental stages. FATP4 knockout in intestines or adipose tissues did not show any apparent phenotype (Shim J et al.

2009; Lenz LS et al. 2011), except a mild weight gain and adipose hypertrophy in the adipose tissue-specific knockout mice under a high-fat diet (Lenz LS et al 2011). To conclude, these studies using knockout mice suggest no serious effect of FATP4 inhibition, at least in adulthood. However, it is possible that FATP4 plays more important roles in humans, and simultaneous inhibition of FATP3 and FATP4 can be synergistically detrimental. FATP3 and FATP4 double knockout mice, in this regard, can be useful to evaluate this possibility.

Regulation of BCAA metabolism by PGC-1s

Here we identified a novel link between PGC-1s and BCAA metabolism. We found that overexpression of either PGC-1α or PGC-1β in myotubes (Figure 2.24a and c) or in skeletal muscle of transgenic mice (Figure 3.6a and c) strongly induced almost all genes of BCAA catabolic enzymes. Consistently, there is an increased generation of 3-HIB both *in vitro* (Figure 2.24b) and *in vivo* (Figure 3.6b), demonstrating that valine catabolism is elevated. As loss-of-function studies, we have generated PGC-1α knockout myotube using the Crispr-Cas9 system (Figure 2.25b) as well as PGC-1α and PGC-1β muscle-specific double knockout mice (DKO mice, Figure 2.25a and Figure 3.7), and found that profound repression of BCAA catabolic genes only in the double knockout cells or mice. How can PGC-1s regulate these BCAA catabolic gene programs? PGC-1s are transcription co-activators. Therefore, there must be transcription factors that actually bind to and activate promoters of these genes, with the help of PGC-1s. Since BCAA catabolism mainly occurs in mitochondria and PGC-1s are known to induce mitochondrial biogenesis, it is possible that PGC-1s increase expression of these genes indirectly to replenish newly-made mitochondria with these enzymes. However, it is worth noting that BCAT1 and BCKDH-B are cytoplasmic proteins and they are also induced by PGC-1s,

suggesting that it may not be an indirect consequence of increased number of mitochondria. Then what transcription factors could be involved? There are many candidate transcription factors that are activated by PGC-1s. Among them, nuclear receptors such as PPARδ and ERRα are the strongest candidates because they are known to regulate fatty acid metabolism and angiogenesis in myotubes, respectively (Handschin C and Spiegelman BM. 2006). However, we found that neither knockdown of these genes nor treatment of a chemical inhibitor affected gene induction of valine catabolic enzymes by PGC-1α (Figure 4.1).

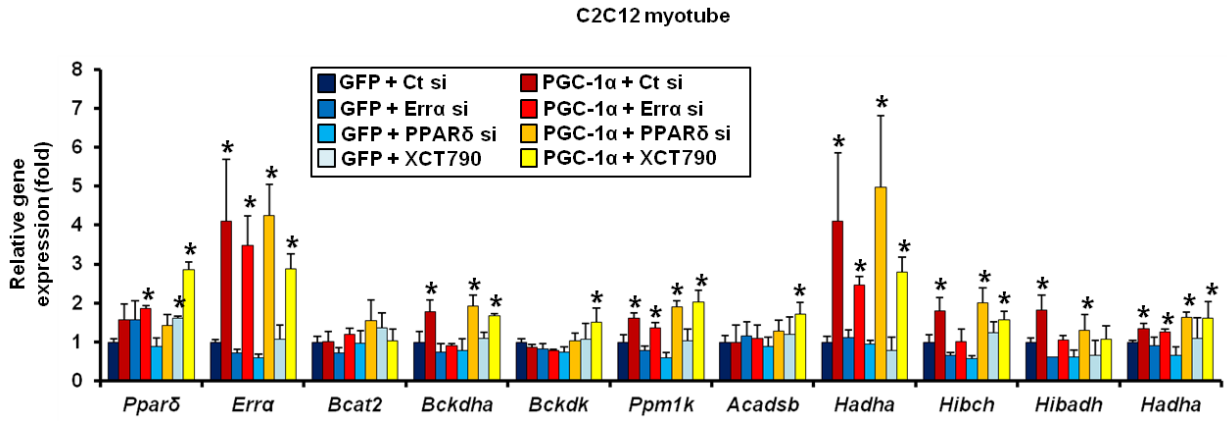


Figure 4.1: Inhibition of ERRα or PPARδ does not block the induction of valine catabolism genes by PGC-1α. qPCR analysis of C2C12 myotubes infected with adenovirus expressing PGC-1α after transfection with the indicated siRNA or treatment with XCT790, an ERRα inverse agonist for 48 hr. *p<.05 vs. control. Data are mean ± s.d. of at least three biological replicates.

Another strong candidate is a Kruppel-like factor (KLF) family. There are several experimental data supporting this possibility. First, these Zinc-finger domain-containing transcription factors are shown to regulate fatty acid metabolism and mitochondrial biogenesis. A recent report using heart-specific KLF4 knockout mice showed that KLF4 directly binds to PGC-1s and ERRα to regulate mitochondrial genes (Liao X et al. 2015). Second, KLF15 is known to regulate one of the key genes of BCAA catabolism, BCAT2. KLF15 whole-body knockout mice showed dramatic reduction of BCAT2 protein levels in the liver and skeletal

muscle and consequently elevated BCAA levels in the blood, suggesting a blunted systemic BCAA catabolism (Gray S et al. 2007; Jeyaraj D et al. 2012). More interestingly, these mice exhibited higher free fatty acid levels in blood and lower trigylcerides levels in skeletal muscle and the heart (Haldar SM et al. 2012; Prosdocimo DA et al. 2014), consistent with our proposal that increased BCAA catabolism (and thus increased 3-HIB production) is important for fatty acid flux into muscle. Third, KLF15 is known to be increased by exercise and fasting in muscle (Yamamoto J et al. 2004; Gray S et al. 2007; Haldar SM et al. 2012), the two physiological conditions where 3-HIB generation and fatty acid trafficking are both increased (Figure 3.16) (Pechlivanis A et al. 2010; Overmyer KA et al. 2015). Fourth, bioinformatics and chromatin-immunoprecipitation (CHIP)-based analysis predicted KLF4 as a top transcription factor that could bind to promoter regions of many of BCAA catabolic enzymes (Hatazawa Y et al. 2014; Hatazawa Y et al. 2015). Lastly, we found

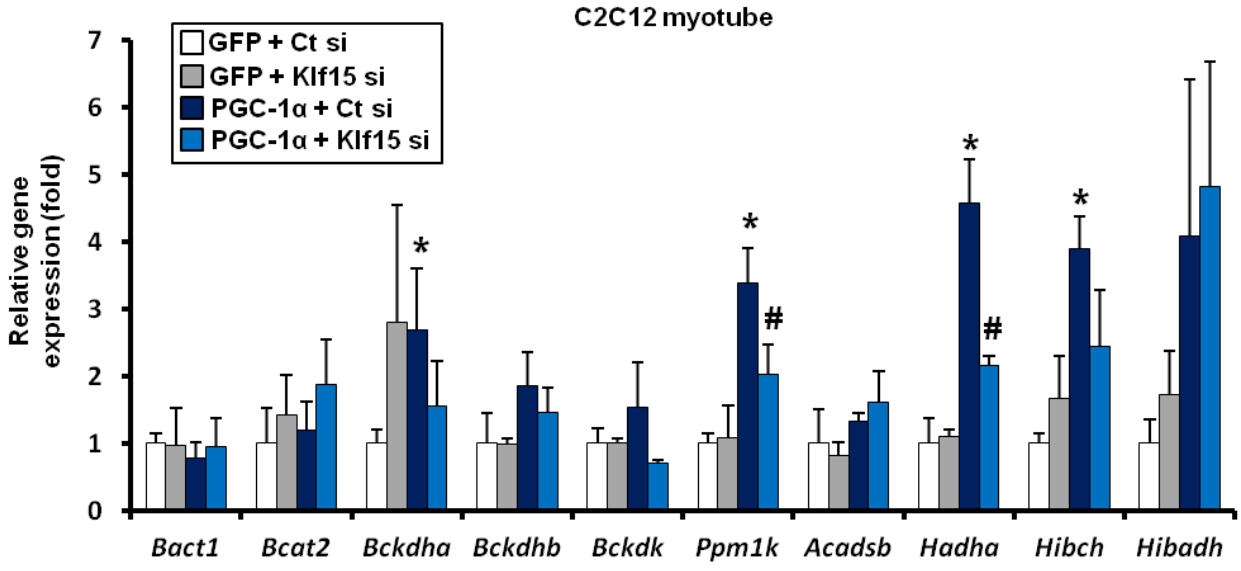


Figure 4.2: Knockdown of Klf15 blocks some of valine catabolism genes induced by PGC-1α. qPCR analysis of C2C12 myotubes infected with adenovirus expressing PGC-1α after transfection of Klf15 siRNA. *p<.05 vs. control. #p<.05 vs. PGC-1α overexpression. Data are mean ± s.d. of at least three biological replicates.

that some of valine catabolic enzymes induced by PGC-1α overexpression are slightly but significantly suppressed by KLF15 knockdown in myotubes (Figure. 4.2). The incomplete inhibition may be due to insufficient knockdown of KLF15 and/or compensation by other KLFs. Therefore, future studies are required to examine which KLF(s) are responsible for PGC-1α-dependent regulation of BCAA catabolism.

Beyond 3-HIB and beyond muscle.

Our study is about the intercellular communication between muscle cells and endothelial cells. Is 3-HIB only the factor secreted from muscle cells that can facilitate endothelial fatty acid transport? We identified 3-HIB as the major active molecule in α-CM with unbiased biochemical fractionation and mass-spectrometry analysis. It is still possible, however, that there are other factors (e.g. VEGF-B) that potentially have a similar biological activity to 3-HIB. In fact, the α-CM activity is higher than the activity achieved by 3-HIB treatment alone, with a concentration of 3-HIB in the α-CM measured by mass-spectrometry. Consistent with this notion, we observed two separate fractions in C18 column chromatography that contained the fatty acid uptake inducing activity (data not shown). One of them was confirmed to contain 3-HIB, but the other did not (data not shown). Thus, it is important to identify this unknown factor as well.

We showed that the increase of fatty acid uptake by α-CM treatment is quite specific to endothelial cells (Figure 2.7a). However, do only muscle cells stimulate endothelial cells to transport fatty acids? It is possible that generation of 3-HIB happens in other tissues, most likely in the liver and adipose tissues. The endothelium in the liver is fenestrated, meaning that these endothelial cells do not have tight junctions but rather have many holes to allow free diffusion of

most nutrients and bulky molecules toward hepatocytes. In this sense, active transport of fatty acids through endothelial walls may not be critical in the liver. Not much is known about the structure of the endothelium in adipose tissues. Contrary to muscle cells that mostly take up extracellular fatty acids (unidirectional transport), fat cells work in both ways (bidirectional transport). They take up and release fatty acids according to certain metabolic conditions. For instance, insulin signaling stimulates fat cells to absorb fatty acids from the blood stream to store them as triglycerides, while fasting signaling does the opposite. Brown adipose tissues are more similar to muscle cells in that they mostly take up fatty acids and have abundant mitochondria with a potentially high capacity of BCAA catabolism (Lopez-Soriano FJ et al. 1988). Collectively, it would be interesting to test if the PGC-1s / 3-HIB signaling axis is also conserved in other metabolically active tissues.

Systemic versus local levels of BCAAs and metabolites

As above mentioned, there are numerous epidemiological studies that correlate plasma BCAA levels with insulin resistance. Ours and other studies demonstrate that there is a clear increase in 3-HIB production in diabetic conditions (Giesbertz P et al. 2015). However, one might expect that enhanced degradation of valine and other BCAAs - which would be necessary to produce 3-HIB - would lead to reduced rather than elevated BCAA levels in the plasma. How can we explain this seemingly paradoxical phenomenon? The answer might be the difference between systemic and local BCAA catabolism. Plasma BCAA levels reflect whole body BCAA metabolism, while BCAA levels in muscle can be very different from those in whole body. We propose that high circulating BCAAs are driving elevations in muscle 3-HIB, i.e. valine catabolism increases in response to excess BCAA in muscle. At least two mechanisms can lead

to excess BCAA delivery to muscle: 1) excess dietary intake of BCAA, and 2) insufficient catabolism of BCAAs in tissues other than muscle, requiring muscle to make up the difference. Many groups have reported tissue-specific alterations in BCAA metabolism, especially in obesity and type II diabetes (Lynch CJ and Adams SH. 2014). For example, in insulin-resistant *ob*/*ob* mice and Zucker rats, two key BCAA enzymes, BCATs and BCKDHs, are dramatically downregulated or inactivated in the liver and adipose tissue but not in muscle (She P et al. 2007; Kuzuya T et al. 2008; Lynch CJ and Adams SH. 2014). These inhibitions of BCAA catabolism in tissues other than muscle would be expected to increase flux of BCAAs to catabolism in muscle, thus increasing 3-HIB. Consistent with this notion, our data show more than 2-fold higher 3-HIB levels in muscle from *db*/*db* mice or in muscle biopsies from human diabetic patients (Figure 3.17a and b), even as it was shown that *db*/*db* mice and diabetic patients have higher plasma BCAA levels. These findings thus show that 3-HIB levels can be high in muscle even when plasma BCAA is high.

Potential caveats of muscle 3-HIB concentration

We have measured 3-HIB concentration in PGC-1α CM, using our mass-spectrometry, and calculate it to be ~700 μM compared to ~200 μM in control CM (Figure 2.24b). However, it is very difficult to conclusively measure the relevant concentration of 3-HIB in skeletal muscle *in vivo* for a number of reasons: 1) we found that variable processing of muscle tissue and/or impurities affecting ion suppression in the mass spectrometer render calculated absolute values variable; and 2) any measured concentration is likely a significant underestimate of the 3-HIB concentrations in the relevant biological space: the interstitium. In other words, we have measured 3-HIB concentrations in the whole muscle but these are potentially much lower than

the actual local 3-HIB concentrations in the interstitial space between myocytes and blood vessels. There is no established method to quantify metabolites in interstitial fluids from muscle. We have tried to isolate the interstitial fluid from muscle, using a low speed centrifugation method previously used for tumor interstitial fluid isolation (Figure 4.3a) (Wiig H et al. 2003; Haslene-Hox H et al. 2011). Briefly, mice were anesthetized and perfused intracardially with PBS to completely remove blood. Tibialis anterior muscle was then isolated from tendon to tendon to prevent cell damage. The muscle was then put on a nylon sieve into an EP tube and centrifuged at 106 g for 10 min. A small volume of fluid (~2 µL) on the bottom of the tube was then collected for mass-spectrometry analysis. Samples from 5 mice were pooled to get enough amount of fluid for one MS/MS run.

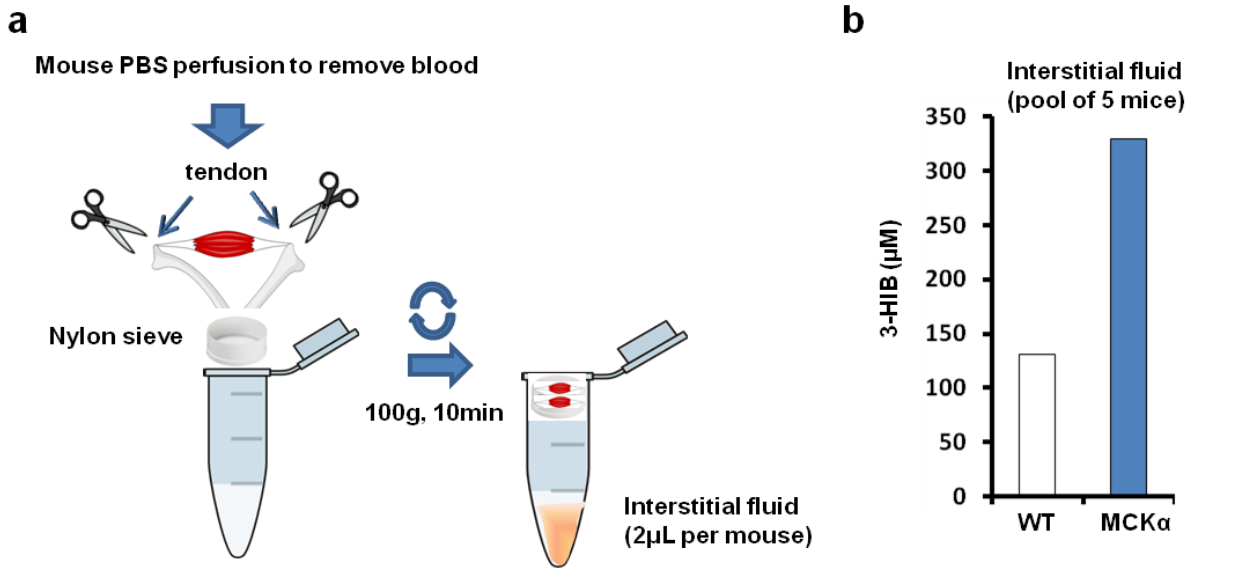


Figure 4.3: Quantification of 3-HIB in muscle interstitial fluid. a, Schematic of preparation of samples enriched with interstitial fluid from skeletal muscle. Mice were anesthetized and perfused intracardially with PBS to completely remove blood. The tibialis anterior muscle was then isolated from tendon to tendon to prevent cell damage. The muscle was then put on a nylon sieve into an EP tube and centrifuged at 106 g for 10 min. A small volume of fluid (~2 µL) on the bottom of the tube was then collected for mass-spec analysis. **b**, MCKα mice have higher 3-HIB levels in a 5 mice-pooled sample enriched with interstitial fluid.

As shown in the Figure 4.3b, the fluid enriched with interstitial fluids contains ~330 μM of 3-HIB in PGC-1α-transgenic mouse versus ~130 μM of 3-HIB in control. These data suggest that 3-HIB in muscle interstitial fluid is high enough to trigger fatty acid accumulation in muscle and consequent insulin resistance. New technological advances should be made to convincingly quantify metabolites in the interstitial fluids of animal and human tissues.

Conclusion

In summary, our data unveil 3-HIB as a novel bioactive paracrine metabolite that regulates trans-endothelial flux of fatty acids. The data highlight the importance of the vasculature in whole-body metabolic homeostasis. The data also uncover a novel cross-regulatory link between the catabolism of BCAAs and fatty acids. Finally, the data provide a mechanistic explanation for how excess catabolic flux of BCAAs can lead to insulin resistance, suggesting this pathway as a new target to treat diabetes.

References

Ahmed K, Tunaru S, Offermanns S. (2009). GPR109A, GPR109B and GPR81, a family of hydroxy-carboxylic acid receptors. Trends Pharmacol Sci. 30:557-62.

Ahmed K, Tunaru S, Tang C, Muller M, Gille A, Sassmann A, Hanson J, Offermanns S. (2010). An autocrine lactate loop mediates insulin-dependent inhibition of lipolysis through GPR81. Cell Metab. 11:311-9.

Andriamampandry C, Taleb O, Kemmel V, Humbert JP, Aunis D, Maitre M. Cloning and functional characterization of a gamma-hydroxybutyrate receptor identified in the human brain. FASEB J. 21:885-95.

Blad CC, Tang C, Offermanns S. (2012). G protein-coupled receptors for energy metabolites as new therapeutic targets. Nat Rev Drug Discov. 11:603-19.

Blackburn C, Guan B, Brown J, Cullis C, Condon SM, Jenkins TJ, Peluso S, Ye Y, Gimeno RE, Punreddy S, Sun Y, Wu H, Hubbard B, Kaushik V, Tummino P, Sanchetti P, Yu Sun D, Daniels T, Tozzo E, Balani SK, Raman P. (2006). Identification and characterization of 4-aryl-3,4 -dihydropyrimidin-2(1H)-ones as inhibitors of the fatty acid transporter FATP4. Bioorg Med Chem Lett. 16:3504-9.

Cismowski MJ, Lanier SM. (2005). Activation of heterotrimeric G-proteins independent of a G-protein coupled receptor and the implications for signal processing. Rev Physiol Biochem Pharmacol. 155:57-80.

DiRusso CC, Li H, Darwis D, Watkins PA, Berger J, Black PN. (2005). Comparative biochemical studies of the murine fatty acid transport proteins (FATP) expressed in yeast. J Biol Chem. 280:16829-37.

Giesbertz P, Padberg I, Rein D, Ecker J, Hofle AS, Spanier B, Daniel H. (2015). Metabolite profiling in plasma and tissues of ob/ob and db/db mice identifies novel markers of obesity and type 2 diabetes. Diabetologia. 58:2133-43.

Gray S, Wang B, Orihuela Y, Hong EG, Fisch S, Haldar S, Cline GW, Kim JK, Peroni OD, Kahn BB, Jain MK. (2007). Regulation of gluconeogenesis by Kruppel-like factor 15. Cell Metab. 5:305-12.

Hagberg CE, Falkevall A, Wang X, Larsson E, Huusko J, Nilsson I, van Meeteren LA, Samen E, Lu L, Vanwildemeersch M, Klar J, Genove G, Pietras K, Stone-Elander S, Claesson-Welsh L, Yla-Herttuala S, Lindahl P, Eriksson U. (2010). Vascular endothelial growth factor B controls endothelial fatty acid uptake. Nature. 464:917-21.

Hagberg CE, Mehlem A, Falkevall A, Muhl L, Fam BC, Ortsater H, Scotney P, Nyqvist D, Samen E, Lu L, Stone-Elander S, Proietto J, Andrikopoulos S, Sjoholm A, Nash A, Eriksson U. (2012). Targeting VEGF-B as a novel treatment for insulin resistance and type 2 diabetes. Nature. 490:426-30.

Haldar SM, Jeyaraj D, Anand P, Zhu H, Lu Y, Prosdocimo DA, Eapen B, Kawanami D, Okutsu M, Brotto L, Fujioka H, Kerner J, Rosca MG, McGuinness OP, Snow RJ, Russell AP, Gerber AN, Bai X, Yan Z, Nosek TM, Brotto M, Hoppel CL, Jain MK. (2012). Kruppel-like factor 15 regulates skeletal muscle lipid flux and exercise adaptation. Proc Natl Acad Sci U S A. 109:6739-44.

Handschin C, Spiegelman BM. (2006). Peroxisome proliferator-activated receptor gamma coactivator 1 coactivators, energy homeostasis, and metabolism. Endocr Rev. 27:728-735.

Haslene-Hox H, Oveland E, Berg KC, Kolmannskog O, Woie K, Salvesen HB, Tenstad O, Wiig H. (2011). A new method for isolation of interstitial fluid from human solid tumors applied to proteomic analysis of ovarian carcinoma tissue. PLoS One. 6:e19217.

Hatazawa Y, Tadaishi M, Nagaike Y, Morita A, Ogawa Y, Ezaki O, Takai-Igarashi T, Kitaura Y, Shimomura Y, Kamei Y, Miura S. (2014). PGC-1α-mediated branched-chain amino acid metabolism in the skeletal muscle. PLoS One. 9:e91006.

Hatazawa Y, Senoo N, Tadaishi M, Ogawa Y, Ezaki O, Kamei Y, Miura S. (2015). Metabolomic analysis of the skeletal muscle of mice overexpressing PGC-1α. PLoS One. 10:e0129084.

He W, Miao FJ, Lin DC, Schwandner RT, Wang Z, Gao J, Chen JL, Tian H, Ling L. (2004). Citric acid cycle intermediates as ligands for orphan G-protein-coupled receptors. Nature. 429:188-93.

Herrmann T, Grone HJ, Langbein L, Kaiser I, Gosch I, Bennemann U, Metzger D, Chambon P, Stewart AF, Stremmel W. (2005). Disturbed epidermal structure in mice with temporally controlled fatp4 deficiency. J Invest Dermatol. 125:1228-35.

Jeyaraj D, Scheer FA, Ripperger JA, Haldar SM, Lu Y, Prosdocimo DA, Eapen SJ, Eapen BL, Cui Y, Mahabeleshwar GH, Lee HG, Smith MA, Casadesus G, Mintz EM, Sun H, Wang Y, Ramsey KM, Bass J, Shea SA, Albrecht U, Jain MK. (2012). Klf15 orchestrates circadian nitrogen homeostasis. Cell Metab. 15:311-23.

Kuzuya T, Katano Y, Nakano I, Hirooka Y, Itoh A, Ishigami M, Hayashi K, Honda T, Goto H, Fujita Y, Shikano R, Muramatsu Y, Bajotto G, Tamura T, Tamura N, Shimomura Y. (2008). Regulation of branched-chain amino acid catabolism in rat models for spontaneous type 2 diabetes mellitus. Biochem Biophys Res Commun. 373:94-8.

Lenz LS, Marx J, Chamulitrat W, Kaiser I, Grone HJ, Liebisch G, Schmitz G, Elsing C, Straub BK, Fullekrug J, Stremmel W, Herrmann T. (2011). Adipocyte-specific inactivation of Acyl-CoA synthetase fatty acid transport protein 4 (Fatp4) in mice causes adipose hypertrophy and alterations in metabolism of complex lipids under high fat diet. J Biol Chem. 286:35578-87.

Liao X, Zhang R, Lu Y, Prosdocimo DA, Sangwung P, Zhang L, Zhou G, Anand P, Lai L, Leone TC, Fujioka H, Ye F, Rosca MG, Hoppel CL, Schulze PC, Abel ED, Stamler JS, Kelly DP, Jain MK. (2015). Kruppel-like factor 4 is critical for transcriptional control of cardiac mitochondrial homeostasis. J Clin Invest. pii: 79964.

Lo IC, Gupta V, Midde KK, Taupin V, Lopez-Sanchez I, Kufareva I, Abagyan R, Randazzo PA, Farquhar MG, Ghosh P. (2015). Activation of Gαi at the Golgi by GIV/Girdin imposes finiteness in Arf1 signaling. Dev Cell. 33:189-203.

Lopez-Soriano FJ, Fernandez-Lopez JA, Mampel T, Villarroya F, Iglesias R, Alemany M. (1988). Amino acid and glucose uptake by rat brown adipose tissue. Effect of cold-exposure and acclimation. Biochem J. 252:843-9.

Lynch CJ, Adams SH. (2014). Branched-chain amino acids in metabolic signalling and insulin resistance. Nat Rev Endocrinol. 10:723-36.

Mangmool S, Kurose H. (2011). G(i/o) protein-dependent and -independent actions of Pertussis Toxin (PTX). Toxins (Basel). 3:884-99.

Moulson CL, Martin DR, Lugus JJ, Schaffer JE, Lind AC, Miner JH. (2003). Cloning of wrinkle-free, a previously uncharacterized mouse mutation, reveals crucial roles for fatty acid transport protein 4 in skin and hair development. Proc Natl Acad Sci U S A. 100:5274-9.

Moulson CL, Lin MH, White JM, Newberry EP, Davidson NO, Miner JH. (2007). Keratinocyte-specific expression of fatty acid transport protein 4 rescues the wrinkle-free phenotype in Slc27a4/Fatp4 mutant mice. J Biol Chem. 282:15912-20.

Overmyer KA, Evans CR, Qi NR, Minogue CE, Carson JJ, Chermside-Scabbo CJ, Koch LG, Britton SL, Pagliarini DJ, Coon JJ, Burant CF. (2015). Maximal oxidative capacity during exercise is associated with skeletal muscle fuel selection and dynamic changes in mitochondrial protein acetylation. Cell Metab. 21:468-78.

Pechlivanis A, Kostidis S, Saraslanidis P, Petridou A, Tsalis G, Mougios V, Gika HG, Mikros E, Theodoridis GA. (2010). (1)H NMR-based metabonomic investigation of the effect of two different exercise sessions on the metabolic fingerprint of human urine. J Proteome Res. 9:6405-16.

Pei Z, Fraisl P, Berger J, Jia Z, Forss-Petter S, Watkins PA. (2004). Mouse very long-chain Acyl-CoA synthetase 3/fatty acid transport protein 3 catalyzes fatty acid activation but not fatty acid transport in MA-10 cells. J Biol Chem. 279:54454-62.

Prosdocimo DA, Anand P, Liao X, Zhu H, Shelkay S, Artero-Calderon P, Zhang L, Kirsh J, Moore D, Rosca MG, Vazquez E, Kerner J, Akat KM, Williams Z, Zhao J, Fujioka H, Tuschl T, Bai X, Schulze PC, Hoppel CL, Jain MK, Haldar SM. (2014). Kruppel-like factor 15 is a critical regulator of cardiac lipid metabolism. J Biol Chem. 289:5914-24.

Sapieha P, Sirinyan M, Hamel D, Zaniolo K, Joyal JS, Cho JH, Honore JC, Kermorvant-Duchemin E, Varma DR, Tremblay S, Leduc M, Rihakova L, Hardy P, Klein WH, Mu X, Mamer O, Lachapelle P, Di Polo A, Beausejour C, Andelfinger G, Mitchell G, Sennlaub F, Chemtob S. (2008). The succinate receptor GPR91 in neurons has a major role in retinal angiogenesis. Nat Med. 14:1067-76.

Stahl A, Hirsch DJ, Gimeno RE, Punreddy S, Ge P, Watson N, Patel S, Kotler M, Raimondi A, Tartaglia LA, Lodish HF. (1999). Identification of the major intestinal fatty acid transport protein. Mol Cell. 4:299-308.

She P, Van Horn C, Reid T, Hutson SM, Cooney RN, Lynch CJ. (2007). Obesity-related elevations in plasma leucine are associated with alterations in enzymes involved in branched-chain amino acid metabolism. Am J Physiol Endocrinol Metab. 293:E1552-63.

Shim J, Moulson CL, Newberry EP, Lin MH, Xie Y, Kennedy SM, Miner JH, Davidson NO. (2009). Fatty acid transport protein 4 is dispensable for intestinal lipid absorption in mice. J Lipid Res. 50:491-500.

Wiig H, Aukland K, Tenstad O. (2003). Isolation of interstitial fluid from rat mammary tumors by a centrifugation method. Am J Physiol Heart Circ Physiol. 284:H416-24.

Yamamoto J, Ikeda Y, Iguchi H, Fujino T, Tanaka T, Asaba H, Iwasaki S, Ioka RX, Kaneko IW, Magoori K, Takahashi S, Mori T, Sakaue H, Kodama T, Yanagisawa M, Yamamoto TT, Ito S, Sakai J. (2004). A Kruppel-like factor KLF15 contributes fasting-induced transcriptional activation of mitochondrial acetyl-CoA synthetase gene AceCS2. J Biol Chem. 279:16954-62.

Youm YH, Nguyen KY, Grant RW, Goldberg EL, Bodogai M, Kim D, D'Agostino D, Planavsky N, Lupfer C, Kanneganti TD, Kang S, Horvath TL, Fahmy TM, Crawford PA, Biragyn A, Alnemri E, Dixit VD. (2015). The ketone metabolite β-hydroxybutyrate blocks NLRP3 inflammasome-mediated inflammatory disease. Nat Med. 21:263-9.